INAF ISTITUTO NAZIONALE DI ASTROFISICA NATIONAL INSTITUTE FOR ASTROPHYSICS

Gaia DPAC

Agenzia Spaziale Italiana

DPCT Data Processing Center Torino

Gaia as local cosmological probe

Mariateresa Crosta
INAF-OATo

Collaborators: V. Akhmetov, W. Beordo, B. Bucciarelli, M.G.Lattanzi, P. Re Fiorentin, A. Spagna

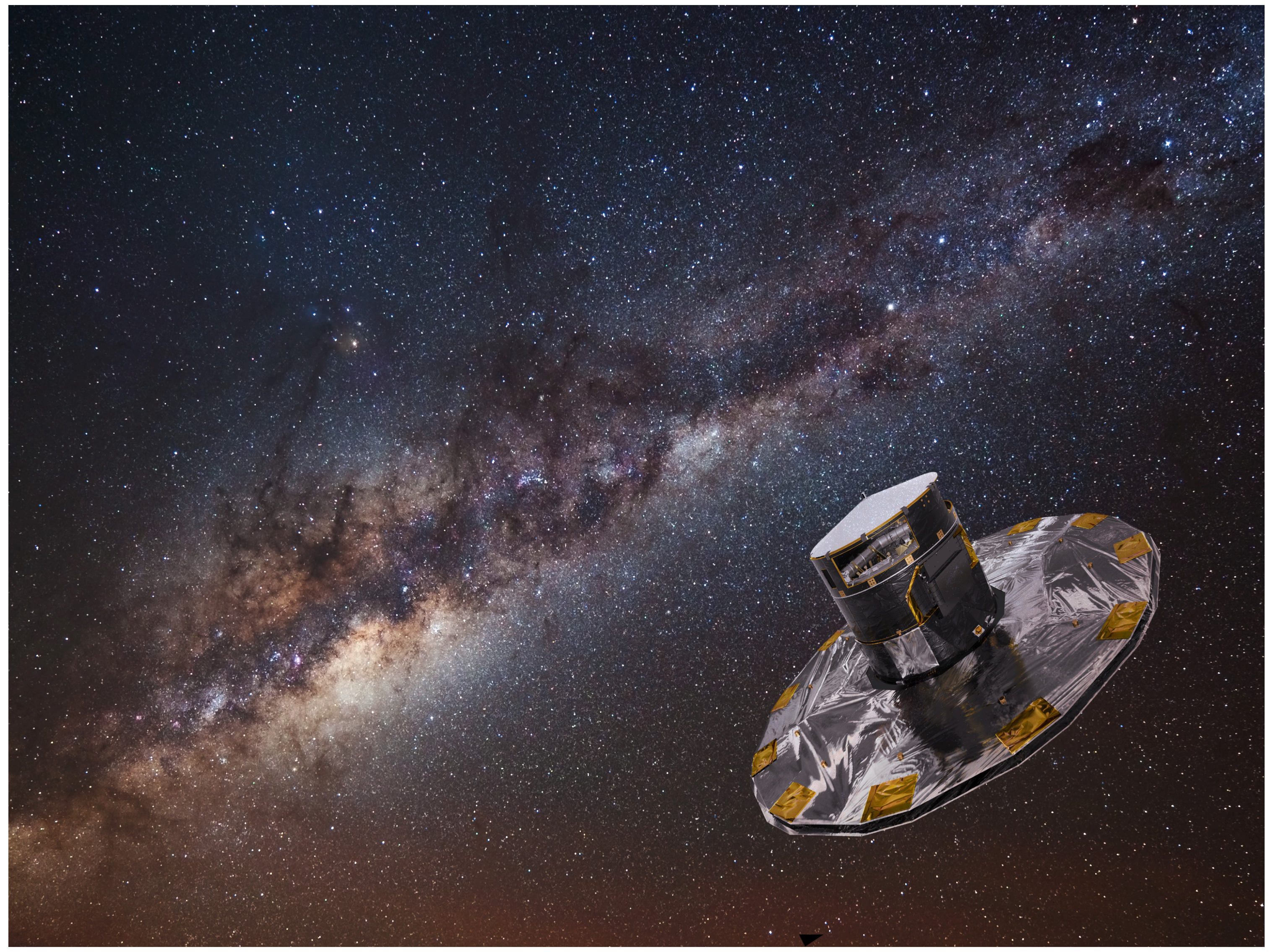

15th International Workshop on the Identification of Dark Matter 2024

Palazzo dell’Emiciclo, Sala Ipogea

July 8-12 2024 L'Aquila (Italy)

Gaia measures at L2 of the Earth-Sun system
position (direction and distance) and velocity
of over 1 billion stars in our Galaxy
with an accuracy of up to 1 microarcsecond

0”,000001 =
micro(μ) arc
sec

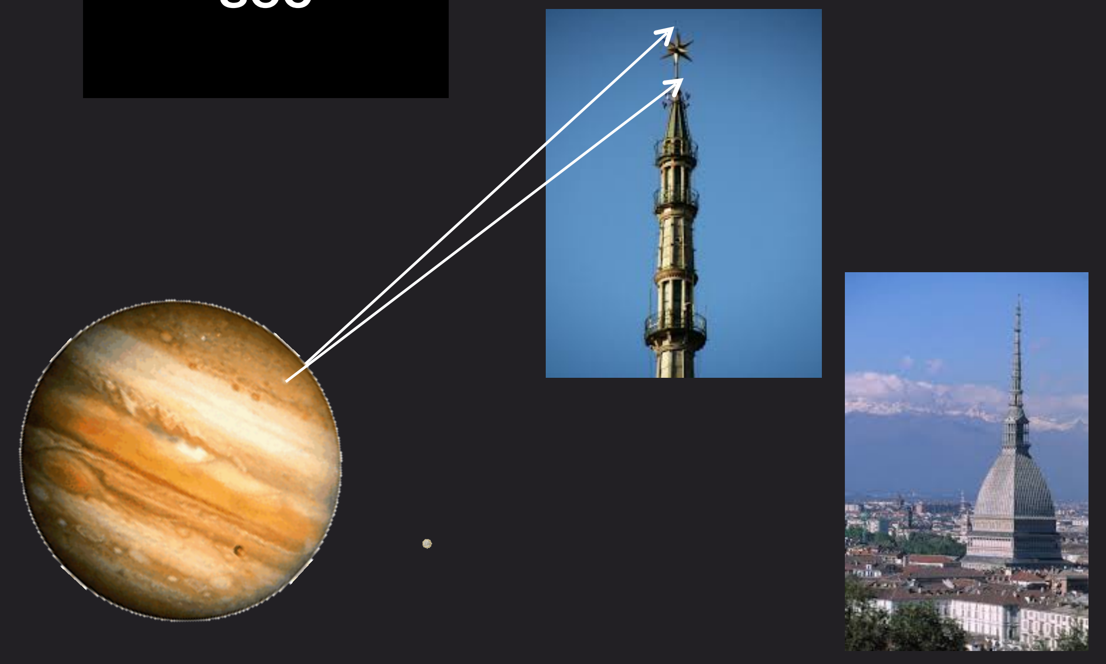

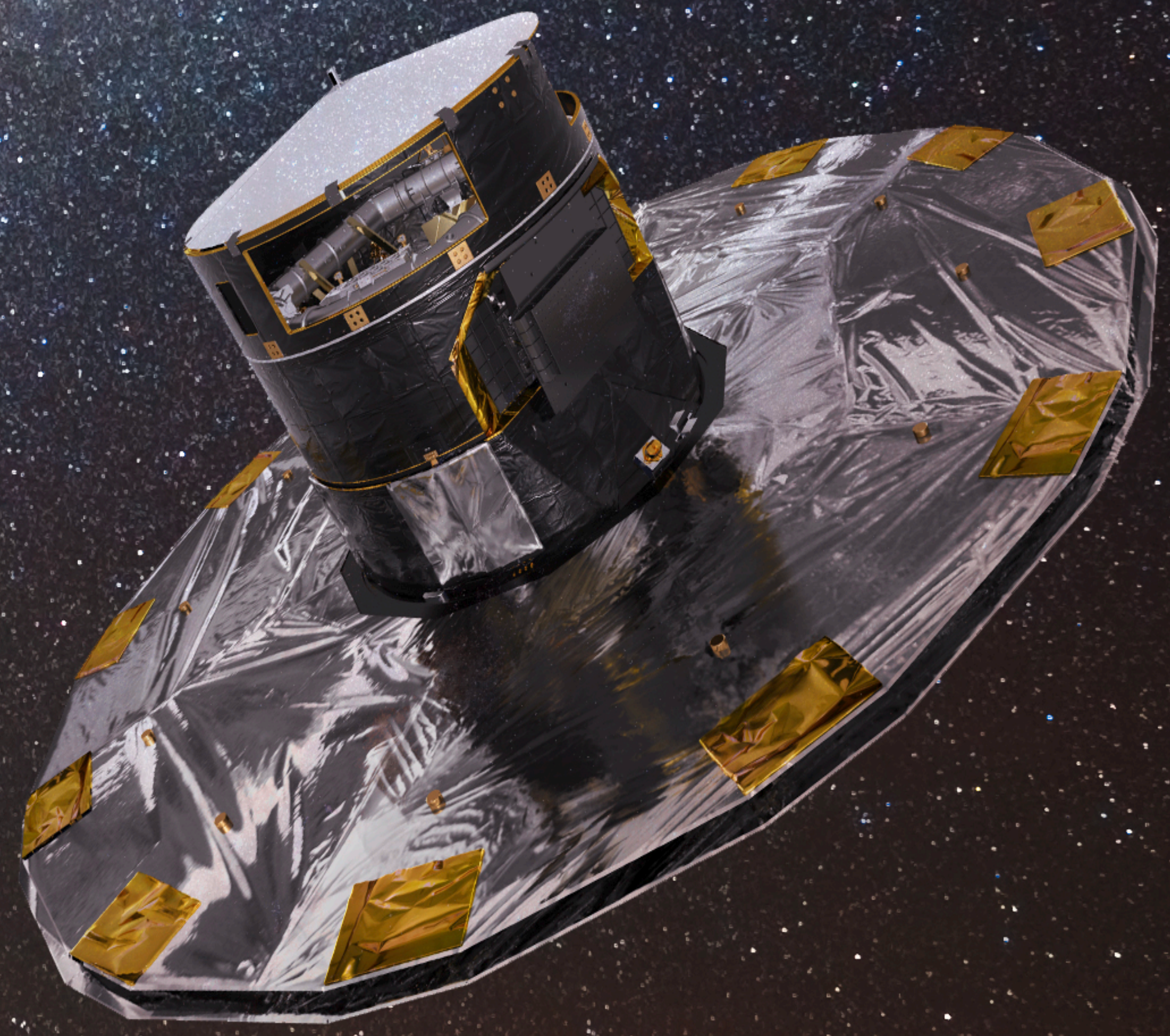

ESA mission launched in 2013, nominal lifetime 5 years, extended up to 2025

The location of an object in astrometry is considered reliable if its relative error is less 10%

parallax $\pi(\text{arcsec}) \approx 1(\text{UA})/d^*(\text{pc})$

Hipparcos $\sigma_\pi = 1 \text{ mas} = 10^{-3}\text{arcsec}$

Gaia $\sigma_\pi = 10\ \mu\text{as} = 10^{-5}\text{arcsec}$

$$\pi \approx \sigma_\pi \cdot 10$$

d* = 100 pc

d*= 10 kpc

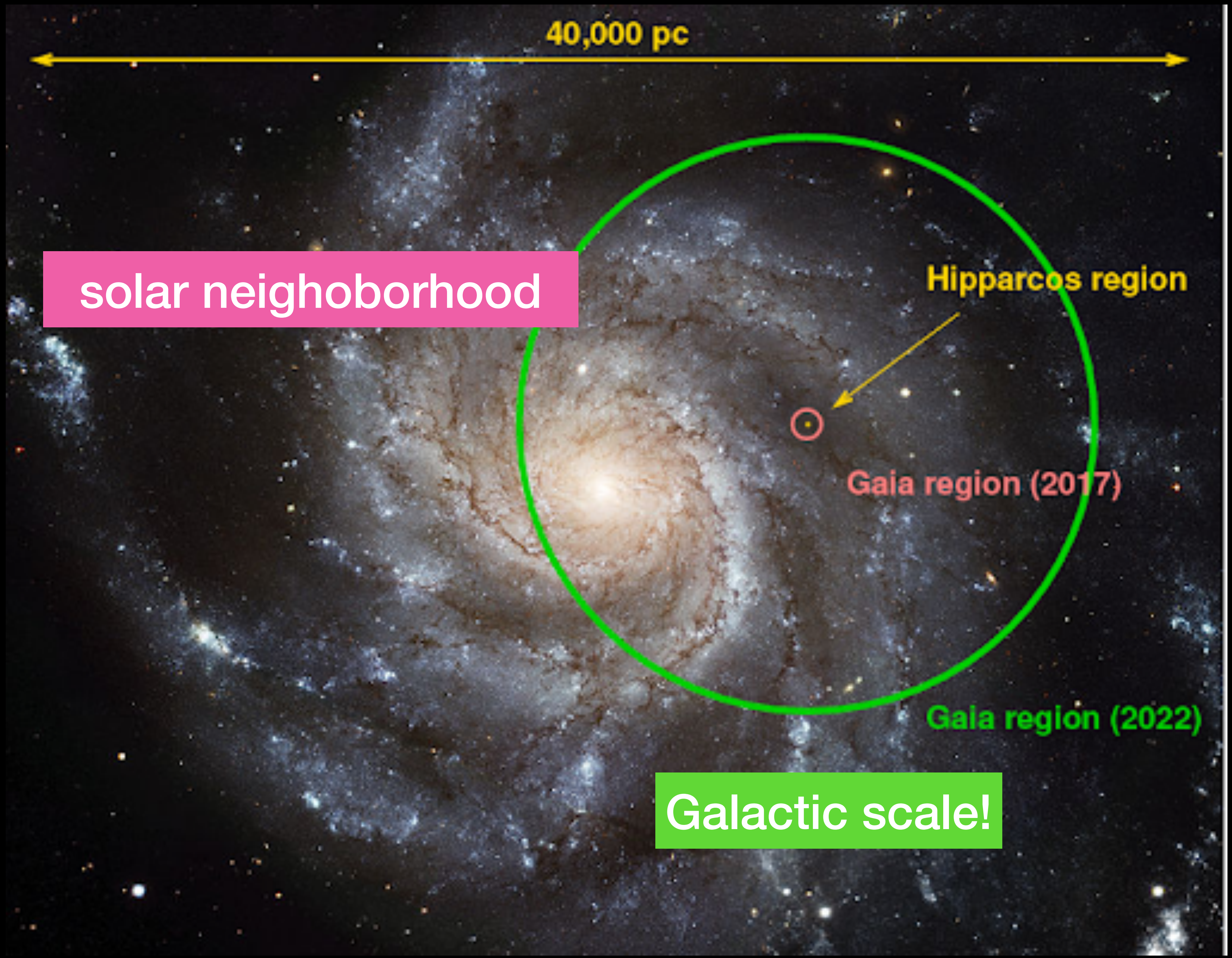

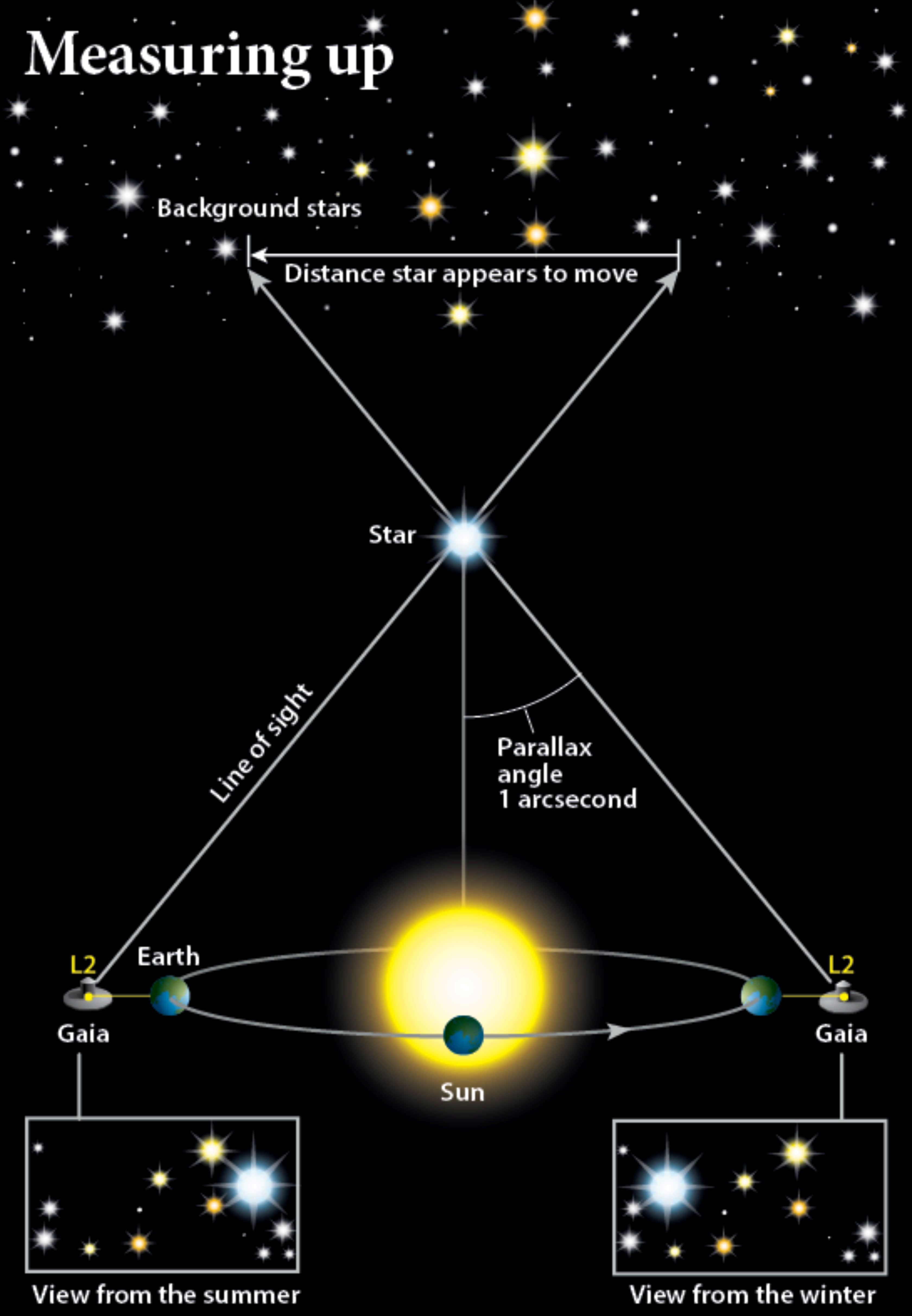

To understand the distances between stars, astronomers rely on a method called parallax. By measuring the distances stars appear to move relative to other stars, astronomers can gauge how far away they are from us and from each other. ASTRONOMY: ROEN KELLY

Science with one/two billion objects in 3 dimension, from structure and evolution of the MW to GR tests

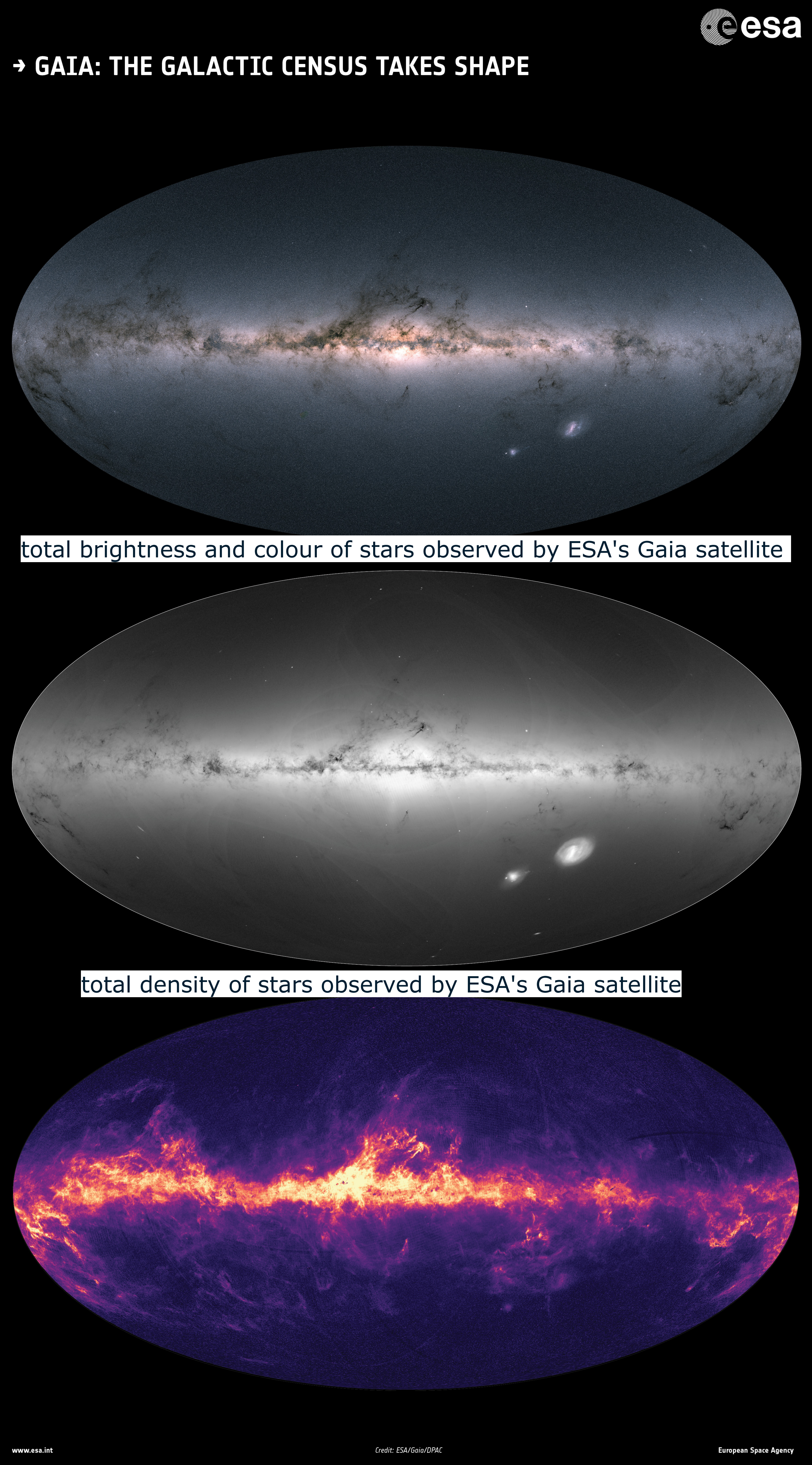

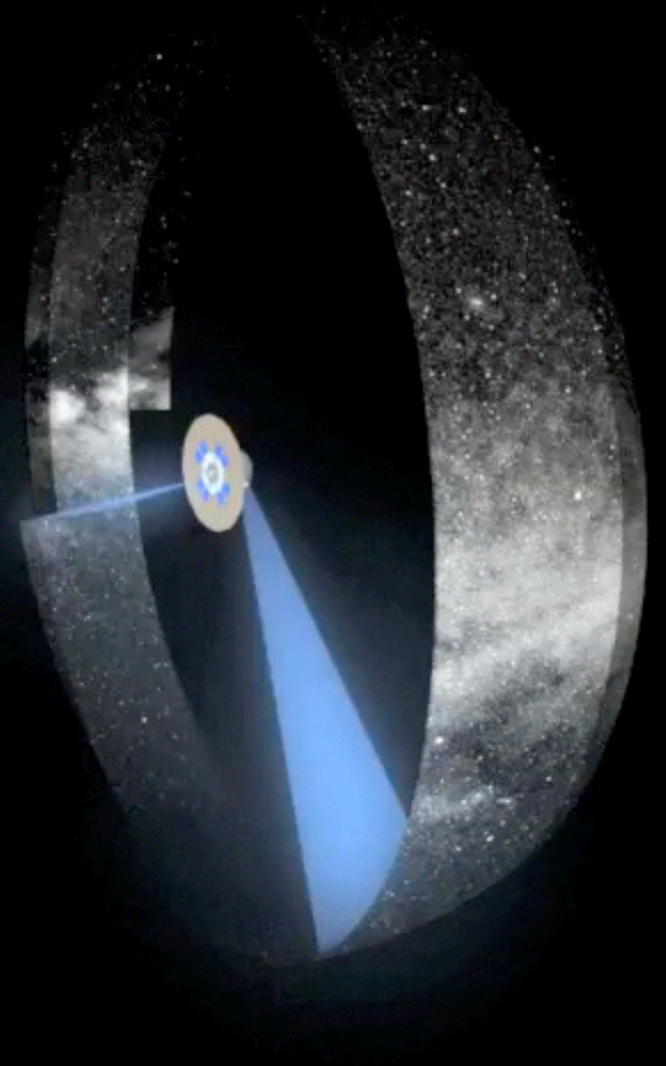

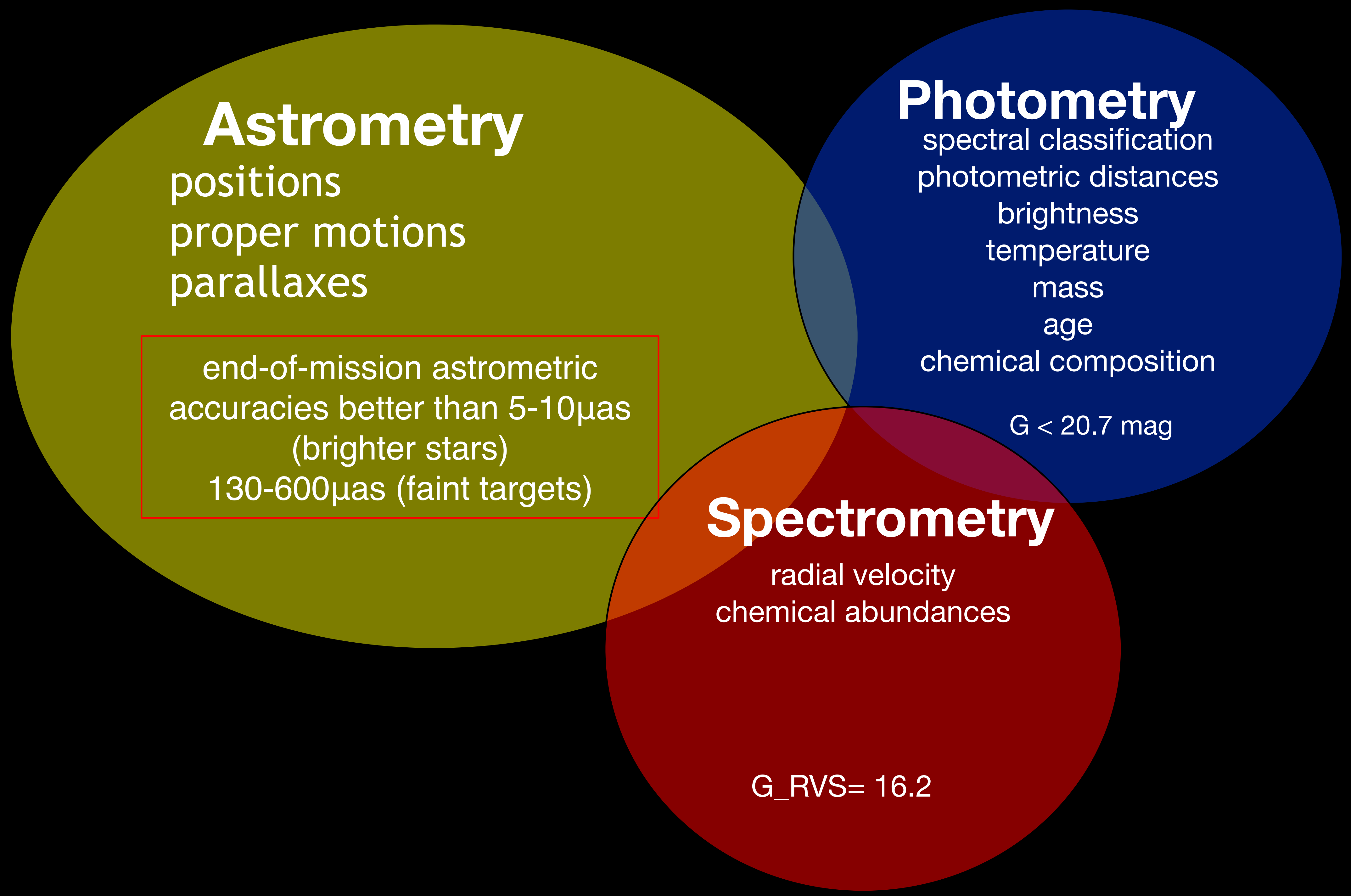

Science with one/two billion objects in 3 dimension, from structure and evolution of the MW to GR tests

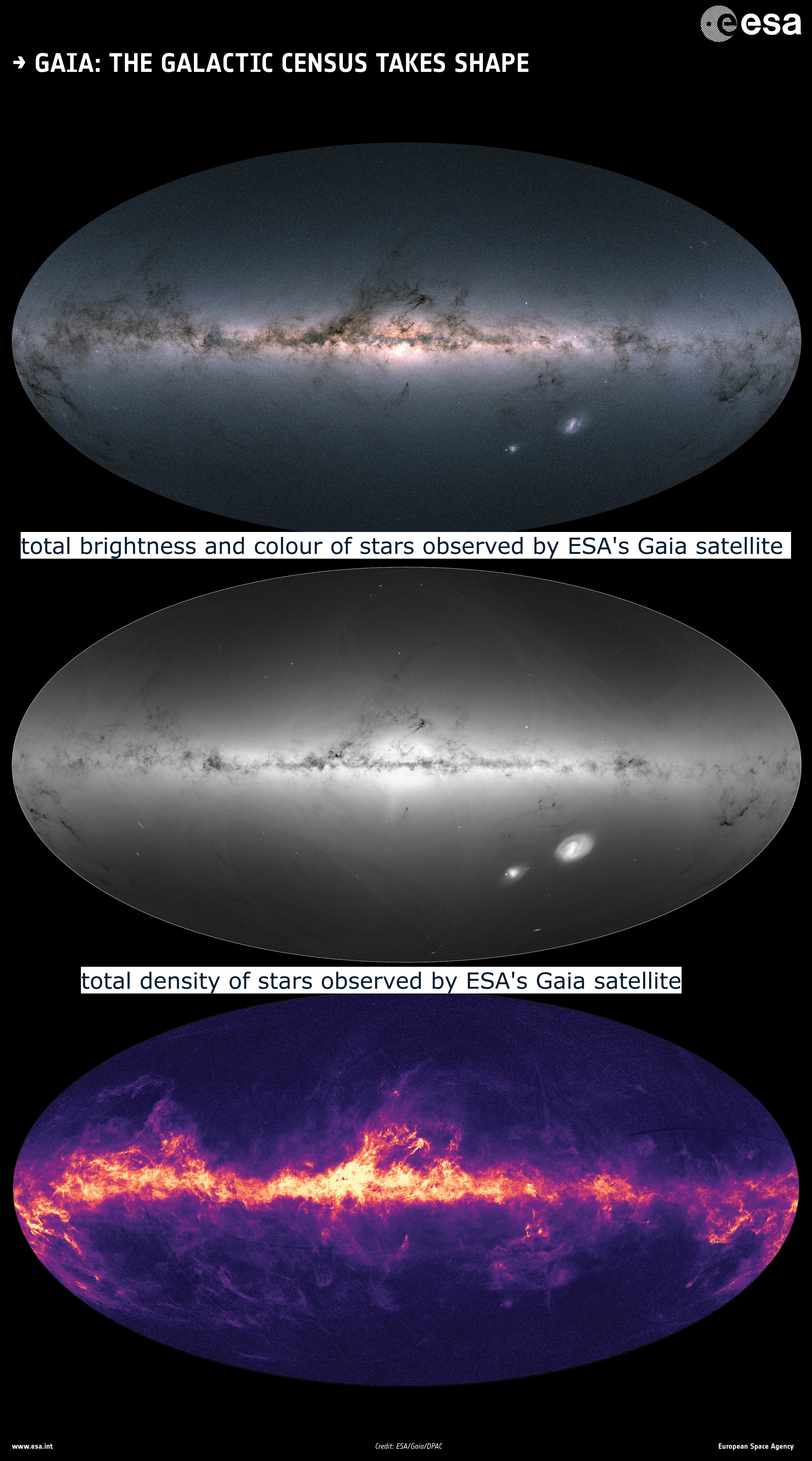

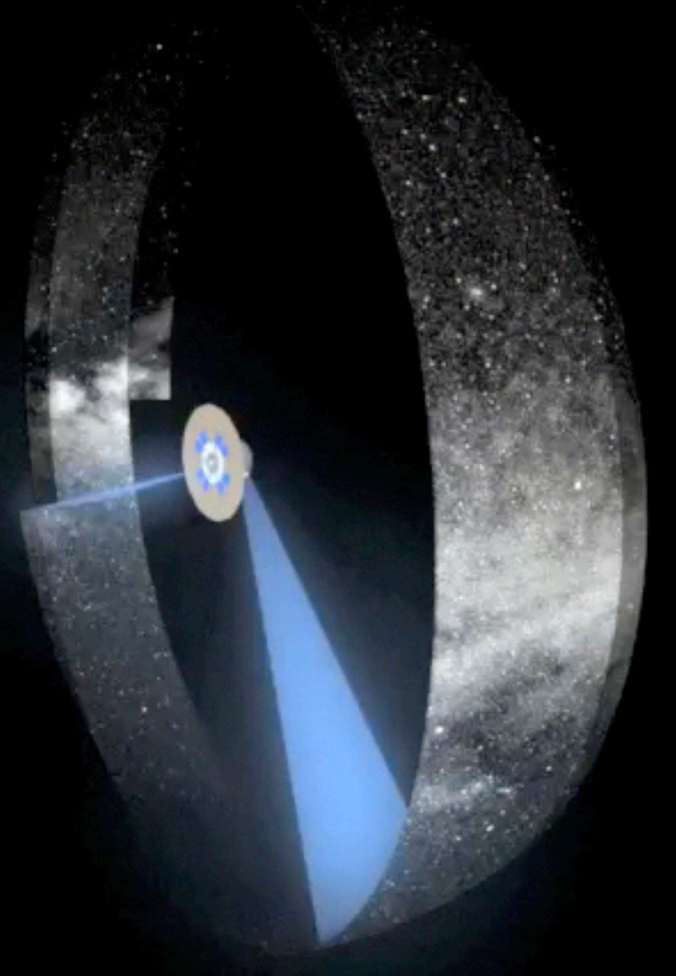

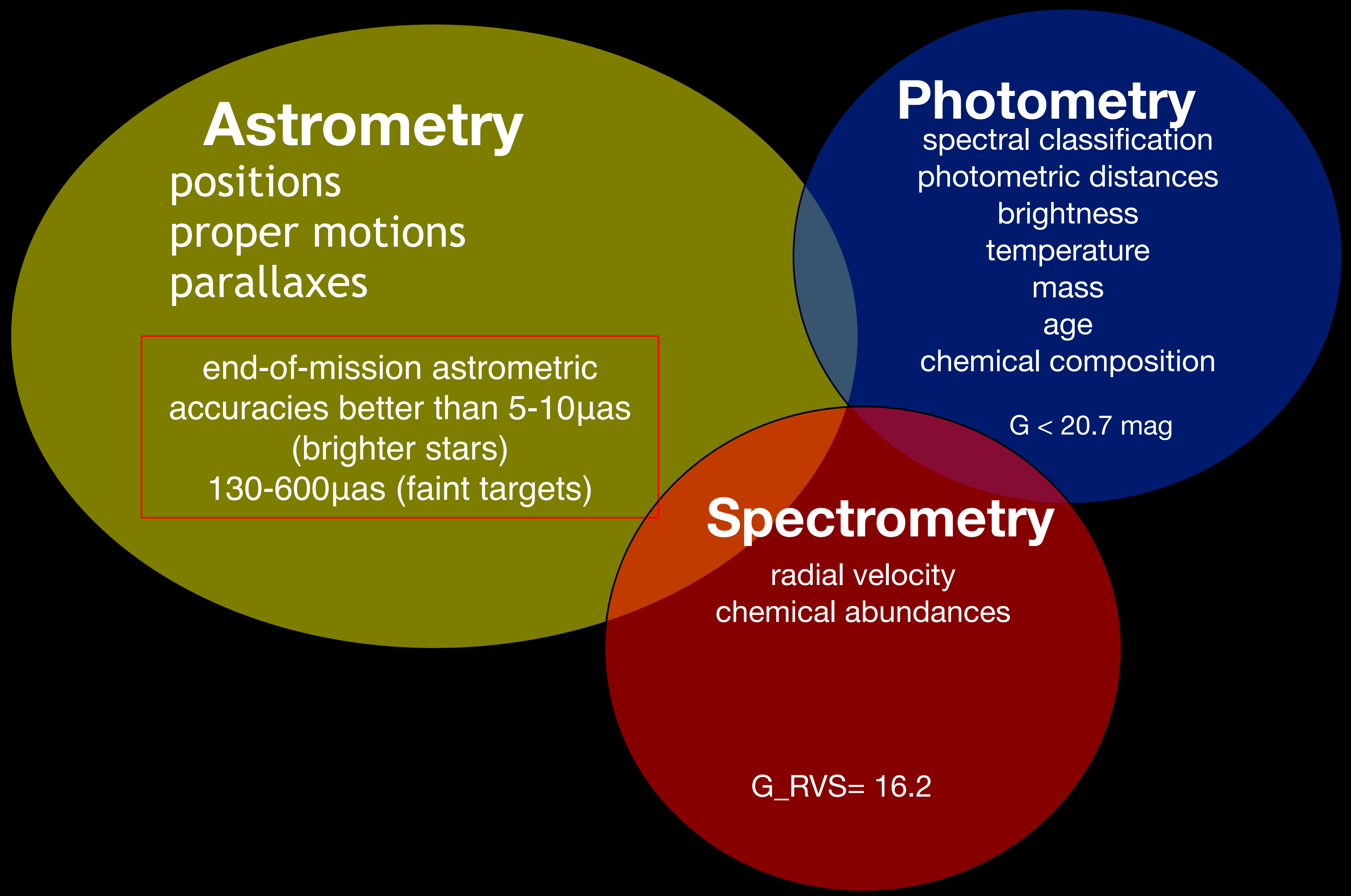

Gaia Data Release 3 in numbers

https://www.cosmos.esa.int/web/gaia/data-release-3

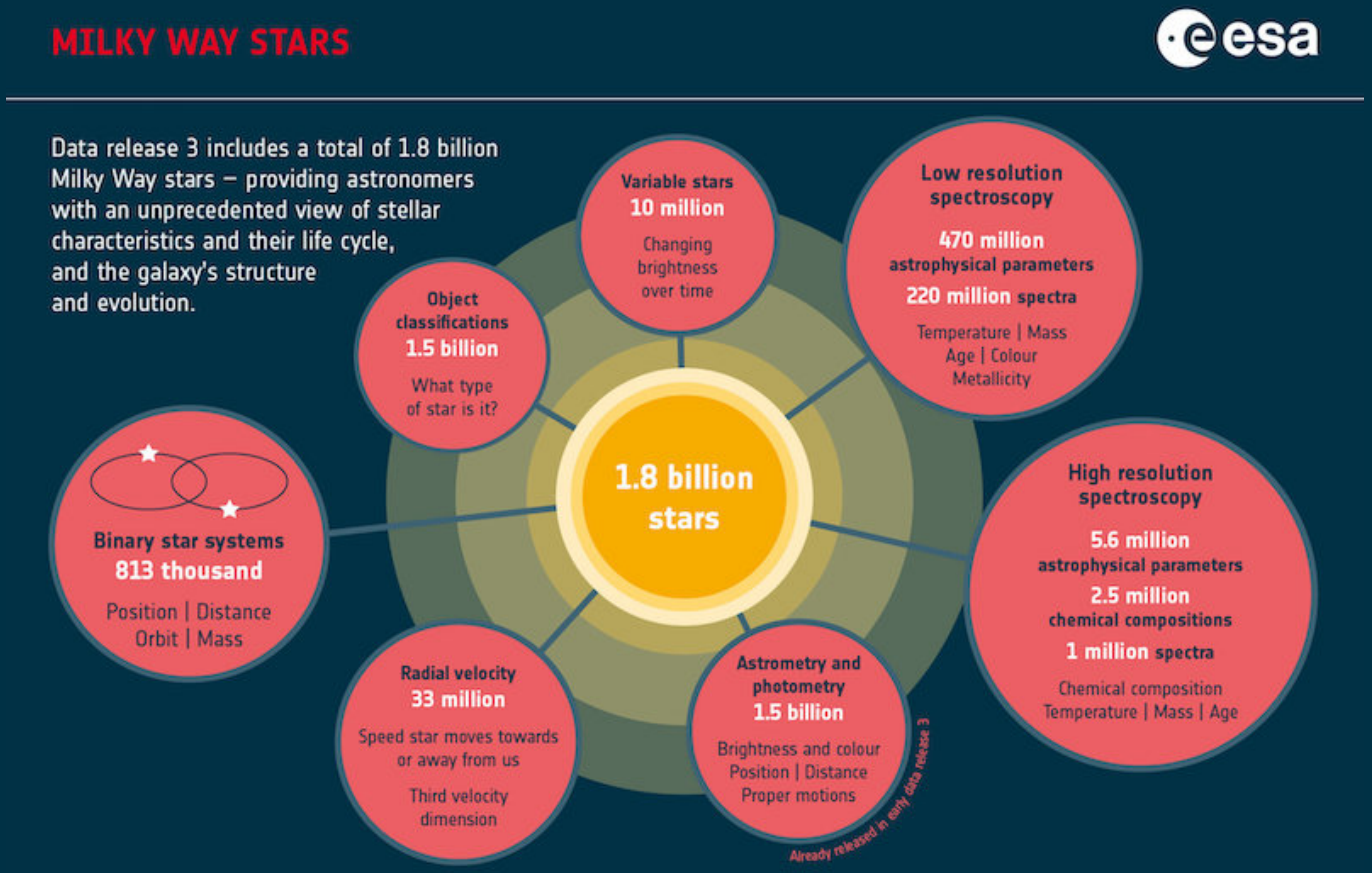

Next Gaia DR4 (based on 66 months of data) not before the first quarter of 2026 will be consisting of:

- Full astrometric, photometric, and radial-velocity catalogues
- All available variable-star and non-single-star solutions
- Source classifications (probabilities) plus multiple astrophysical parameters (derived from BP/RP, RVS, and astrometry) for stars, unresolved binaries, galaxies, and quasars
- An exoplanet list
- **All epoch and transit data for all sources**!

Gaia DR5 (based on all mission data) not before the end of 2030 will be consisting of **Complete Gaia Legacy Archive of all data**

Data Release Scenario http://www.cosmos.esa.int/web/gaia/release

Stars belong to the architecture of spacetime which is dictated by the Einstein equations

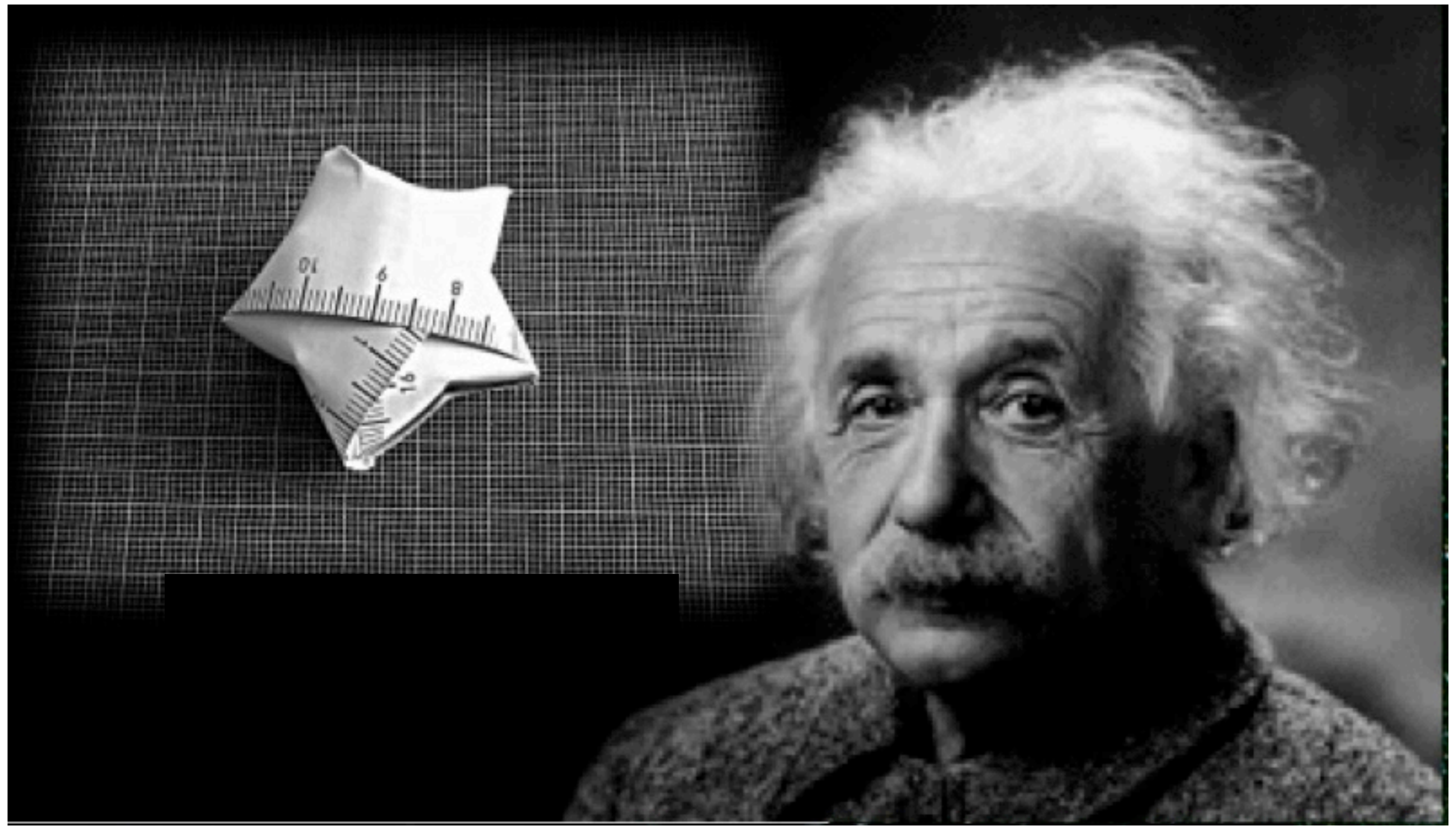

Astrometry

$\alpha, \delta, \mu_\alpha, \mu_\delta, \pi, \ldots$

theoretical, analytical and/or numerical models, completely based on General Relativity and relativistic attitude (satellite or ground based observers)

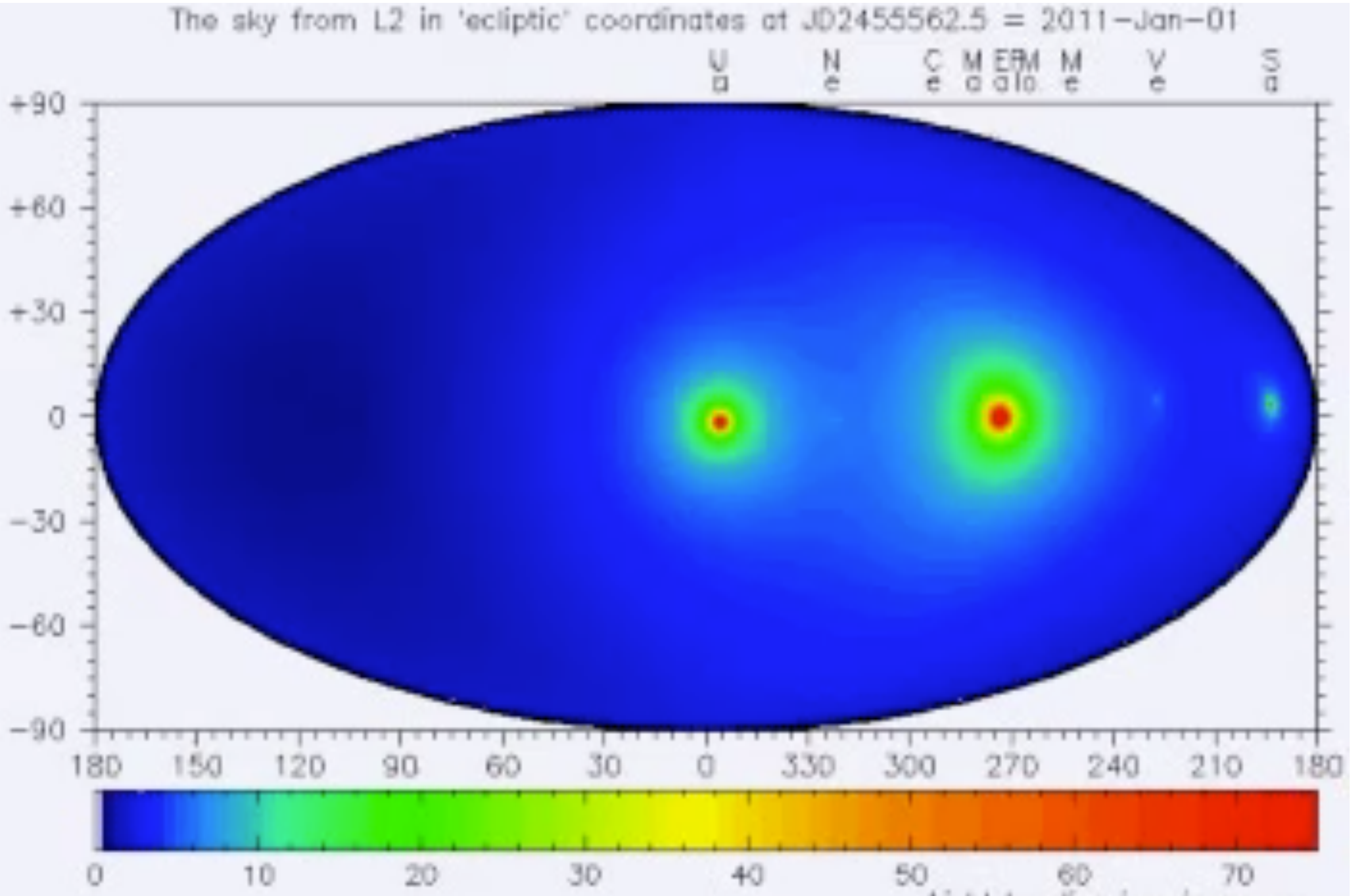

increasingly accurate astronomical data

micro-arcsecond accuracy + Solar System gravitational fields => relativistic models for the light-ray propagation, from the observer to the star

Stars belong to the architecture of spacetime which is dictated by the Einstein equations

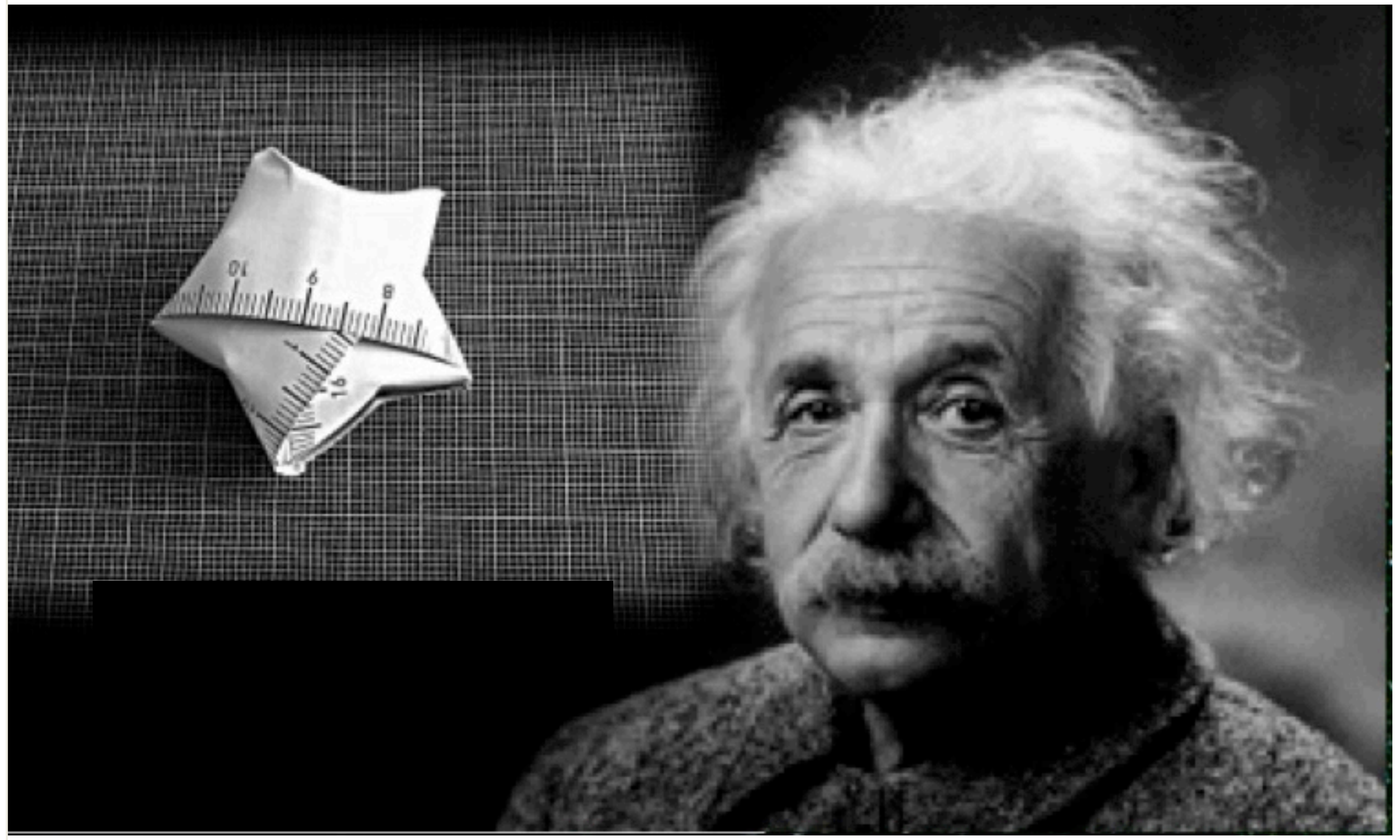

Astrometry

$\underline{\alpha, \delta, \mu_\alpha, \mu_\delta, \pi, \ldots}$

Relativistic Astrometry

theoretical, analytical and/or numerical models, completely based on General Relativity and relativistic attitude (satellite or ground based observers)

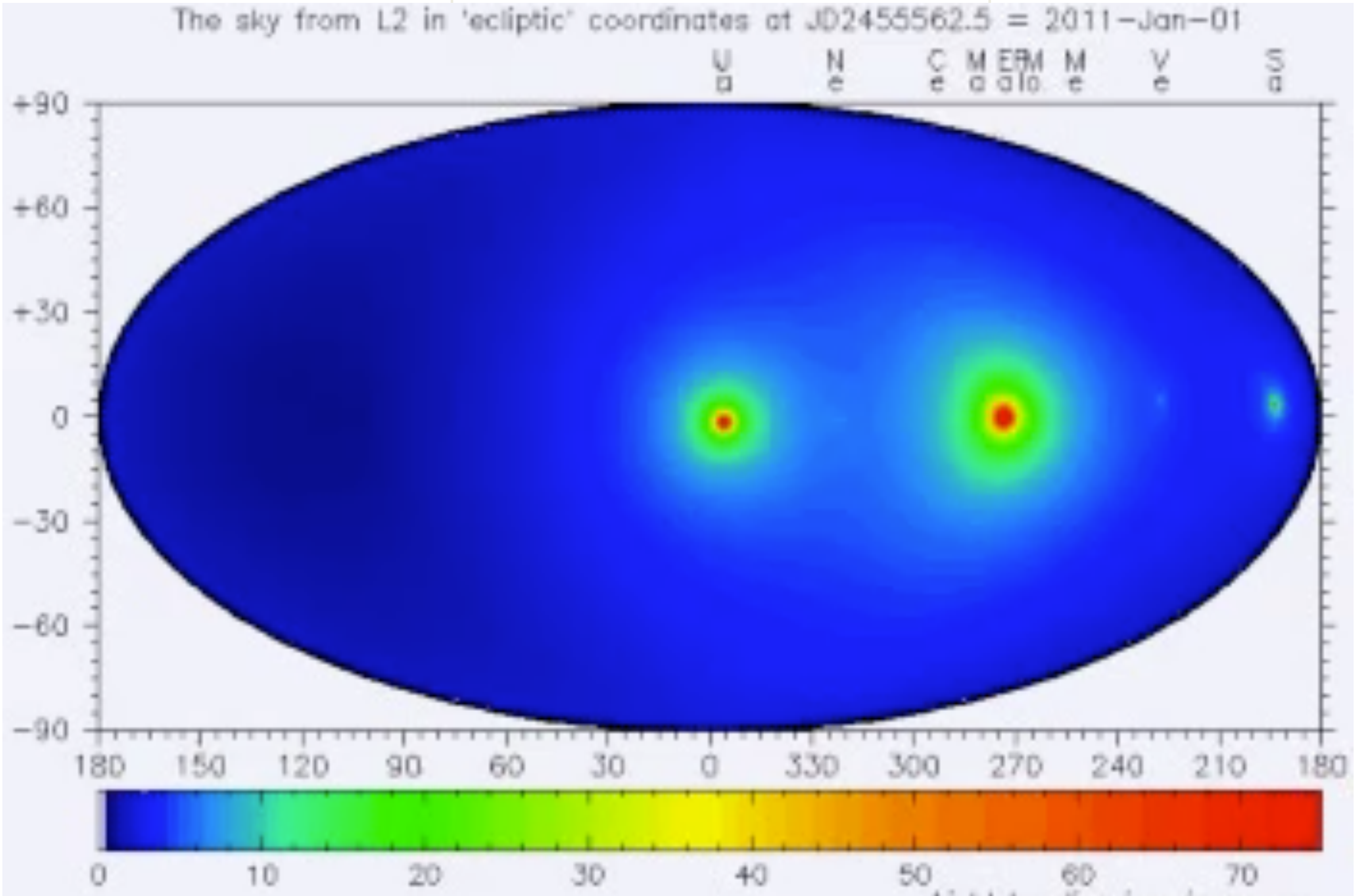

increasingly accurate astronomical data

micro-arcsecond accuracy + Solar System gravitational fields => relativistic models for the light-ray propagation, from the observer to the star

Gaia: the Era of Relativistic Astrometry

the trajectories of photons emitted by the stars
- null geodesics -

should be as fundamental as
the equation of stellar evolution!

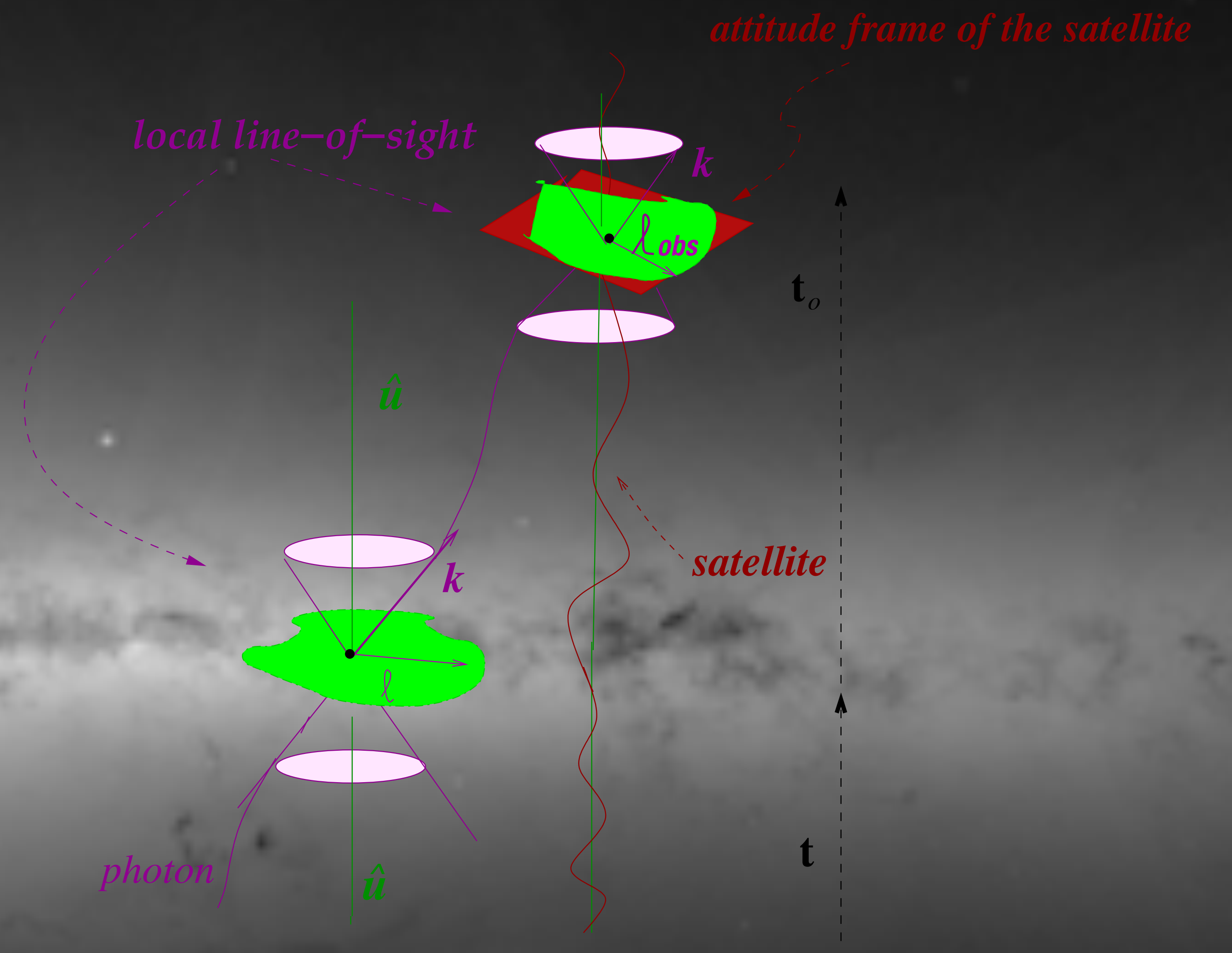

Source count maps based on the Gaia DR3 data.

Acknowledgement: Images were created by André Moitinho and Márcia Barros, University of Lisbon, Portugal

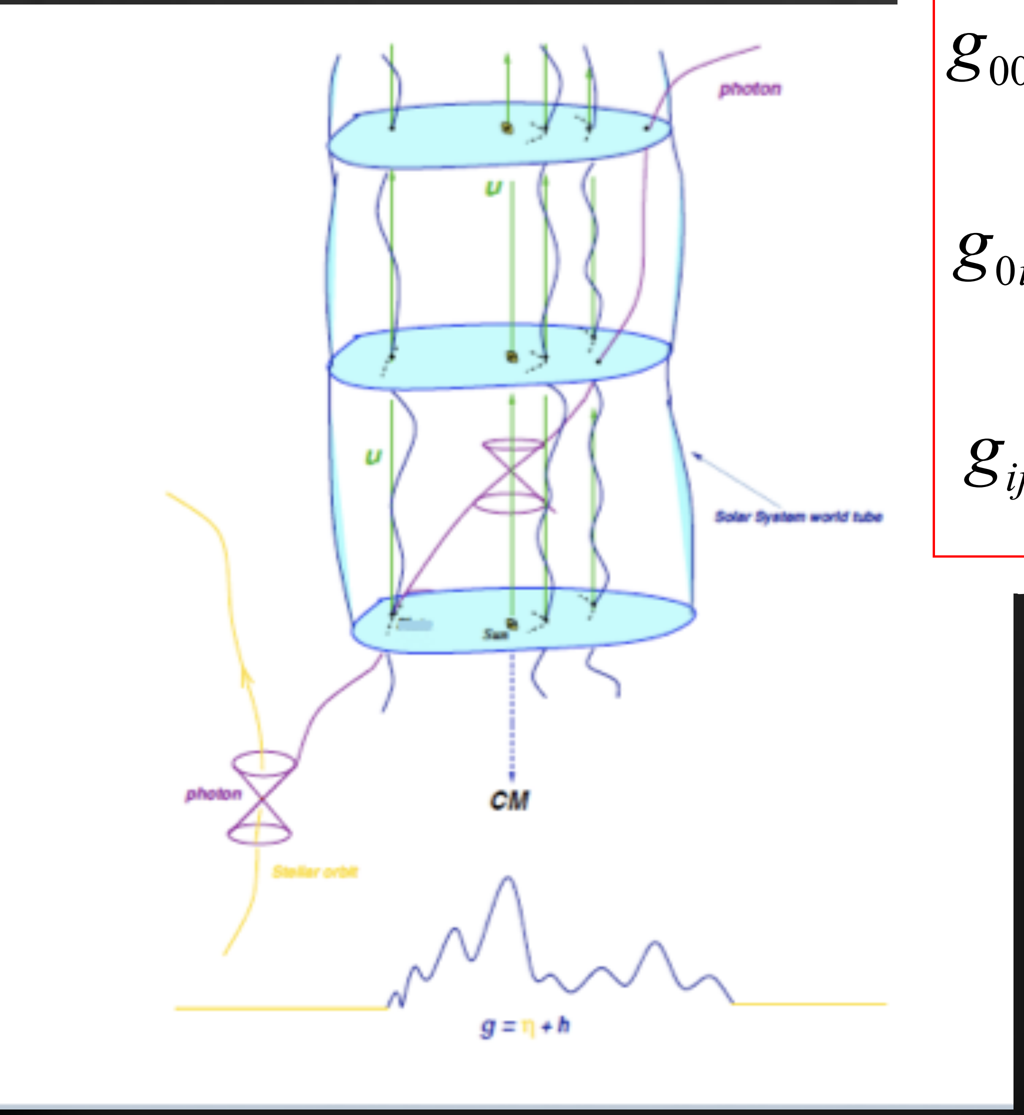

$$g_{00} = -1 + \frac{2}{c^2} w(t, \boldsymbol{x}) - \frac{2}{c^4} w^2(t, \boldsymbol{x}),$$

$$g_{0i} = -\frac{4}{c^3} w^i(t, \boldsymbol{x}),$$

$$g_{ij} = \delta_{ij}\left(1 + \frac{2}{c^2} w(t, \boldsymbol{x})\right).$$

ε ~ v^2/c^2 ~ GM/rc^2 ~ mas accuracy
which requires determination of
g_{oo} even terms in ε, lowest order ε^2~mas
g_{oj} odd terms in ε, lowest order ε^3~μ-as
g_{ij} even terms in ε, lowest order ε^2~mas

the Consortium constitued for the Gaia data reduction (DPAC) agreed to set up, respectively, two independent global sphere solutions and 2 independent GR models:
GREM (Gaia RElativistic Model) - AGIS
RAMOD (Relativistic Astrometric MODel) -GSR

IAU metric for the definition of the Celestial Coordinate Systems (BCRS)

M.Crosta. “Astrometry in the 21st century. From Hipparchus to Einstein” La Rivista del Nuovo Cimento 42 (2019)

M. Crosta et al. “General relativistic observable for gravitational astrometry in the context of the Gaia mission and beyond” PRD 96 (2017)

- the position and velocity data, comprising the outputs of the Gaia mission, are fully GR compliant

Given a relativistic approach for the data analysis and processing, any subsequent exploitations should be consistent with the precepts of the theory underlying the astrometric model

A **fully relativistic model for the Milky Way (MW)** should be pursued!

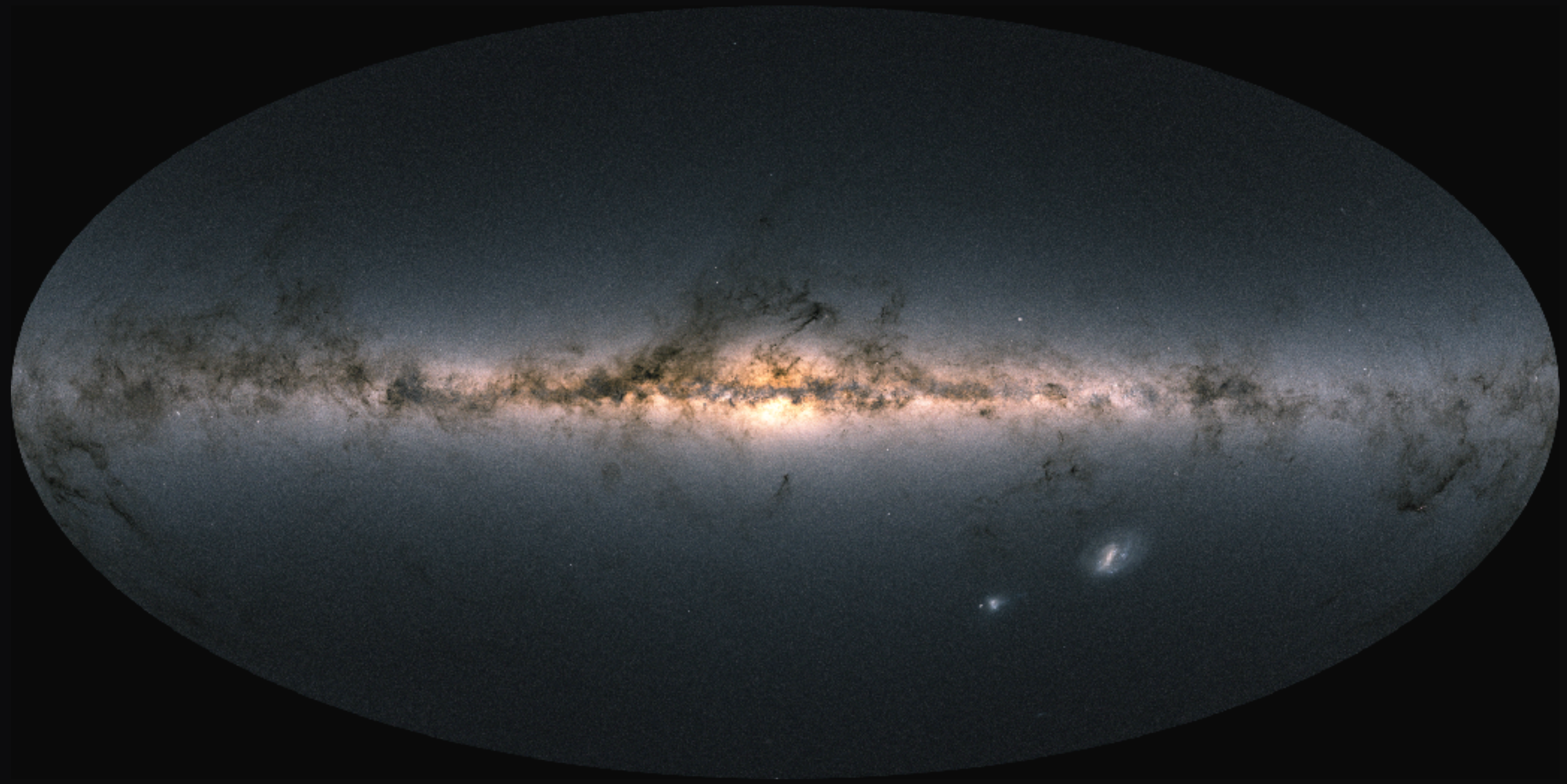

➢ **Local Cosmology:** Lambda-CDM model predictions at the scale of the Milky Way

The use of Gaia data must be parallel with the utilization of the most advanced cosmological simulations with baryonic matter (gas and stars)

Gaia can provide values (true observables) to estimate model parameters

ΛCDM - Hierarchical scenario

The growth of cosmic structures:

- primordial density fluctuations produced during inflation
- dominant mass component is cold dark-matter (CDM)
- fluctuations grow under the action of gravity
- ΛCDM power spectrum: small objects collapse first
- Gas cooling and star formation
- Galaxy evolution and merging

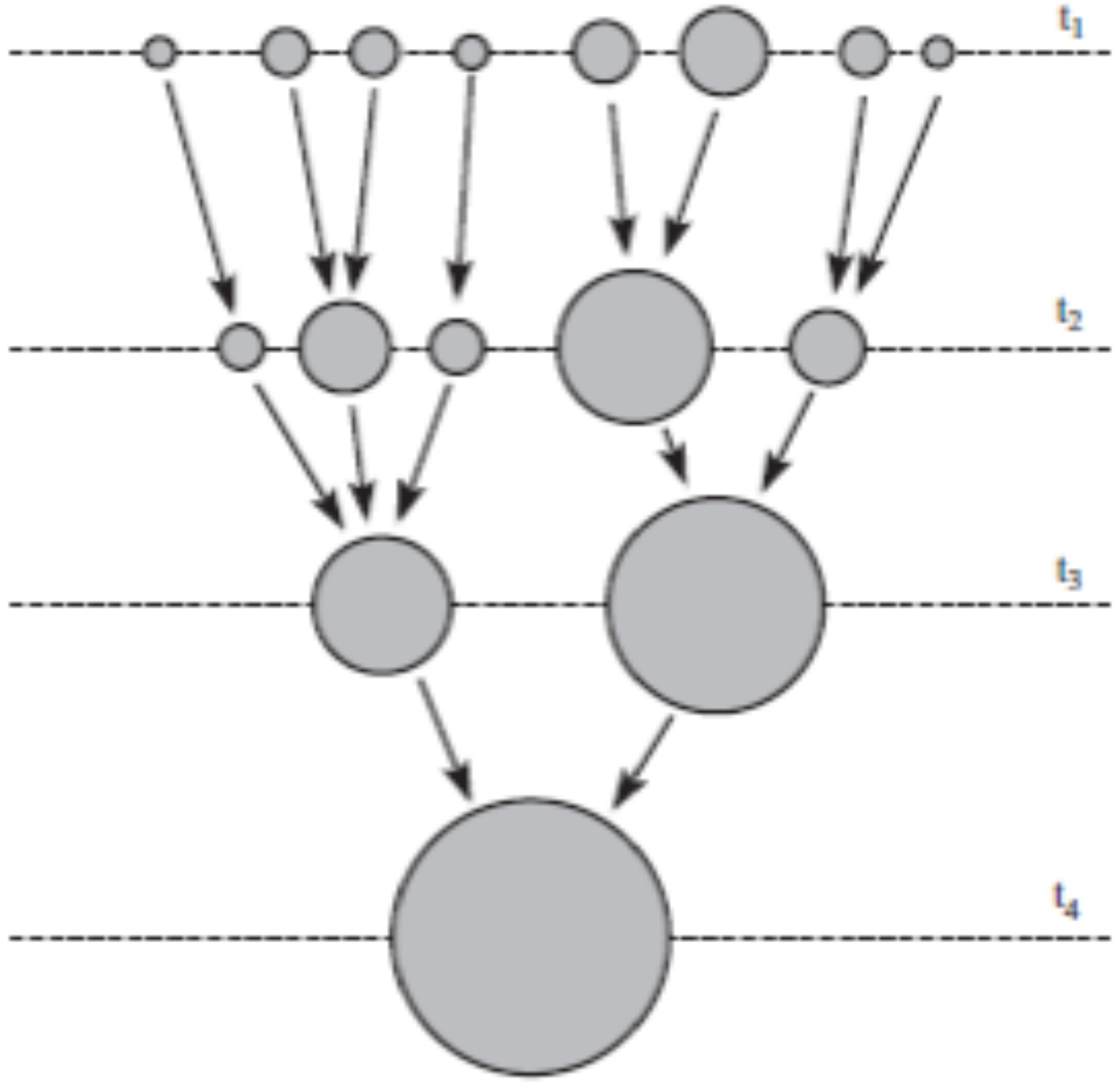

Examples of galactic building blocks in protogalaxies observed by JWST

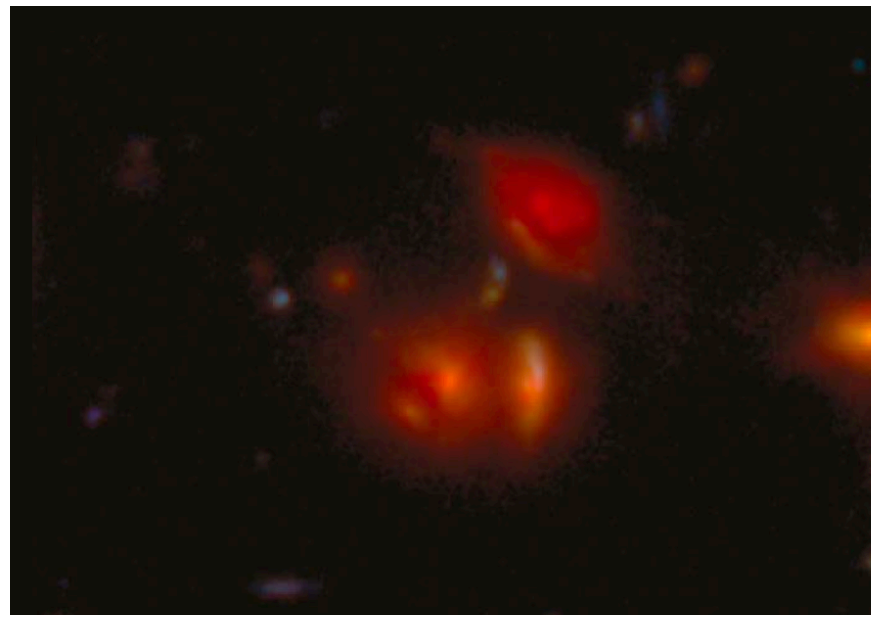

”The cosmic rose” (0.1 Gyr)

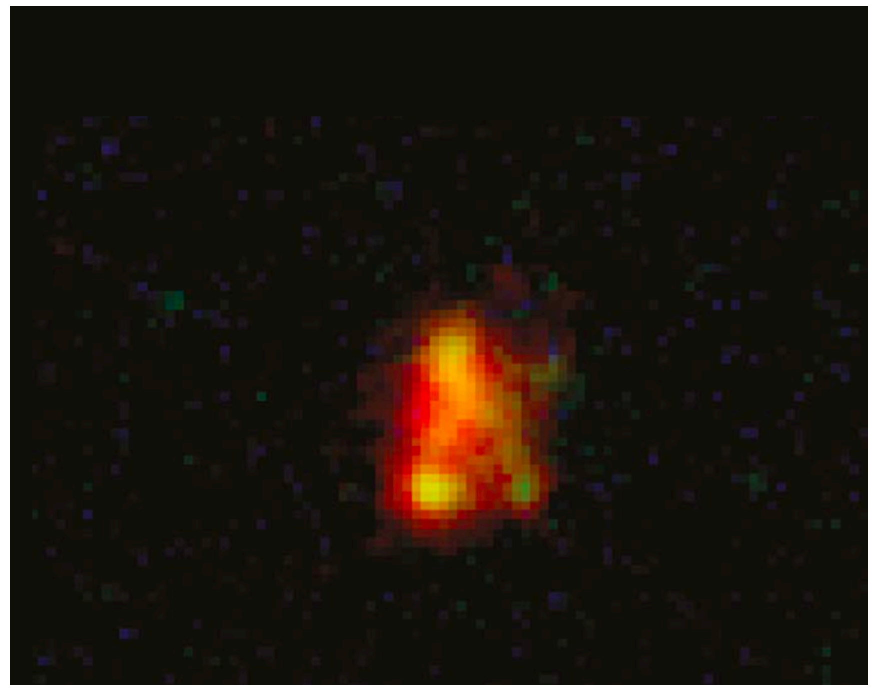

“The big clumpy” (0.3 Gyr)

Open questions

- How many mergers in the history of the Milky Way?
- How large were they?
- When did the mergers take place?
- How the mergers have affected the Milky Way?

Galactic components

Satellites

Halo streams

Stellar halo
(in situ, accreted satellites,
heated disc stars)

Thin/thick disc

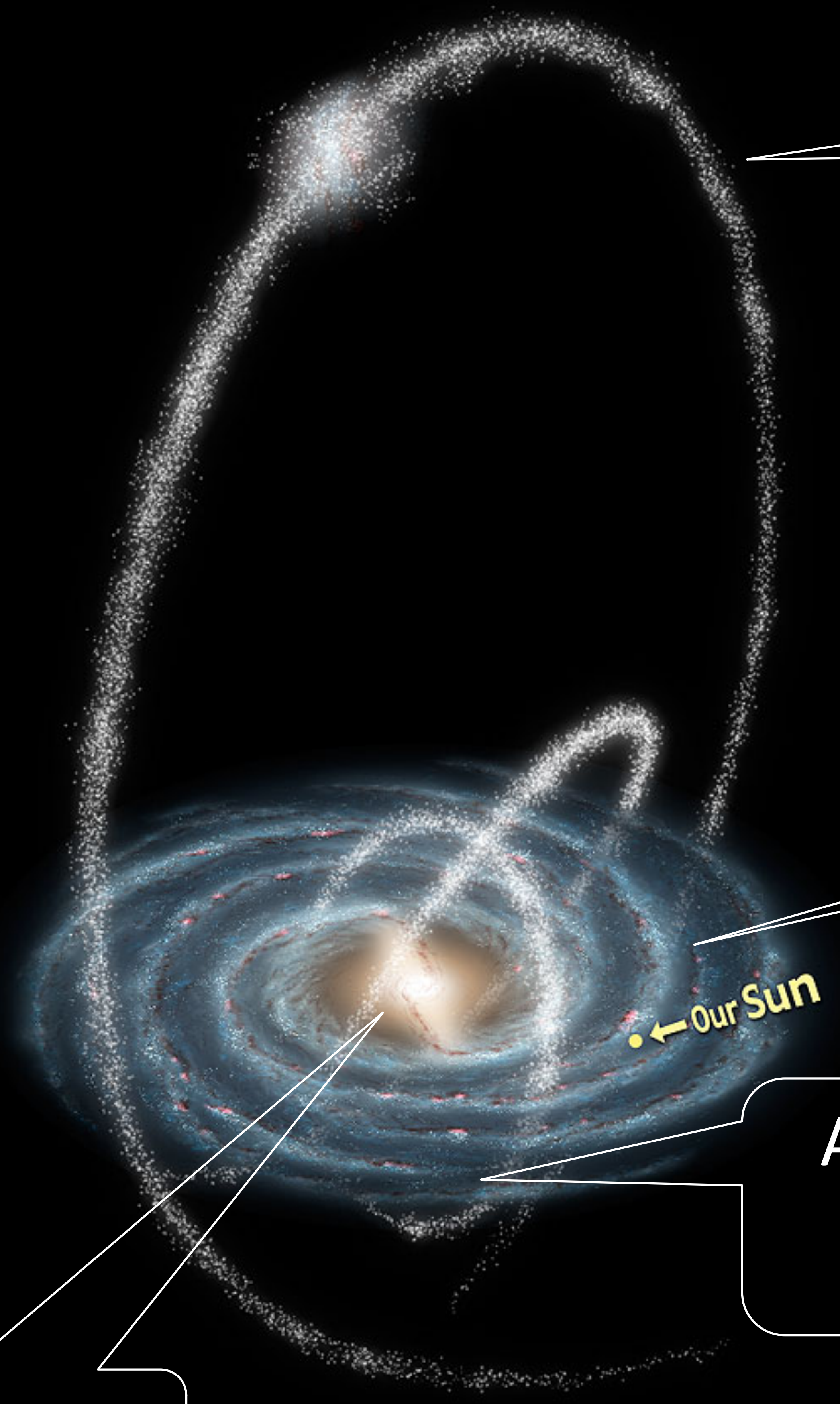

Accreted/unevolved
disc star

Bulge

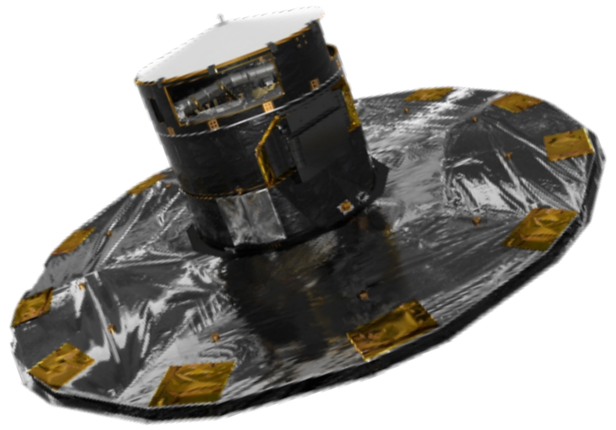

Major merger: *Gaia – Sausage – Enceladus (GSE)*

Amina Helmi et al. 2018, *"The merger that led to the formation of the Milky Way's inner stellar halo and thick disk",* Nature, 563, 85

Abstract. … We demonstrate that the inner halo is dominated by debris from an object which at infall was slightly more massive than the Small Magellanic Cloud ….

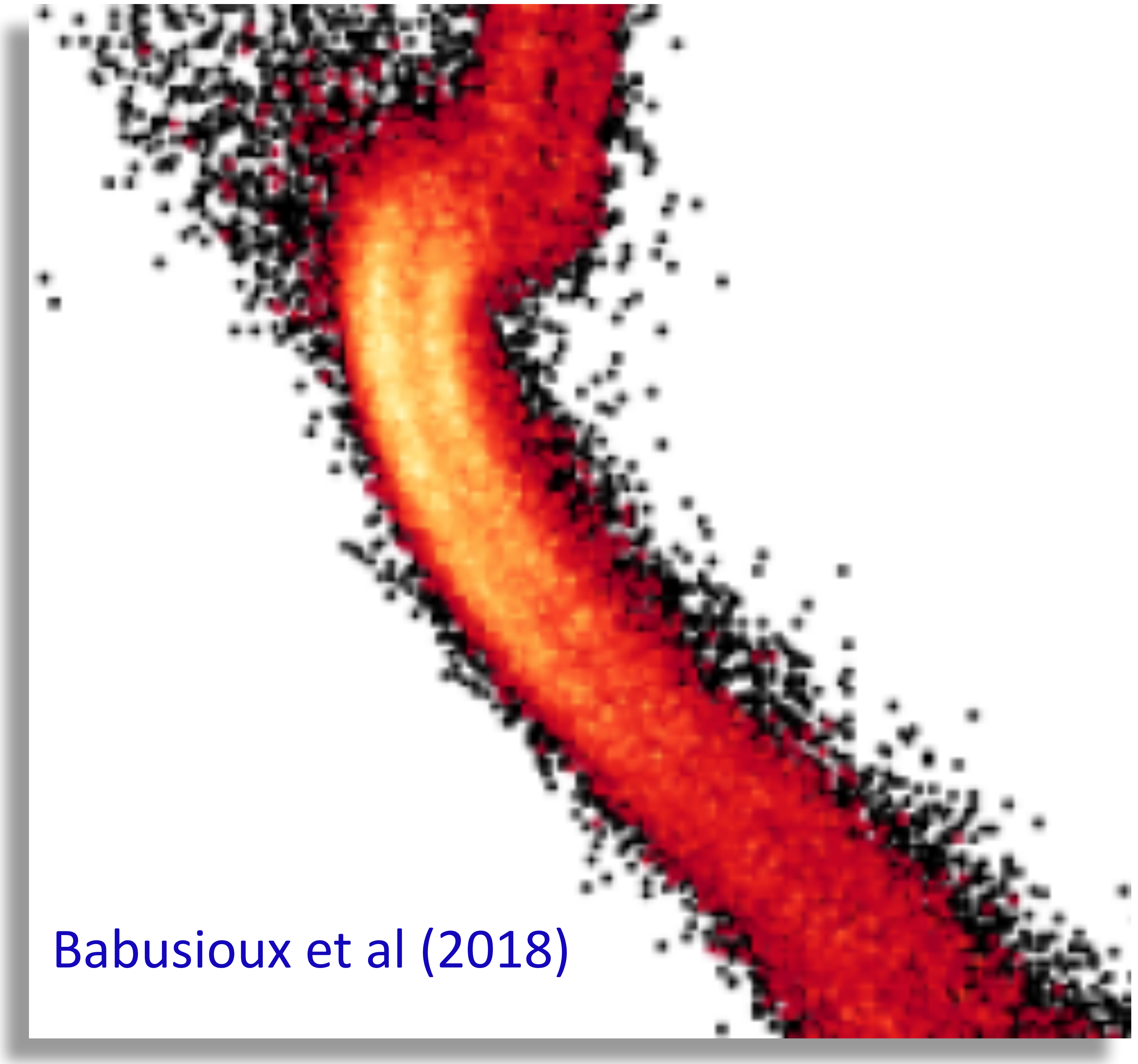

Babusioux et al (2018)

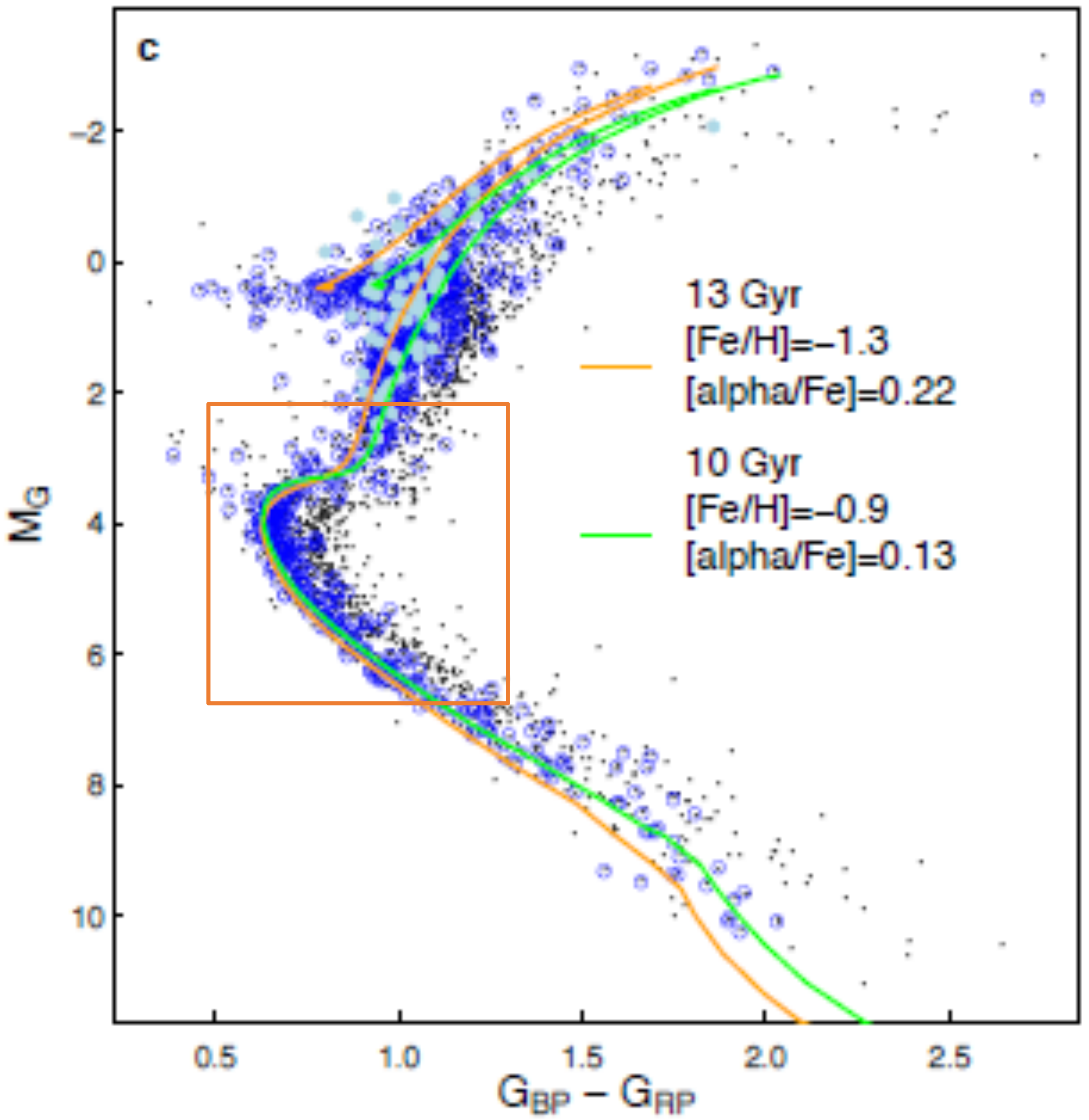

Galactic halo formation - tidal contributions

Sagittarius dwarf galaxy interaction with the MW

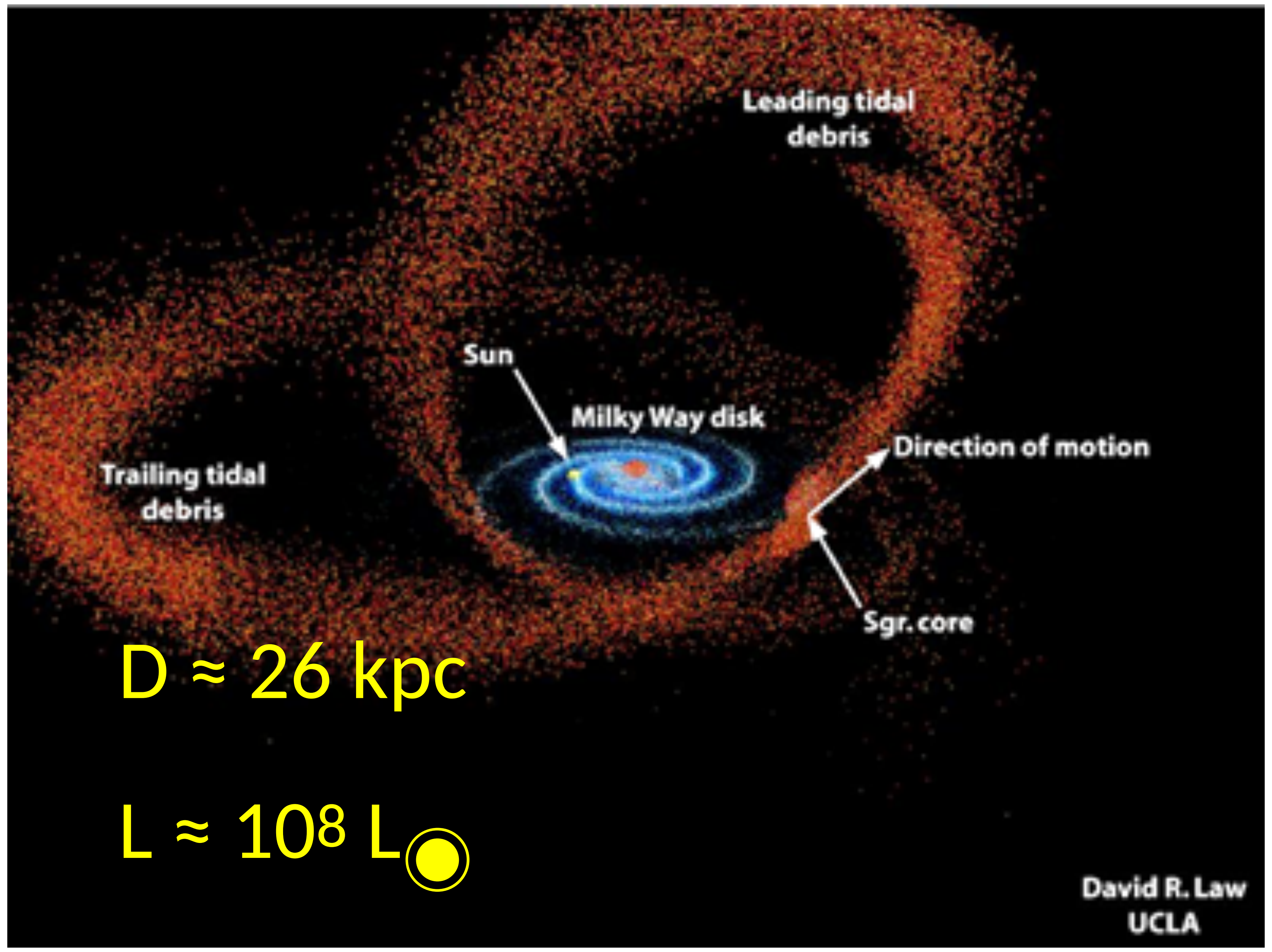

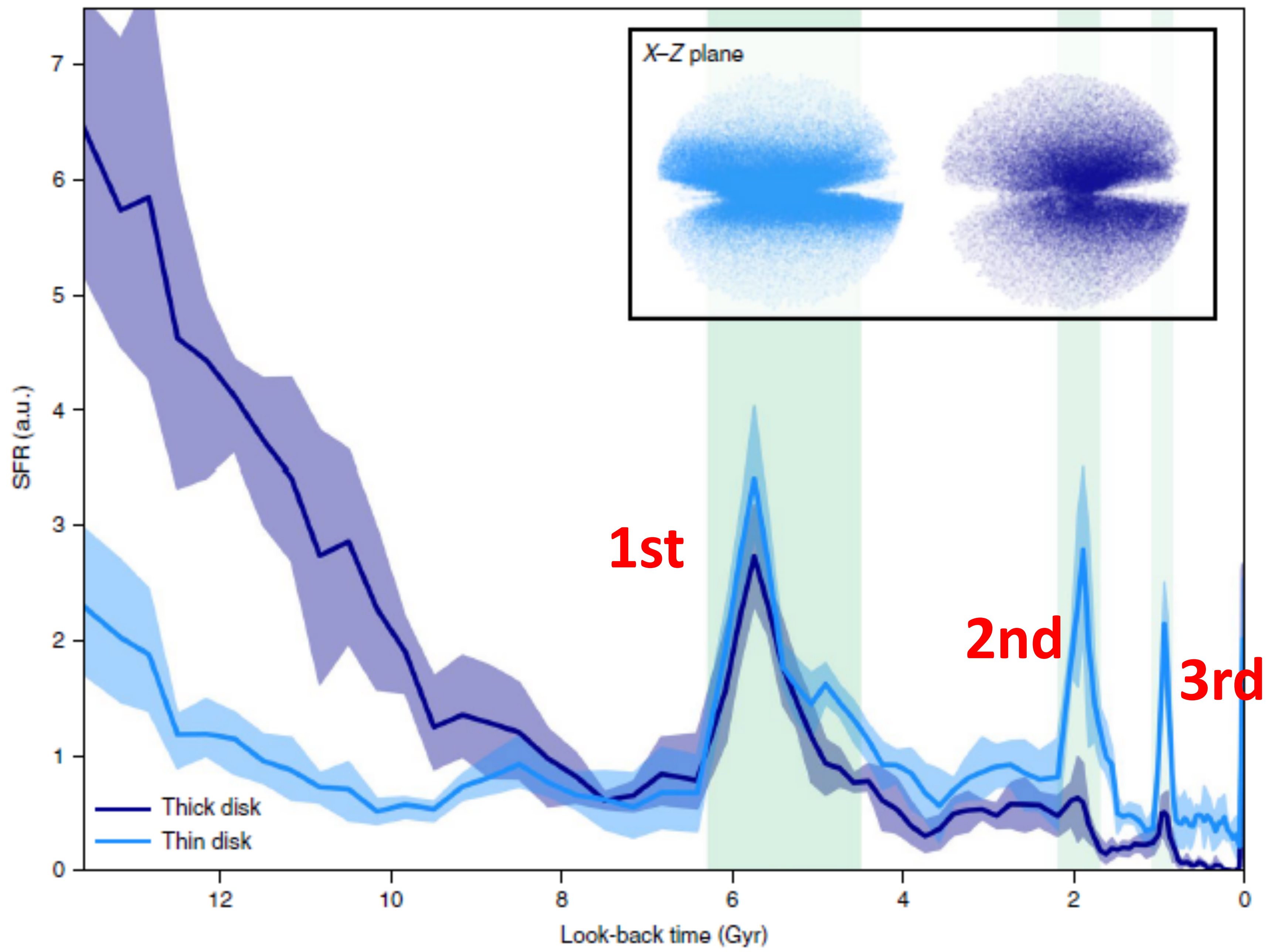

Star Formation History in the ~2-kpc-radius bubble around the Sun distinguishing between the thin and thick disks (selected on the basis of tangential velocity).
Green-shaded areas highlight the location of the detected star-forming bursts.
Three conspicuous and narrow episodes of enhanced star formation that we can precisely date as having occurred 5.7, 1.9 and 1.0 Gyr ago, which coincide with proposed pericentre passages of the Sagittarius dwarf galaxy.

Ruiz Lara et al 2020

Galactic halo formation - substructures

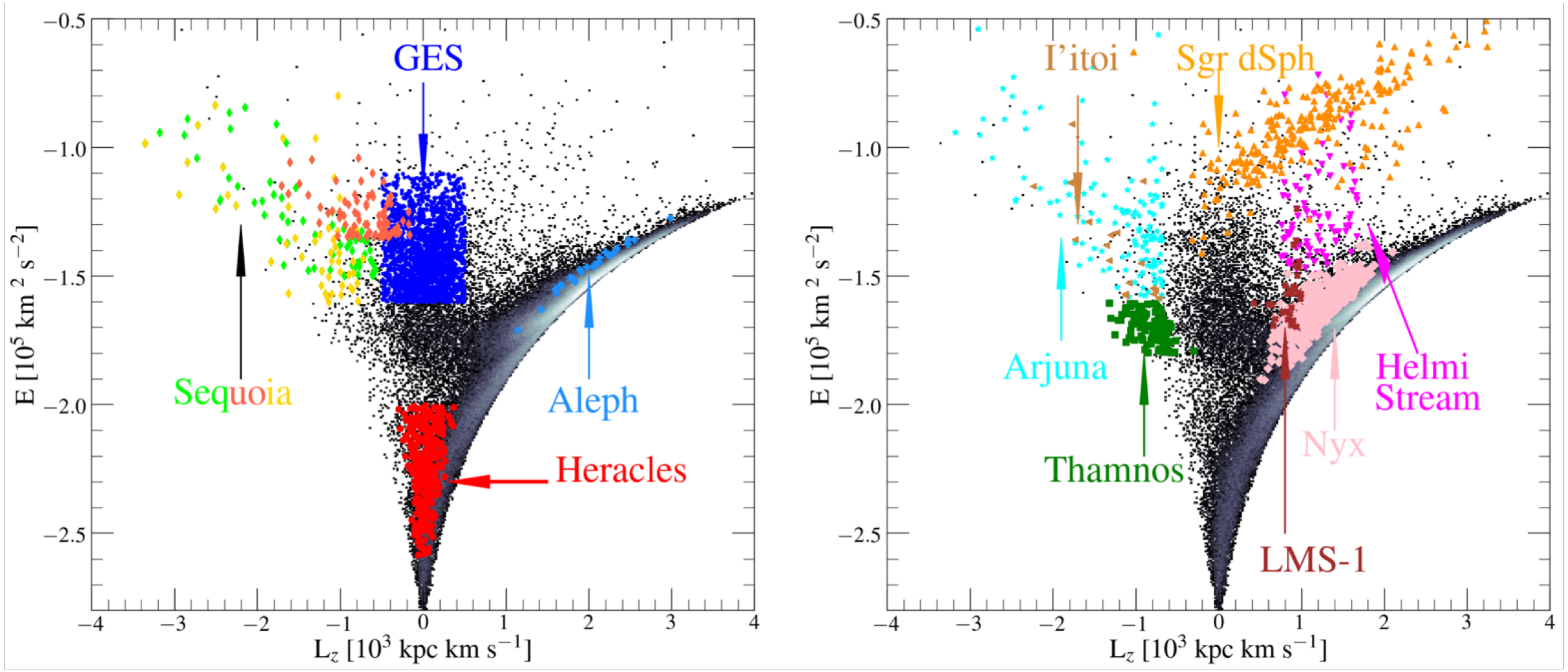

Halo substructures in the orbital energy vs. angular momentum w.r.t. the Galactic disc plane, among the MW sample from Gaia-APOGEE (white/black are high/low density regions). The coloured markers illustrate different halo structures.

(e.g. Ibata+1994; Helmi+1999, 2018; Belokurov+2018; Myeong+2019; Koppelman+2019; Necib+2020; Naidu+2020; Horta+2021,2022)

Galactic disc - Icarus: accreted/unevolved stars

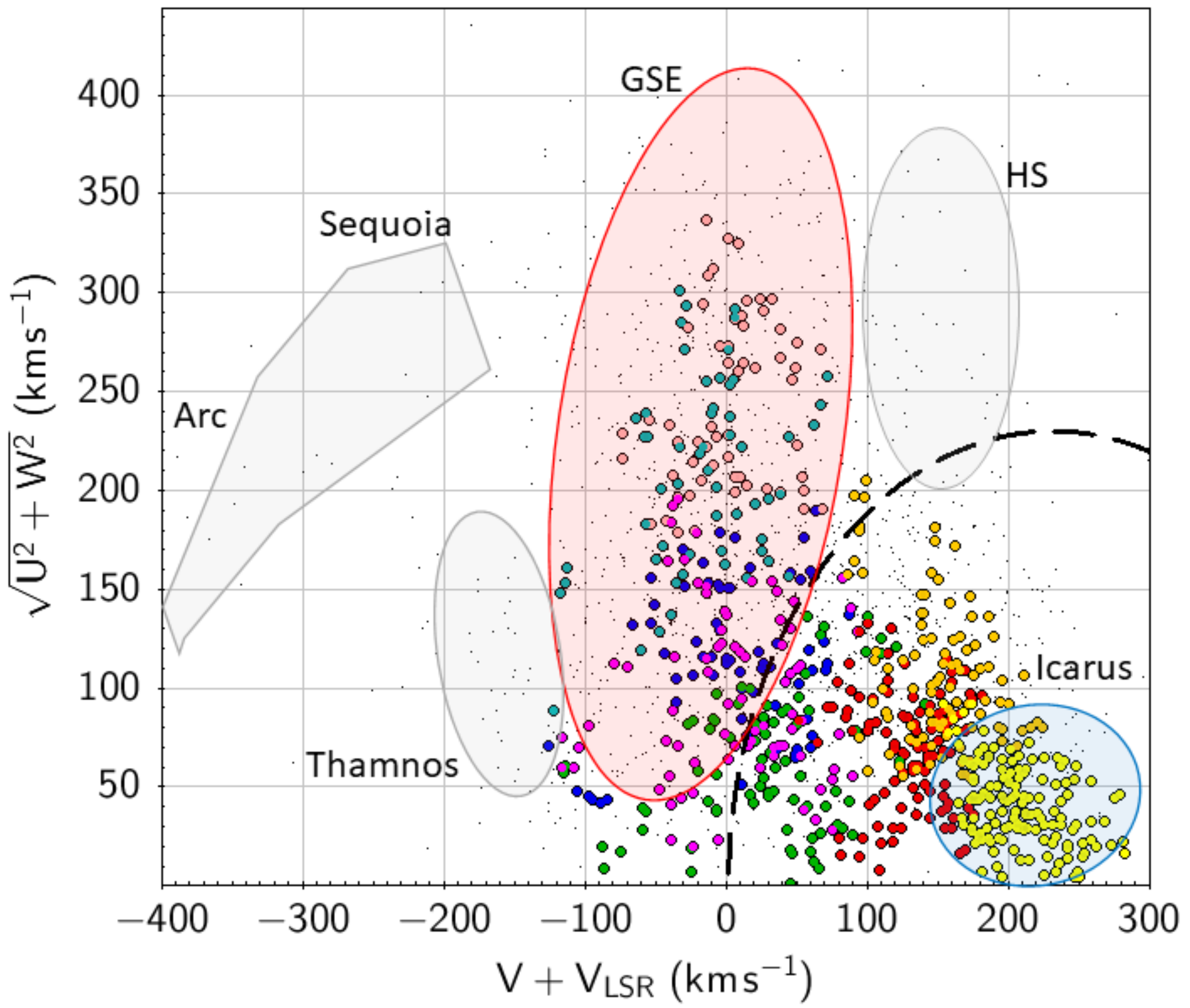

Toomre diagram.
The traditional kinematic selection for halo stars, $|\mathbf{v} - \mathbf{v}_{LSR}| > 230$ km/s, represented by the dashed line.

Re Fiorentin et al (2021, 2024 in preparation)

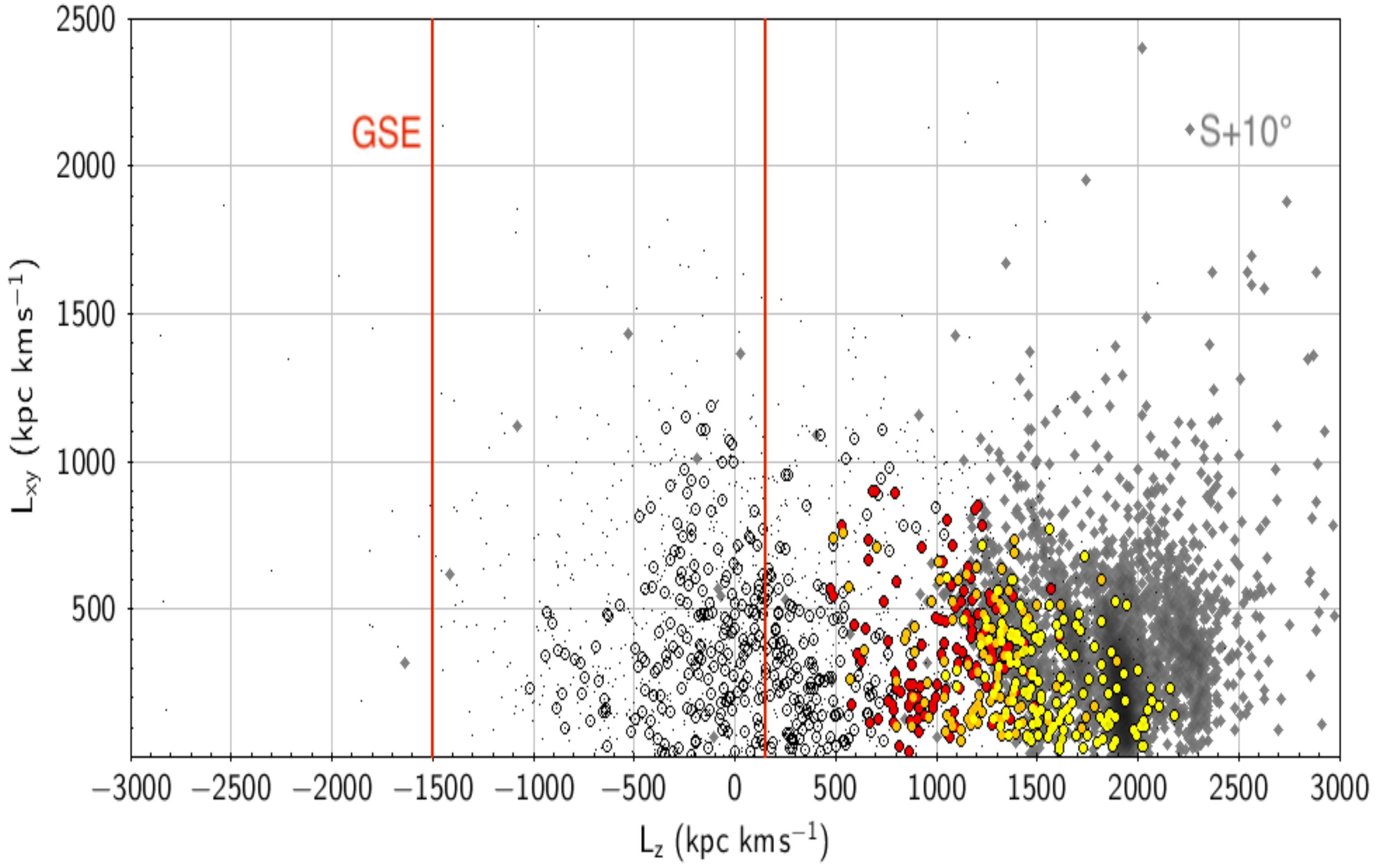

L_{XY} vs. L_Z distribution of Icarus stars (yellow and red dots)

The red solid lines indicate the GSE locus (Helmi+2018). The debris of the simulated 10°-inclination prograde satellite with a stellar mass of **~$10^9 M_{Sun}$** analysed in Re Fiorentin+2015 are overplotted for comparison (grey diamonds).

Galactic disc: rotation curves

Flat rotation curves in disk galaxies - a longest outstanding problem in astronomy - provide the main observational support to the **hypothesis of surrounding dark matter.** Adding a “dark matter” halo **allows a good fit to data**

Rotation curves are distinctive features of spiral galaxies like our Milky Way, a sort of a kinematical/dynamical signature, like the HR diagram for the astrophysical content

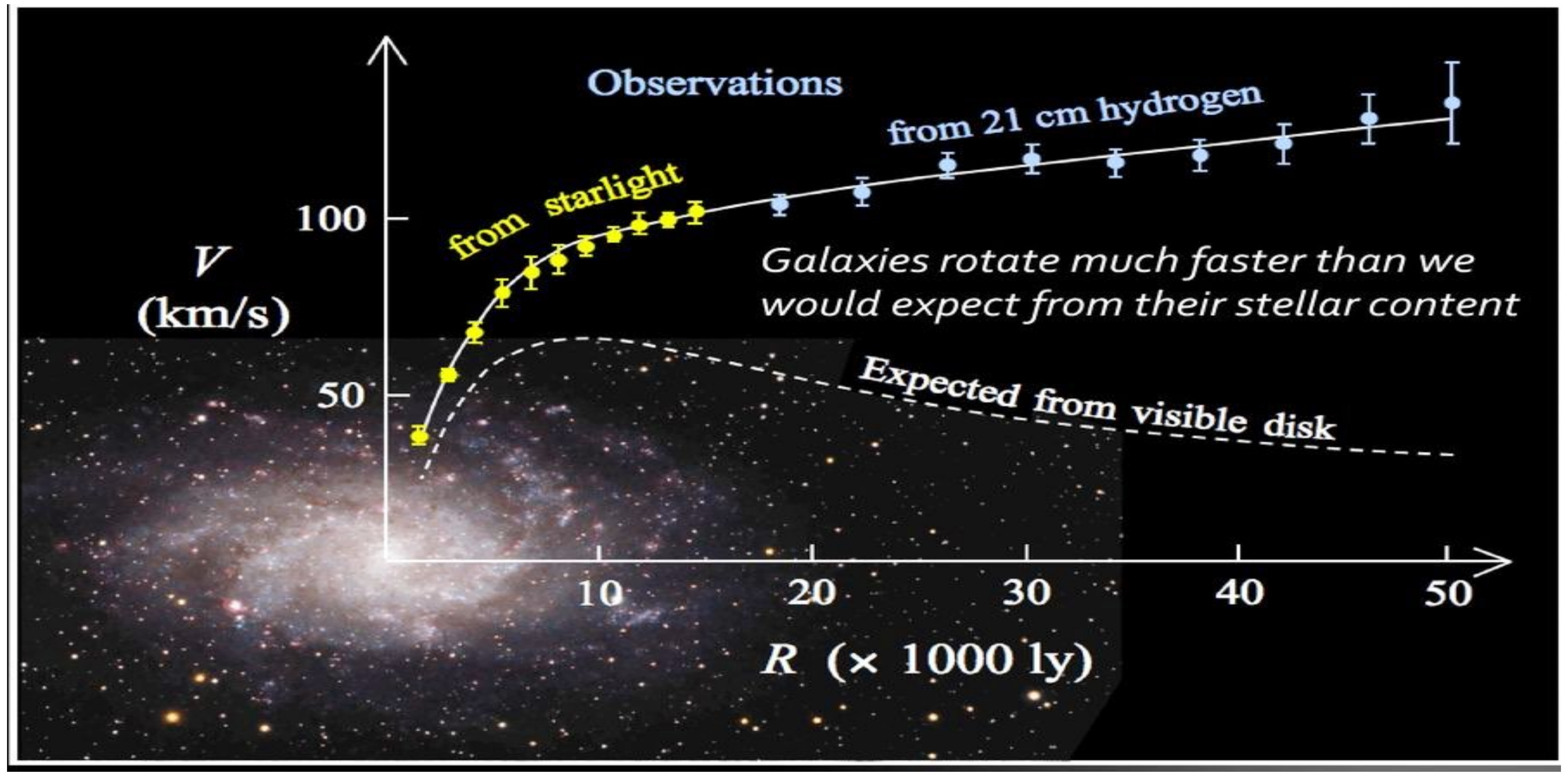

Stellar kinematics, as tracer of gravitational potential, is the most reliable observable for gauging different matter components

By routinely scanning individual sources throughout the whole sky, Gaia directly measures the (relativistic) kinematics of the stellar component

-> the rotation curve of the MW used as a first test for a GR Galaxy

weak field regime @Milky Way scale

In general one assumes that:
gravitational potential or "relativistic effects" at the MW scale are usually "small", then

✓negligible..

- ✓locally Newton approximation is retained valid at each point..

weak field regime @Milky Way scale

In general one assumes that:
gravitational potential or “relativistic effects” at the MW scale are usually “small”, then

✓negligible..

✓locally Newton approximation is retained valid at each point..

but $(v_{Gal}/c)^2 \sim 0{,}69 \times 10^{-6}$ (rad) ~100 mas

$(v_{Gal}/c)^3 \sim 0{,}57 \times 10^{-9}$ (rad) ~ $120\mu as$

the individual astrometric error is $\leq 100\mu as$
throughout most of its magnitude range

weak field regime @Milky Way scale

In general one assumes that:
gravitational potential or "relativistic effects" at the MW scale are usually "small", then

✓negligible..

✓locally Newton approximation is retained valid at each point..

but $(v_{Gal}/c)^2 \sim 0{,}69 \times 10^{-6}$ (rad) ~100 mas

$(v_{Gal}/c)^3 \sim 0{,}57 \times 10^{-9}$ (rad) ~ $120\mu as$

the individual astrometric error is $\leq 100\mu as$
throughout most of its magnitude range

For the Gaia-like observer the weak gravitational regime turns out to be "strong" when one has to perform high accurate measurements

ε ~ v^2/c^2 ~ GM/rc^2 ~ mas accuracy

which requires determination of

g_{oo} even terms in ε, lowest order ε^2~mas

g_{oj} odd terms in ε, lowest order ε^3~μ-as

g_{ij} even terms in ε, lowest order ε^2~mas

weak field regime @Milky Way scale

In general one assumes that:
gravitational potential or “relativistic effects” at the MW scale are usually “small”, then

✓negligible..
✓locally Newton approximation is retained valid at each point..

but $(v_{Gal}/c)^2 \sim 0{,}69 \times 10^{-6}$ (rad) ~100 mas
$(v_{Gal}/c)^3 \sim 0{,}57 \times 10^{-9}$ (rad) ~ $120\mu as$

the individual astrometric error is $\leq 100\mu as$
throughout most of its magnitude range

“weakly” relativistic effect could be relevant?

For the Gaia-like observer the weak gravitational regime turns out to be "strong" when one has to perform high accurate measurements

ε ~ v^2/c^2 ~ GM/rc^2 ~ mas accuracy
which requires determination of
g_{oo} even terms in ε, lowest order ε^2~mas
g_{oj} odd terms in ε, lowest order ε^3~μ-as
g_{ij} even terms in ε, lowest order ε^2~mas

Lesson from the past

- Neptune (as “dark” planet in the orbit of Uranus….a new “Newtonian” planet!

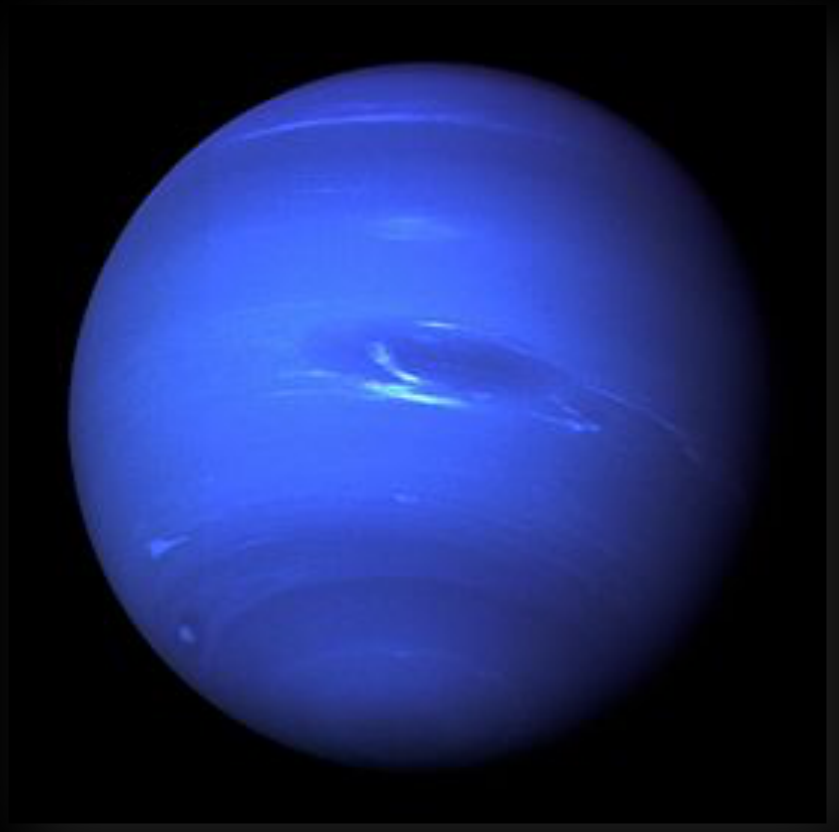

1846 observed by Johann Galle within a degree of the position predicted by Le Verrier

Lesson from the past

- Neptune (as “dark” planet in the orbit of Uranus….a new “Newtonian” planet!

  1846 observed by Johann Galle within a degree of the position predicted by Le Verrier

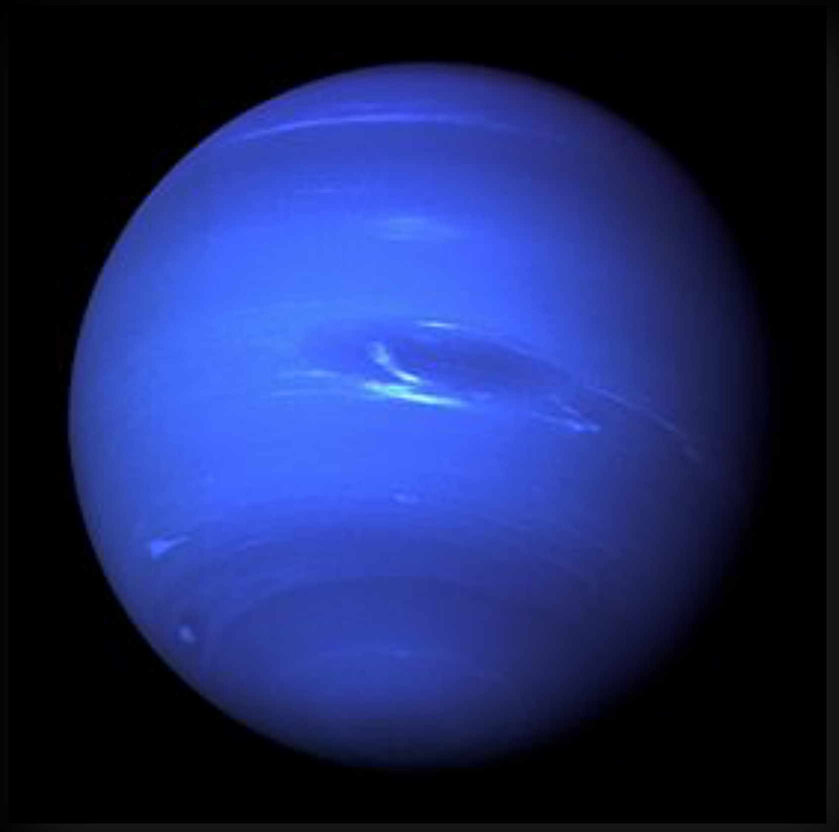

- advancement of Mercury’s perihelion: instead of correcting the dynamics by adding a "dark planet" (Vulcano) following the case of Neptune, GR cured the anomalous precession by accounting for the weak non-linear gravitational fields overlapping nearby the Sun.

  It amounts to only 43"/century, because of the small curvature, however the effect was ”strong” enough to justify a modification of the Newtonian theory

excess of the perihelion shift of Mercury, 43”/100yr

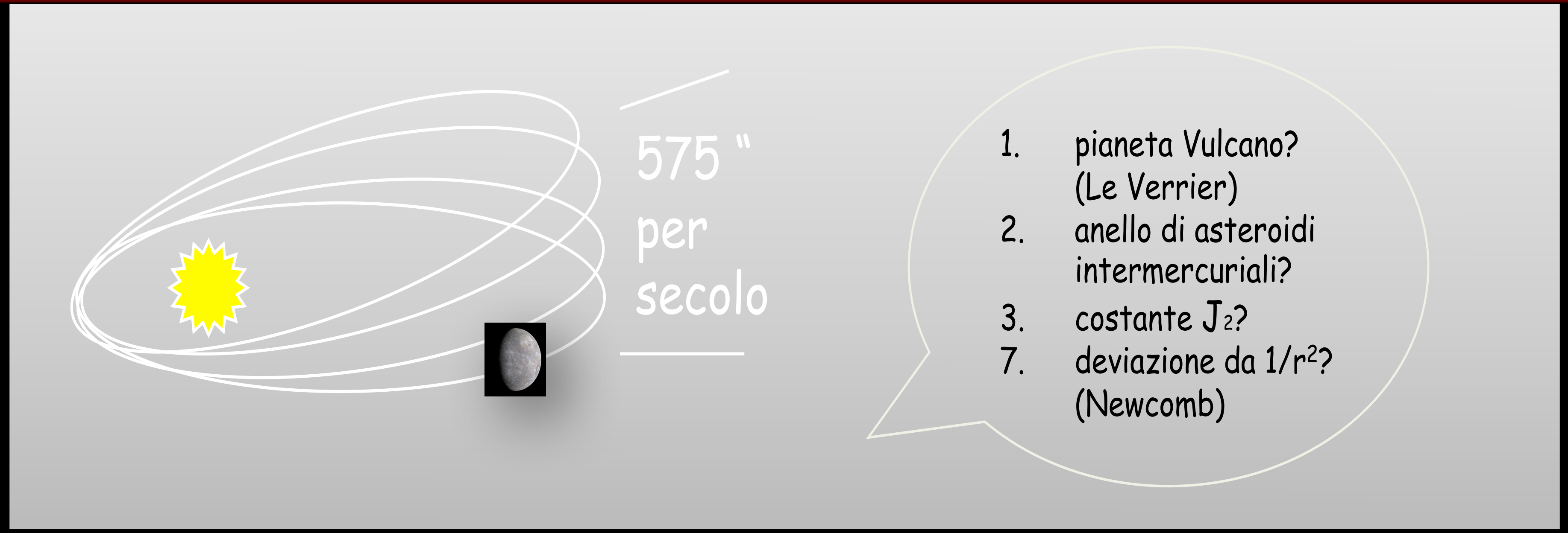

Lesson from the past

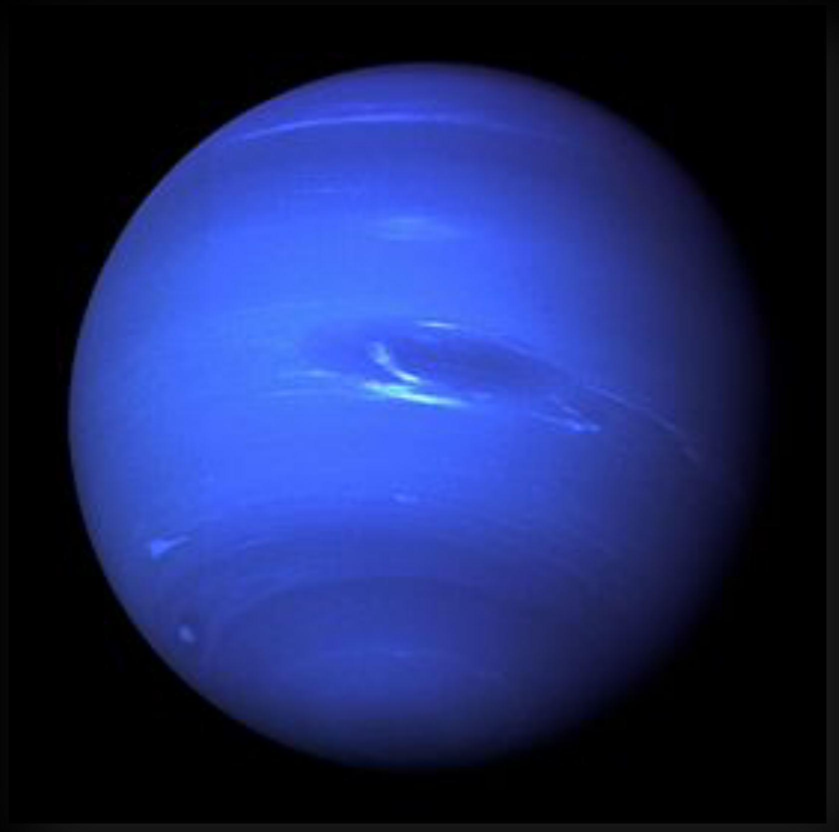

- Neptune (as “dark” planet in the orbit of Uranus….a new “Newtonian” planet!

1846 observed by Johann Galle within a degree of the position predicted by Le Verrier

- advancement of Mercury’s perihelion: instead of correcting the dynamics by adding a "dark planet" (Vulcano) following the case of Neptune, GR cured the anomalous precession by accounting for the weak non-linear gravitational fields overlapping nearby the Sun.

It amounts to only 43"/century, because of the small curvature, however the effect was ”strong” enough to justify a modification of the Newtonian theory

excess of the perihelion shift of Mercury, 43”/100yr

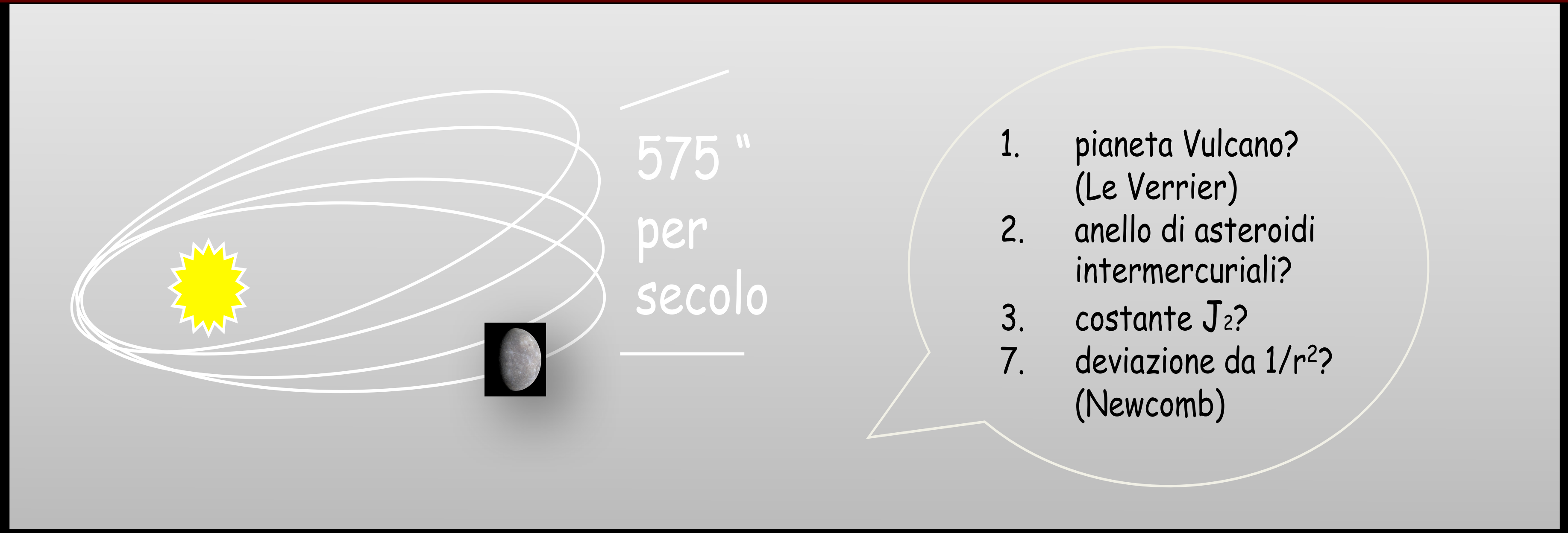

Lense-Thirring effect, the distortion of space-time due to rotating masses: new (weak) relativistic effect!

Lensing-Thirring effect

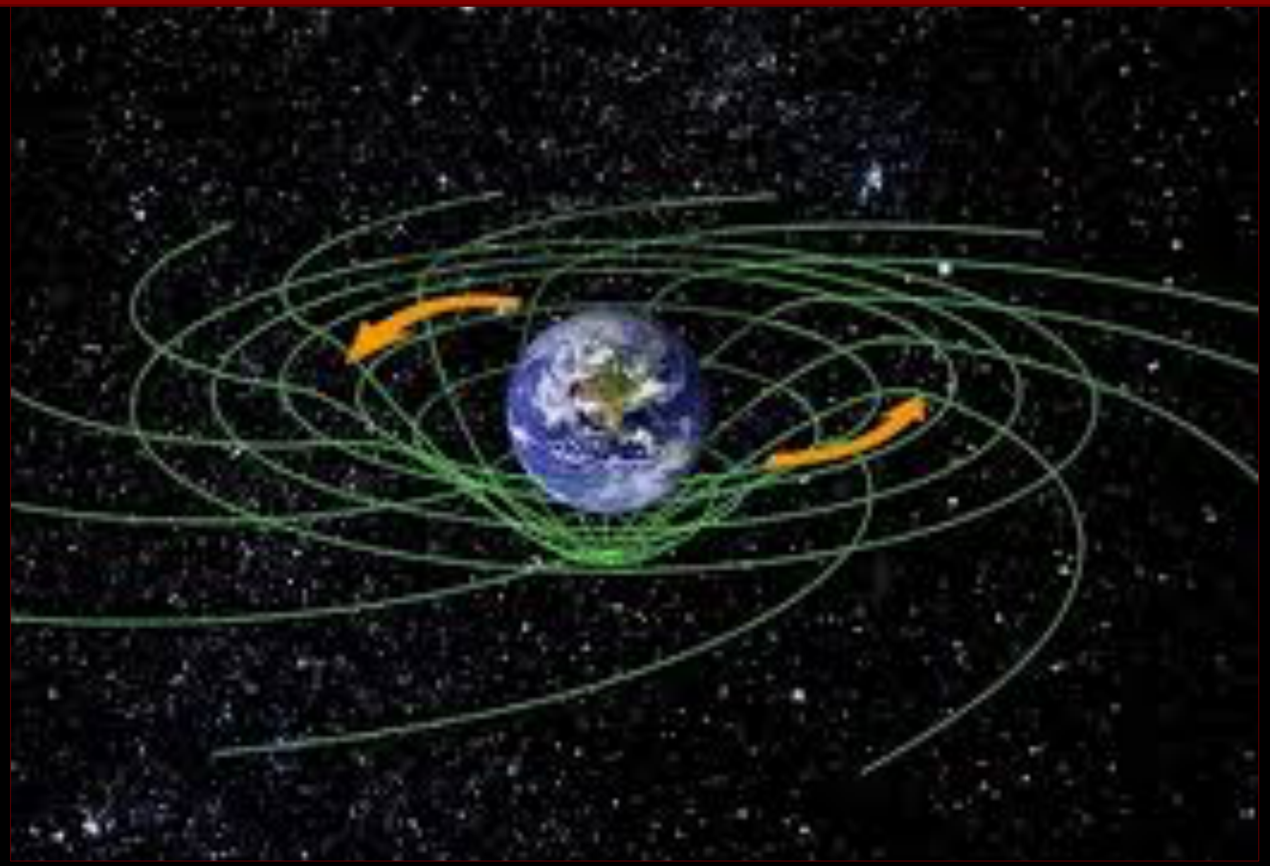

Lesson from the past

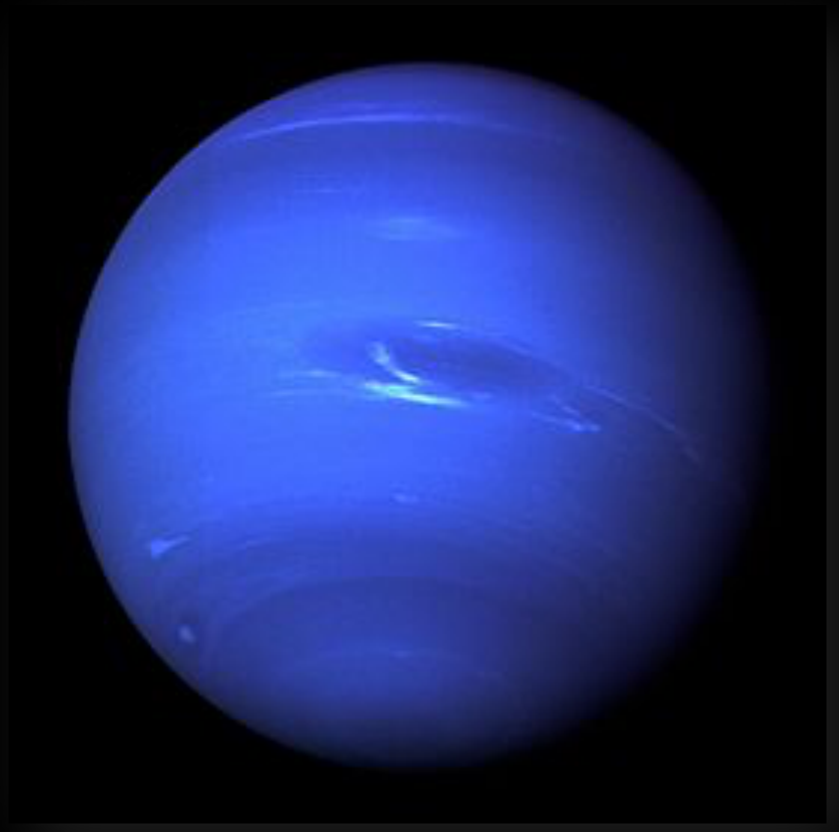

- Neptune (as "dark" planet in the orbit of Uranus….a new "Newtonian" planet!

1846 observed by Johann Galle within a degree of the position predicted by Le Verrier

- advancement of Mercury's perihelion: instead of correcting the dynamics by adding a "dark planet" (Vulcano) following the case of Neptune, GR cured the anomalous precession by accounting for the weak non-linear gravitational fields overlapping nearby the Sun.

It amounts to only 43"/century, because of the small curvature, however the effect was "strong" enough to justify a modification of the Newtonian theory

excess of the perihelion shift of Mercury, 43"/100yr

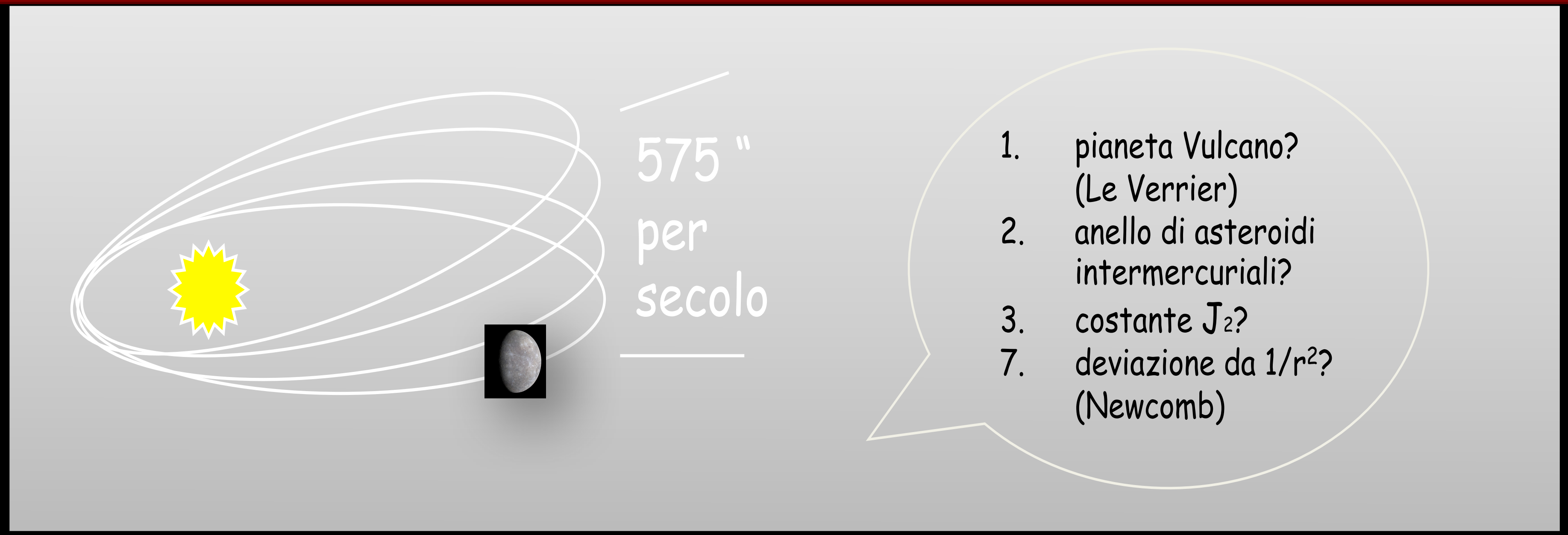

Lense-Thirring effect, the distortion of space-time due to rotating masses: new (weak) relativistic effect!

Lensing-Thirring effect

The small curvature limit in General Relativity may not coincide with the Newtonian regime

Lesson from the past

- Neptune (as "dark" planet in the orbit of Uranus….a new "Newtonian" planet!

1846 observed by Johann Galle within a degree of the position predicted by Le Verrier

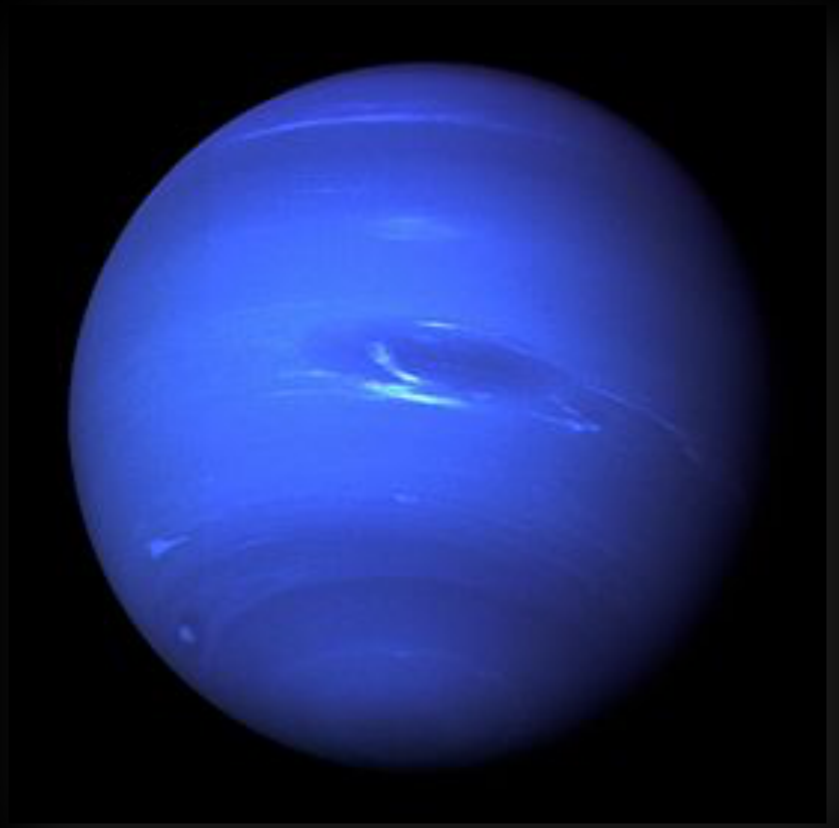

- advancement of Mercury's perihelion: instead of correcting the dynamics by adding a "dark planet" (Vulcano) following the case of Neptune, GR cured the anomalous precession by accounting for the weak non-linear gravitational fields overlapping nearby the Sun.

It amounts to only 43"/century, because of the small curvature, however the effect was "strong" enough to justify a modification of the Newtonian theory

excess of the perihelion shift of Mercury, 43"/100yr

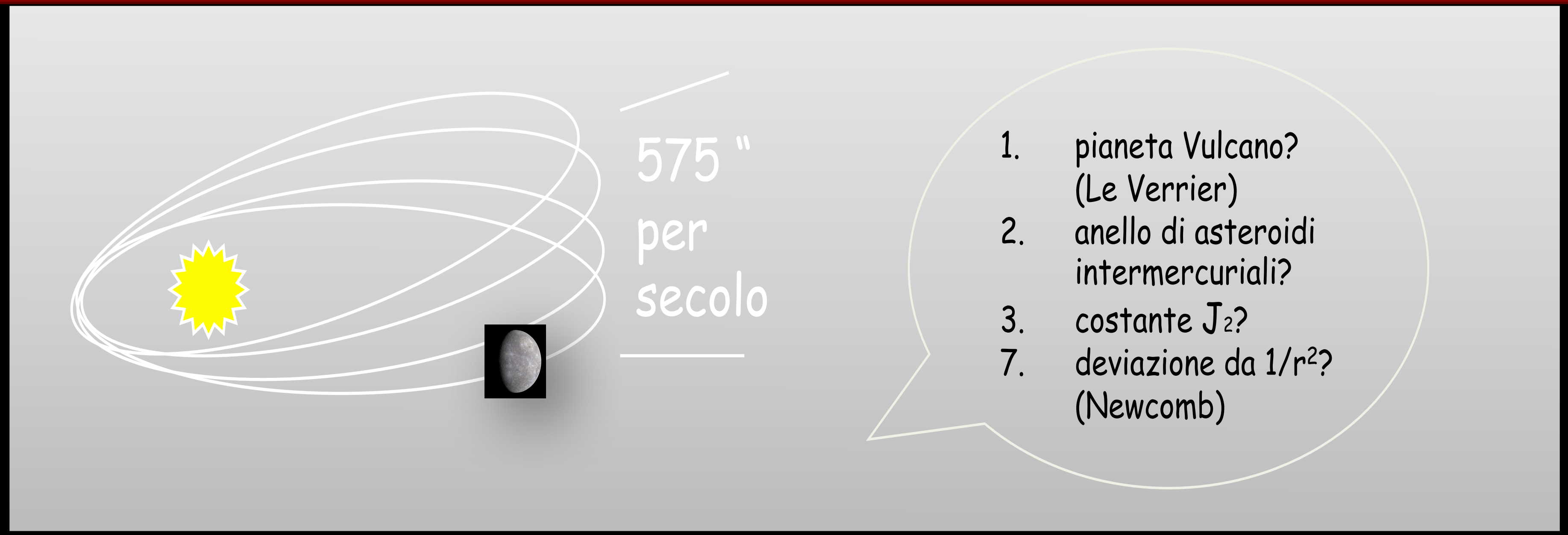

Lensing-Thirring effect

Lense-Thirring effect, the distortion of space-time due to rotating masses: new (weak) relativistic effect!

The small curvature limit in General Relativity may not coincide with the Newtonian regime

need to compare the GR model and the classical one

"Classic" Milky Way (MWC) model with NFW dark matter halo

- Newtonian limit applied for Galactic dynamics -> Poisson's equation

$$\nabla^2\Phi = 4\pi G(\rho_b + \rho_d + \rho_h)$$

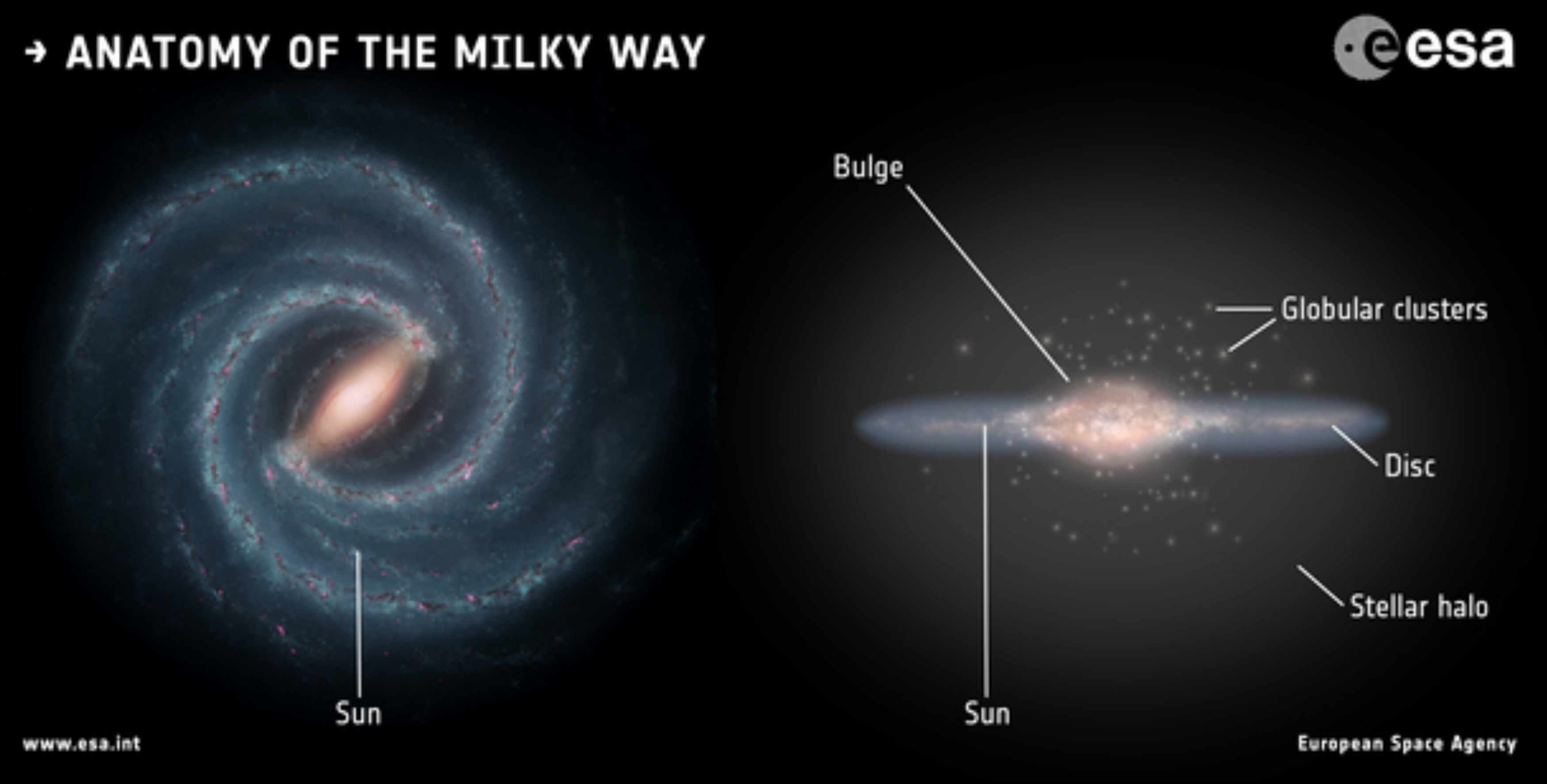

"Classic" Milky Way (MWC) model with NFW dark matter halo

- Newtonian limit applied for Galactic dynamics -> Poisson's equation

$$\nabla^2 \Phi = 4\pi G(\rho_b + \rho_d + \rho_h)$$

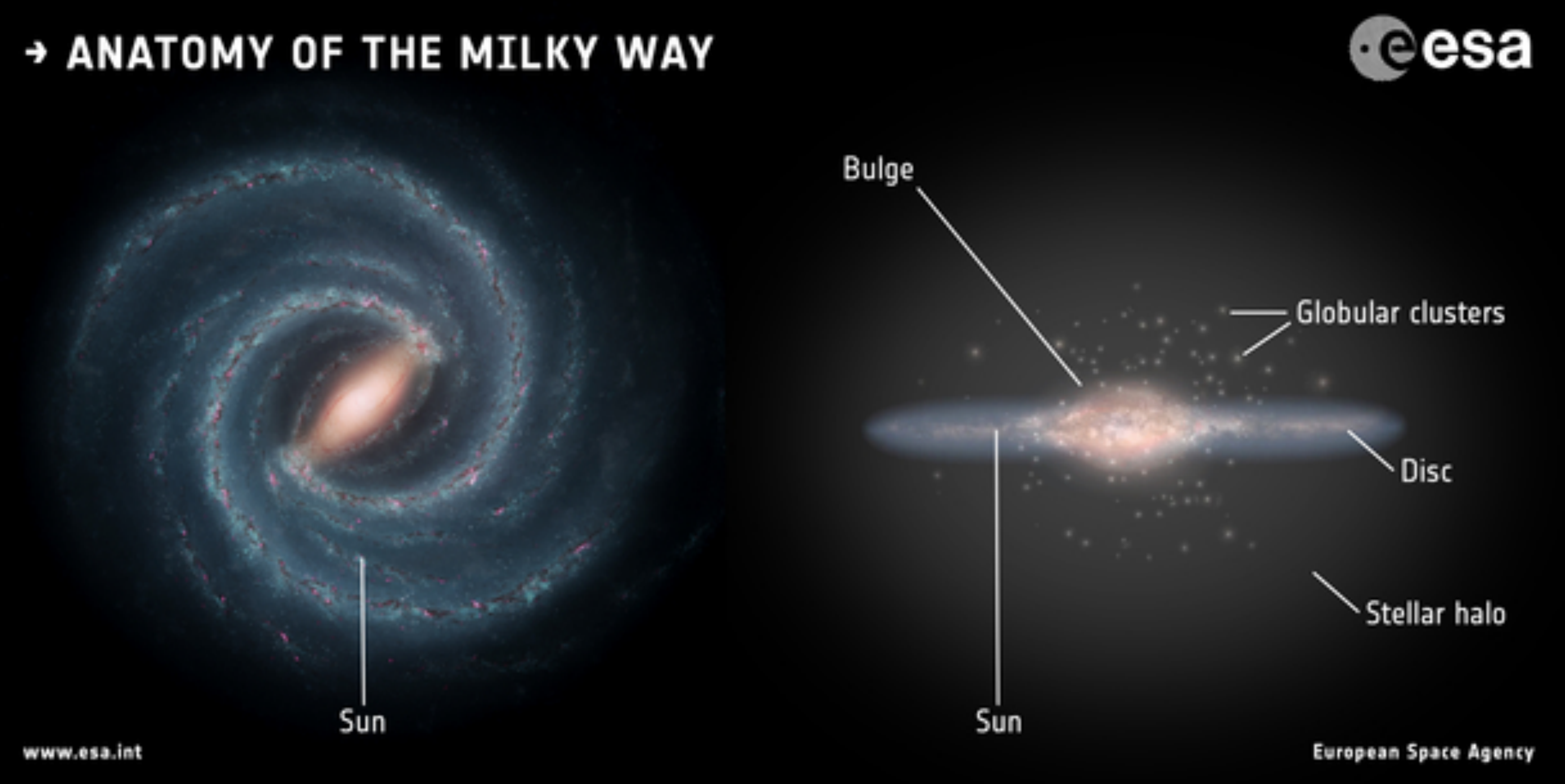

1. Plummer **bulge**

$$\rho_b = \frac{3b_b^2 M_b}{4\pi(r^2 + b_b^2)^{5/2}}$$

Pouliasis, E., Di Matteo, P.

Haywood, M. 2017, A&A, 598, A66

2. Miyamoto-Nagai **thin and thick discs**

$$\rho_d(R,z) = \frac{M_d b_d^2}{4\pi} \frac{\left[a_d R^2 + (a_d + 3\sqrt{z^2+b_d^2})(a_d + \sqrt{z^2+b_d^2})^2\right]}{\left[R^2 + (a_d + \sqrt{z^2+b_d^2})^2\right]^{5/2} (z^2+b_d^2)^{3/2}}$$

Bovy, J. 2015, ApJs, 216, 29

Korol, Rossi & Barausse (2019)

3. Navarro-Frank-White DM halo

$$\rho_h(r) = \rho_0^{halo} \frac{1}{(r/A_h)(1 + r/A_h)^2}$$

McMillan, P. J. 2017, MNRAS, 465, 76-94

Navarro, J. F., Frenk, C. S. and White, S. D. M. 1996, ApJ, 462, 563

M_b, M_{td}, M_{Td}, a_{td}, a_{Td} , b_b, bd, ρ_0^{halo} and **A_h** correspond to the bulge mass, the masses and the scale lengths/heights of the thin and thick discs, the halo scale density, and the halo radial scale

"Classic" Milky Way (MWC) model with NFW dark matter halo

- Newtonian limit applied for Galactic dynamics -> Poisson's equation

$$\nabla^2\Phi = 4\pi G(\rho_b + \rho_d + \rho_h)$$

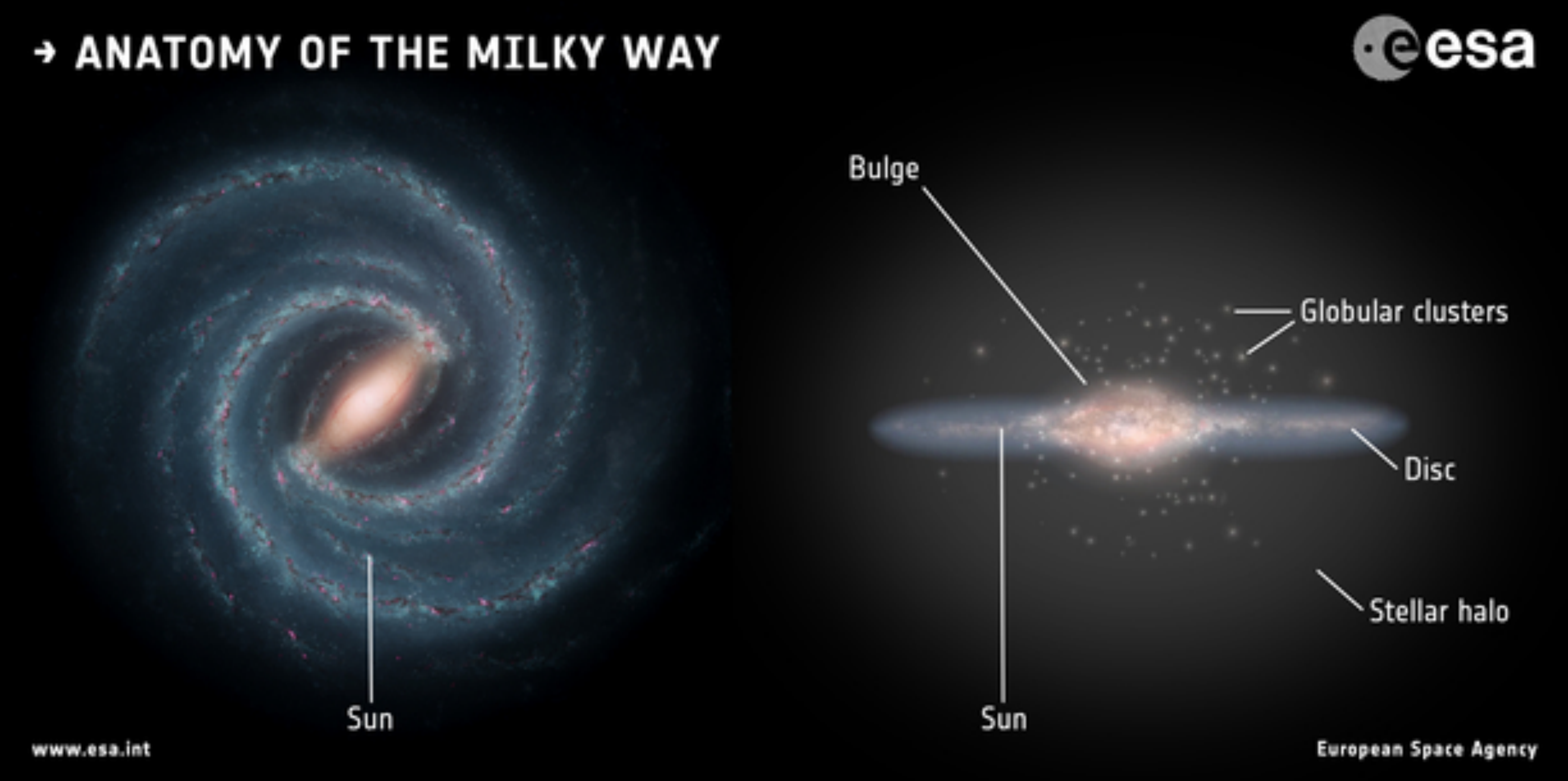

1. Plummer **bulge**

$$\rho_b = \frac{3b_b^2 M_b}{4\pi(r^2 + b_b^2)^{5/2}}$$

Pouliasis, E., Di Matteo, P.

Haywood, M. 2017, A&A, 598, A66

2. Miyamoto-Nagai **thin and thick discs**

$$\rho_d(R,z) = \frac{M_d b_d^2}{4\pi} \frac{\left[a_d R^2 + (a_d + 3\sqrt{z^2+b_d^2})(a_d + \sqrt{z^2+b_d^2})^2\right]}{\left[R^2 + (a_d + \sqrt{z^2+b_d^2})^2\right]^{5/2}(z^2+b_d^2)^{3/2}}$$

Bovy, J. 2015, ApJs, 216, 29

Korol, Rossi & Barausse (2019)

3. Navarro-Frank-White DM halo

$$\rho_h(r) = \rho_0^{halo} \frac{1}{(r/A_h)(1 + r/A_h)^2}$$

McMillan, P. J. 2017, MNRAS, 465, 76-94

Navarro, J. F., Frenk, C. S. and White, S. D. M. 1996, ApJ, 462, 563

M_b, M_{td}, M_{Td}, a_{td}, a_{Td} , b_b, bd, ρ_0^{halo} and **A_h** correspond to the bulge mass, the masses and the scale lengths/heights of the thin and thick discs, the halo scale density, and the halo radial scale

$$\nabla^2\Phi_{tot} = 4\pi G(\rho_b + \rho_{td} + \rho_{Td} + \rho_h)$$ ➡ $$V_c^2 = R\left(d\Phi_{tot}/dR\right)$$

MWC velocity profile

MOND

EINASTO DENSITY PROFILE

Same baryonic distribution of MWC

$$\mathbf{g}_{MOND} = \eta\left(\frac{g_N}{g_0}\right)\mathbf{g}_0$$

gravitational acceleration, g_N conventional Newtonian acceleration, baryonic matter alone

$$\eta\left(\frac{g_N}{g_0}\right) = (1 - e^{-\sqrt{g_N/g_0}})^{-1}$$

interpolation function setting the transition between the Newtonian and the deep MOND regimes through the acceleration scale g_0

$$\mathbf{g_0} = (\mathbf{1.20 \pm 0.02})\mathbf{10^{-10}}\mathrm{ms}^{-2}$$

acceleration scale, constrained to extremely tight values by the observed Radial Acceleration Relation of external galaxies (Lelli et al. 2017)

gravitational acceleration g_{MOND} = centripetal acceleration

$$V_{MOND}(R, V_{bar}) = \frac{V_{bar}}{\sqrt{1 - e^{-V_{bar}/\sqrt{Rg_0}}}}$$

$$\rho_{\mathrm{Einasto}}(r) = \rho_\mathrm{s}\ \exp\left\{-\frac{2}{\alpha}\left[\left(\frac{r}{r_\mathrm{s}}\right)^\alpha - 1\right]\right\}$$

Cold dark matter distribution

parameters of the Einasto profile

$C_{200} \equiv r_{200}/r_s$. halo concentration Li et al. (2019)

virial radius r_{200}: the enclosed average density is 200 times the critical density of the Universe (Planck Collaboration et al. 2014; Dutton & Maccio` 2014)

$$V_{200} = 10 C_{200} r_s H_0$$

rotation velocity

$$M_{200} = \frac{V_{200}^3}{10 G^2 H_0^2}$$

enclosed halo mass at the virial radius

GR model for the Milky Way

Einstein equation are very difficult to solve analytically and Galaxy is a multi-structured object making it even the more difficult to detail a metric for the whole Galaxy

GR model for the Milky Way

Einstein equation are very difficult to solve analytically and Galaxy is a multi-structured object making it even the more difficult to detail a metric for the whole Galaxy

Galactic metric-disc

Stationarity and axisymmetry spacetime

$$ds^2 = -e^{2U}(dt + Ad\phi)^2 + e^{-2U}\left(e^{2\gamma}(dr^2 + dz^2) + Wd\phi^2\right)$$

Lewis-Papapetrou class

Reflection symmetry (around the galactic plane)

Disc is an equilibrium configuration of a pressure-less rotating perfect fluid (a GR dust)

Masses inside a large portion of the Galaxy interact only gravitationally and reside far from the central bulge region

GR model for the Milky Way

Einstein equation are very difficult to solve analytically and Galaxy is a multi-structured object making it even the more difficult to detail a metric for the whole Galaxy

Galactic metric-disc

Stationarity and axisymmetry spacetime

$$ds^2 = -e^{2U}(dt + Ad\phi)^2 + e^{-2U}\left(e^{2\gamma}(dr^2 + dz^2) + Wd\phi^2\right)$$

Lewis-Papapetrou class

Reflection symmetry (around the galactic plane)

Disc is an equilibrium configuration of a pressure-less rotating perfect fluid (a GR dust)

Masses inside a large portion of the Galaxy interact only gravitationally and reside far from the central bulge region

For dust (shear free and expansion free)

$$ds^2 = -(dt - Nd\phi)^2 + r^2 d\phi^2 + e^{\nu}(dr^2 + dz^2)$$

Einstein field Eq.

$$r\partial_z \nu + \partial_r N \partial_z N = 0$$

$$2r\partial_r \nu + (\partial_r N)^2 - (\partial_z N)^2 = 0$$

$$2r^2(\partial_r\partial_r \nu + \partial_z\partial_z \nu) + (\partial_r N)^2 + (\partial_z N)^2 = 0$$

$$r(\partial_r\partial_r N + \partial_z\partial_z N) - \partial_r N = 0$$

$$(\partial_r N)^2 + (\partial_z N)^2 = kr^2\rho e^{\nu}$$

GR model for the Milky Way

Einstein equation are very difficult to solve analytically and Galaxy is a multi-structured object making it even the more difficult to detail a metric for the whole Galaxy

Galactic metric-disc

Stationarity and axisymmetry spacetime

$$ds^2 = -e^{2U}(dt + Ad\phi)^2 + e^{-2U}\left(e^{2\gamma}(dr^2 + dz^2) + Wd\phi^2\right)$$

Lewis-Papapetrou class

Reflection symmetry (around the galactic plane)

Disc is an equilibrium configuration of a pressure-less rotating perfect fluid (a GR dust)

Masses inside a large portion of the Galaxy interact only gravitationally and reside far from the central bulge region

For dust (shear free and expansion free)

$$ds^2 = -(dt - Nd\phi)^2 + r^2 d\phi^2 + e^{\nu}(dr^2 + dz^2)$$

the function $N(r,z)$ was solved by Balasin & Grumiller (BG)

(Balasin and Grummiler, Int.J. Mod. Phys., 2008)

$$N(r,z) = V_0(R_{out} - r_{in}) + \frac{V_0}{2}\sum_{\pm}\left(\sqrt{(z \pm r_{in})^2 + r^2} - \sqrt{(z \pm R_{out})^2 + r^2}\right)$$

physical boundaries: for r >> N, far from r = 0, and $|z| < r_{in}$

- r_{in} = **bulge size**
- R_{out} = **extension of the MW disk-> Galaxy size**
- V_0 = **velocity in the flat regime**

✓ Einstein equation allows to treat separately velocities and density

Einstein field Eq.

$$r\partial_z\nu + \partial_r N \partial_z N = 0$$

$$2r\partial_r\nu + (\partial_r N)^2 - (\partial_z N)^2 = 0$$

$$2r^2(\partial_r\partial_r\nu + \partial_z\partial_z\nu) + (\partial_r N)^2 + (\partial_z N)^2 = 0$$

$$r(\partial_r\partial_r N + \partial_z\partial_z N) - \partial_r N = 0$$

$$(\partial_r N)^2 + (\partial_z N)^2 = kr^2\rho e^{\nu}$$

$$\rho(R,z) = e^{-\nu(R,z)}\frac{1}{8\pi R^2}\left[\left(\partial_R N(R,z)\right)^2 + \left(\partial_z N(R,z)\right)^2\right]$$

Stationarity and axisymmetry spacetime may include Kerr solution for the bulge as well as different disc solutions

Stationarity and axisymmetry spacetime may include Kerr solution for the bulge as well as different disc solutions

The Galaxy is a multistructured object, global solutions are unrealistic

Stationarity and axisymmetry spacetime may include Kerr solution for the bulge as well as different disc solutions

Regions around the bulge and the bar need relativistic hydrodynamics, where equilibrium conditions are not possible

The Galaxy is a multistructured object, global solutions are unrealistic

Stationarity and axisymmetry spacetime may include Kerr solution for the bulge as well as different disc solutions

Regions around the bulge and the bar need relativistic hydrodynamics, where equilibrium conditions are not possible

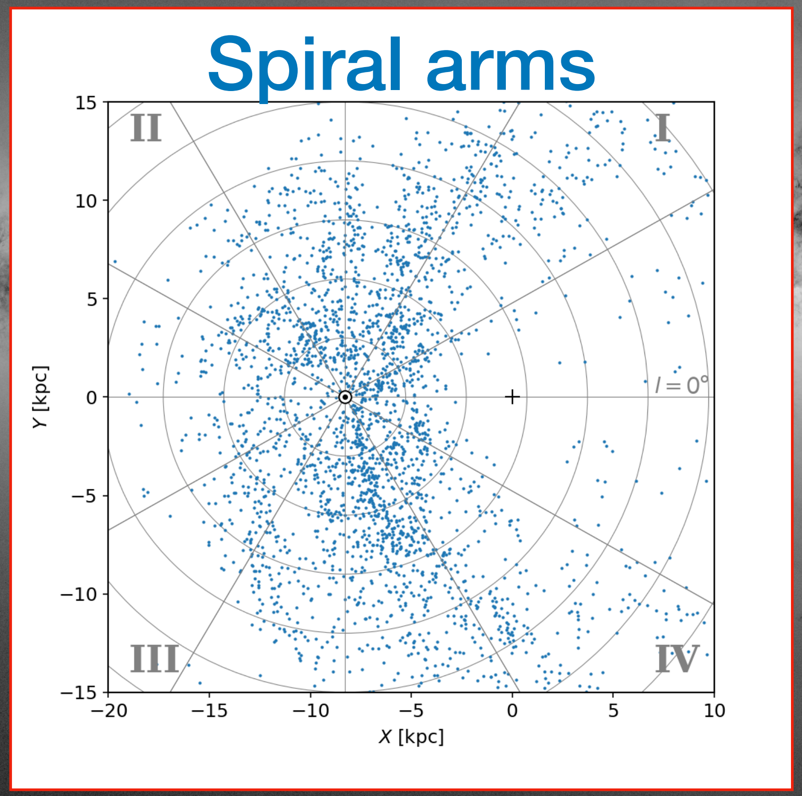

MW core
Relativistic
hydrodynamics for the
bulge/bar?

The Galaxy is a multistructured object, global solutions are unrealistic

Stationarity and axisymmetry spacetime may include Kerr solution for the bulge as well as different disc solutions

Regions around the bulge and the bar need relativistic hydrodynamics, where equilibrium conditions are not possible

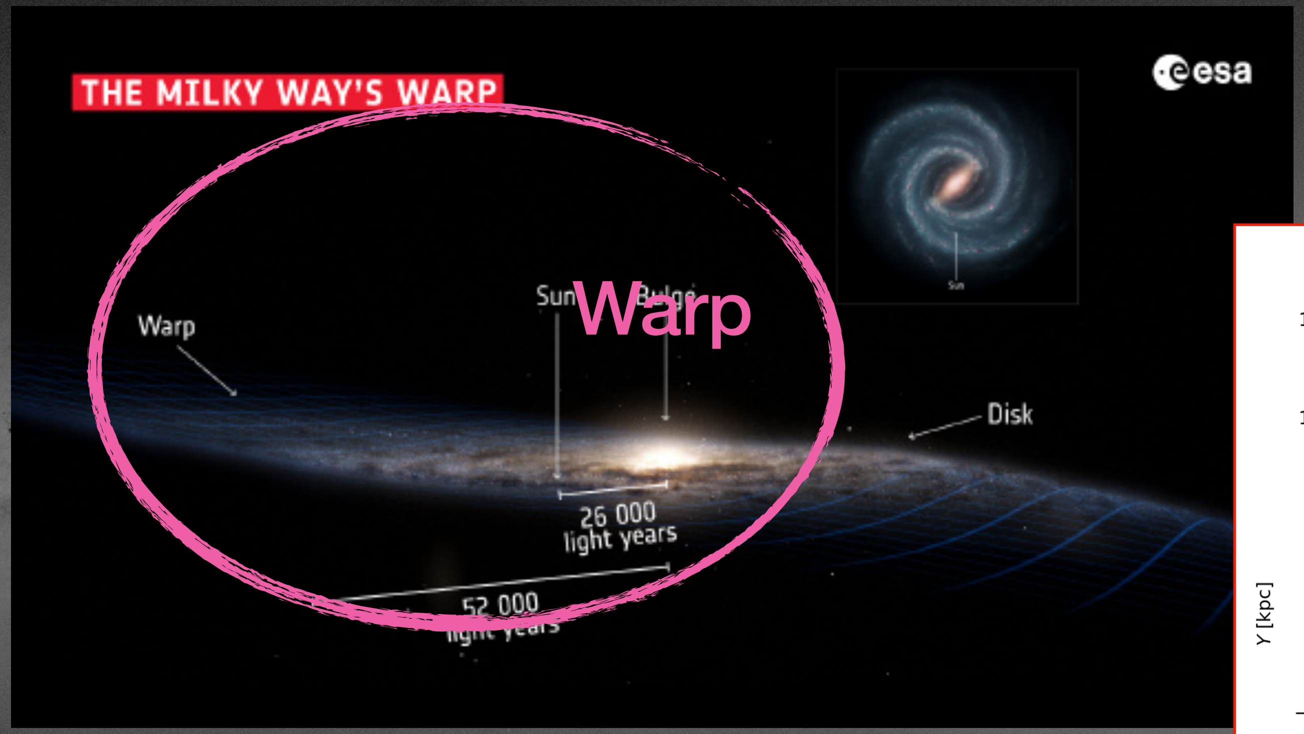

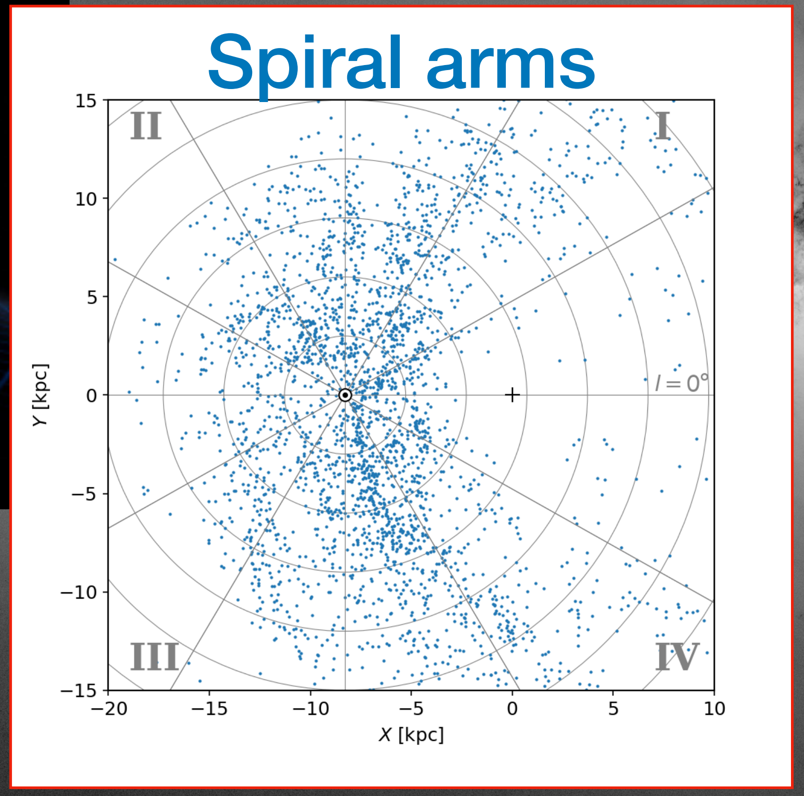

MW core
Relativistic hydrodynamics for the bulge/bar?

The Galaxy is a multistructured object, global solutions are unrealistic

Stationarity and axisymmetry spacetime may include Kerr solution for the bulge as well as different disc solutions

Regions around the bulge and the bar need relativistic hydrodynamics, where equilibrium conditions are not possible

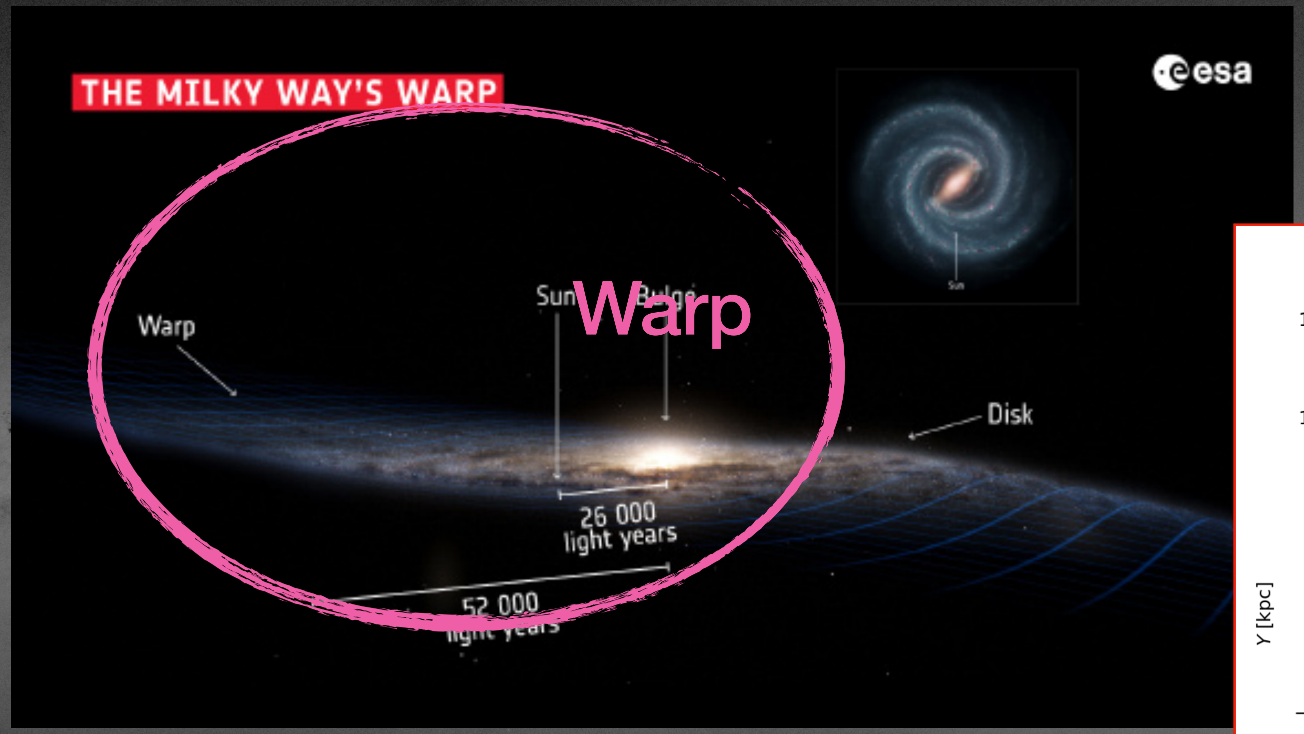

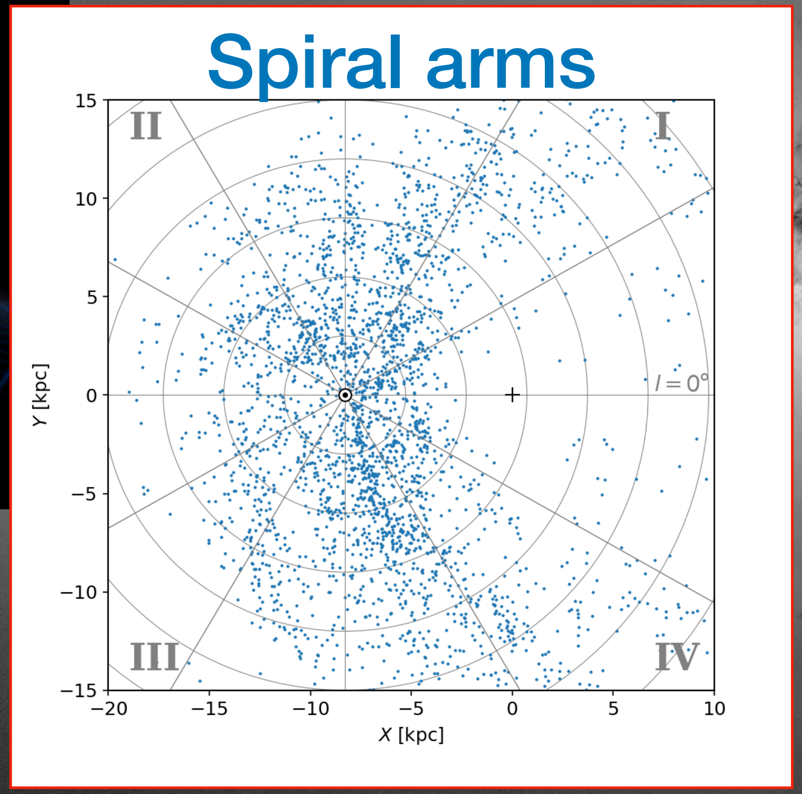

MW core
Relativistic
hydrodynamics for the
bulge/bar?

Flaring?

The Galaxy is a multistructured object, global solutions are unrealistic

Stationarity and axisymmetry spacetime may include Kerr solution for the bulge as well as different disc solutions

Regions around the bulge and the bar need relativistic hydrodynamics, where equilibrium conditions are not possible

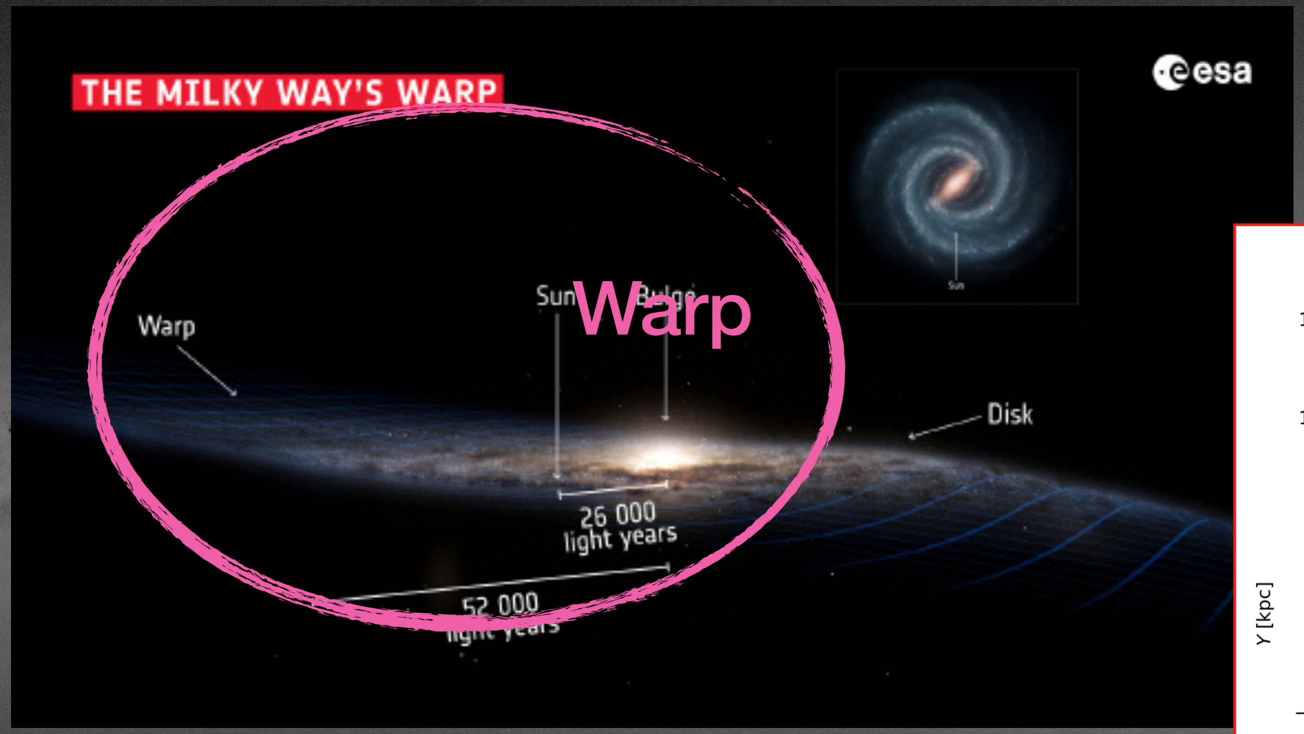

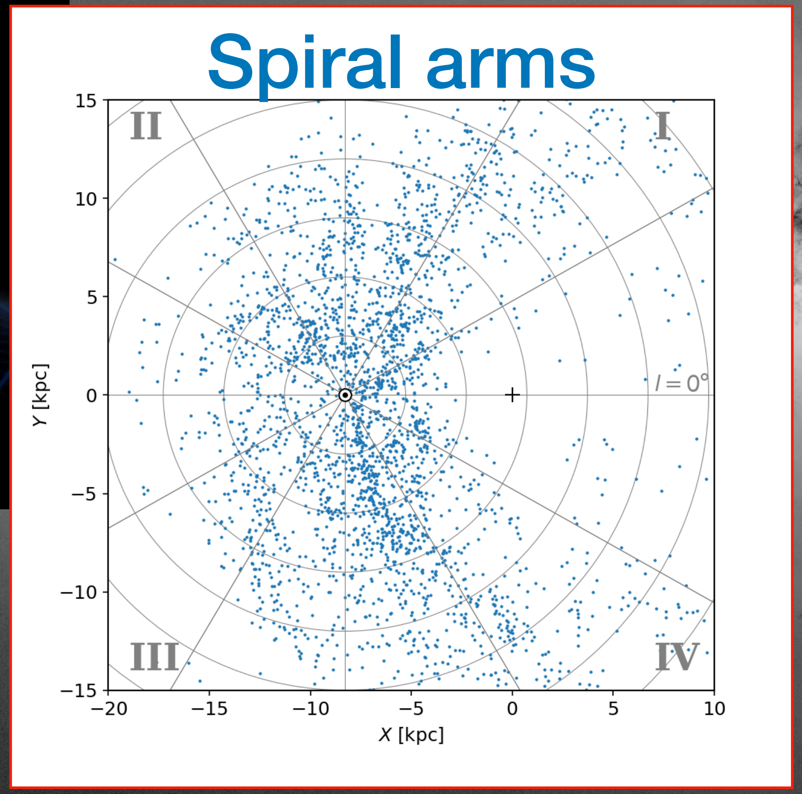

MW core
Relativistic
hydrodynamics for the
bulge/bar?

Disc

Flaring?

The Galaxy is a multistructured object, global solutions are unrealistic

Stationarity and axisymmetry spacetime may include Kerr solution for the bulge as well as different disc solutions

Regions around the bulge and the bar need relativistic hydrodynamics, where equilibrium conditions are not possible

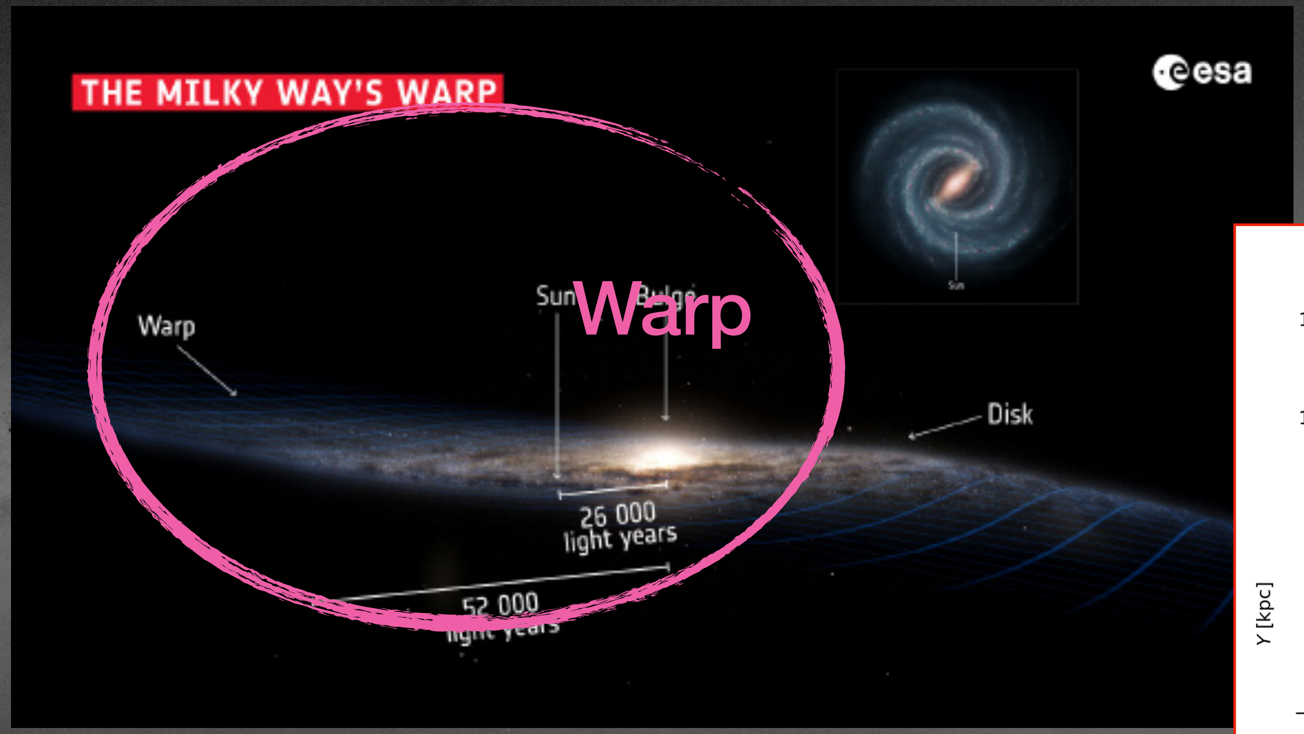

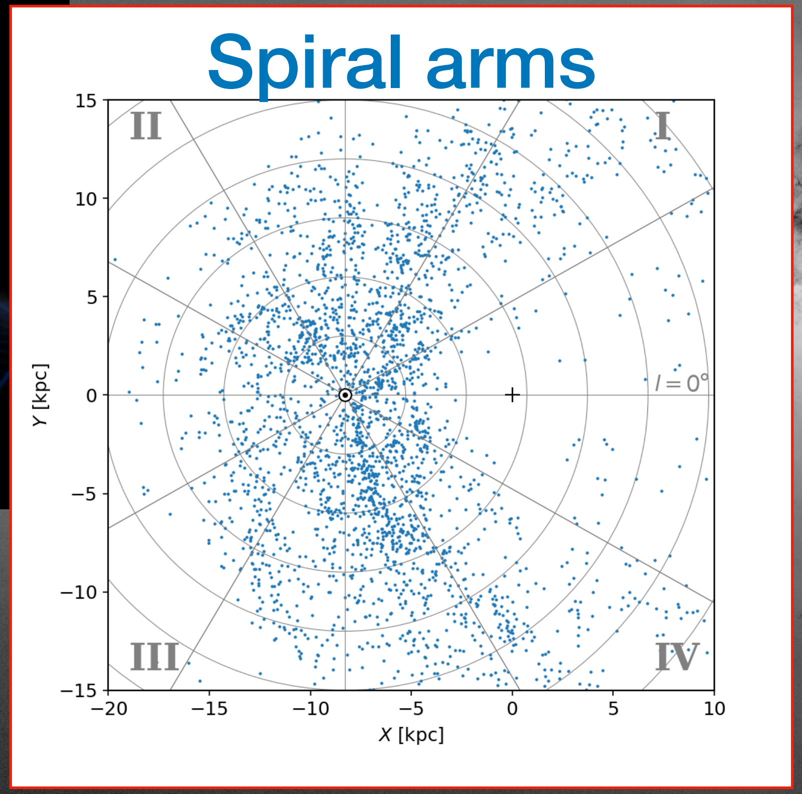

MW core
Relativistic hydrodynamics for the bulge/bar?

Disc

Flaring?

Streams?

The Galaxy is a multistructured object, global solutions are unrealistic

Stationarity and axisymmetry spacetime may include Kerr solution for the bulge as well as different disc solutions

Regions around the bulge and the bar need relativistic hydrodynamics, where equilibrium conditions are not possible

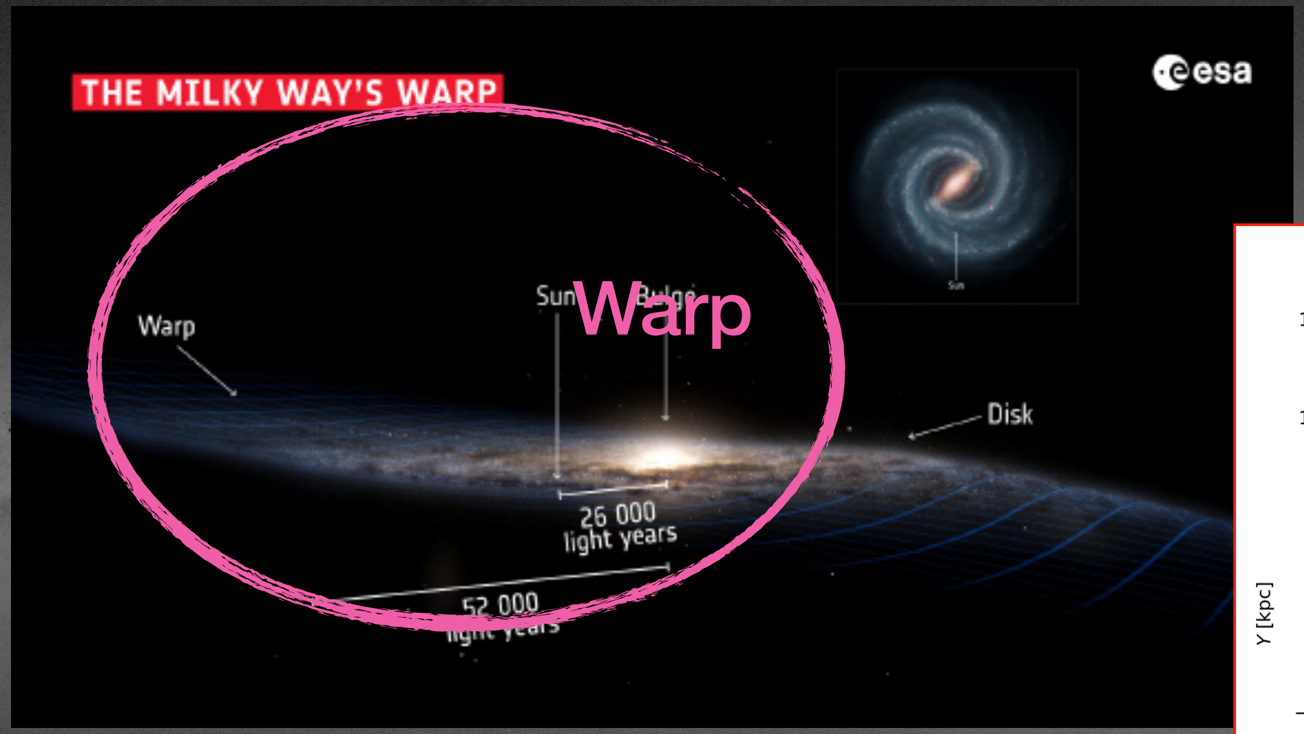

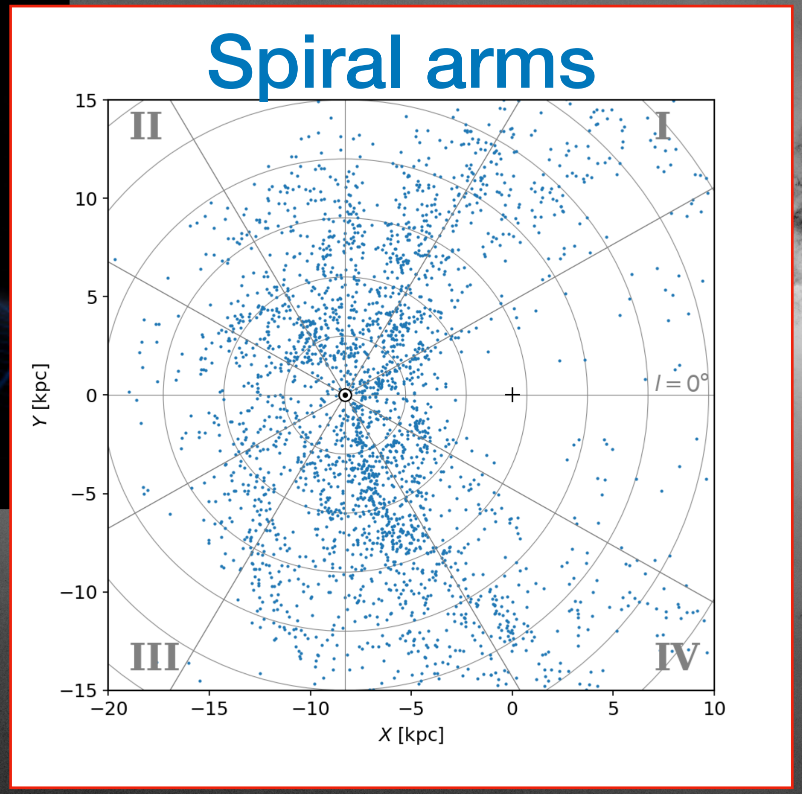

MW core
Relativistic hydrodynamics for the bulge/bar?

Streams?

Disc

Flaring?

The Galaxy is a multistructured object, global solutions are unrealistic

Peering into hidden parts is utmost fundamental to establish boundary matching conditions between internal/external Einstein’s solutions

Stationarity and axisymmetry spacetime may include Kerr solution for the bulge as well as different disc solutions

Regions around the bulge and the bar need relativistic hydrodynamics, where equilibrium conditions are not possible

$k^\alpha = \partial_t, m^\alpha = \partial_\phi$ $\quad u^\alpha = \Gamma\left(k^\alpha + \beta m^\alpha\right)$ **or** $u^\alpha = \gamma\left(e^\alpha_{\hat{0}} + \zeta^{\hat{\phi}} e^\alpha_{\hat{\phi}}\right)$

Relativistic kinematics, valid regardless the geometry

spatial velocity w.r.t the local non-rotating observer

$$\zeta^{\hat{\phi}} = \frac{\sqrt{g_{\phi\phi}}}{M}(\beta + M^\phi)$$

β coordinate angular velocity

$M = r/\sqrt{(r^2 - N^2)}, \quad M^\phi = N/(r^2 - N^2)$

On testing CDM and geometry-driven Milky Way rotation curve models with *Gaia* DR2- Crosta M., Giammaria M., Lattanzi M. G., Poggio E.,MNRAS, Volume 496, Issue 2, August 2020, Pages 2107–2122

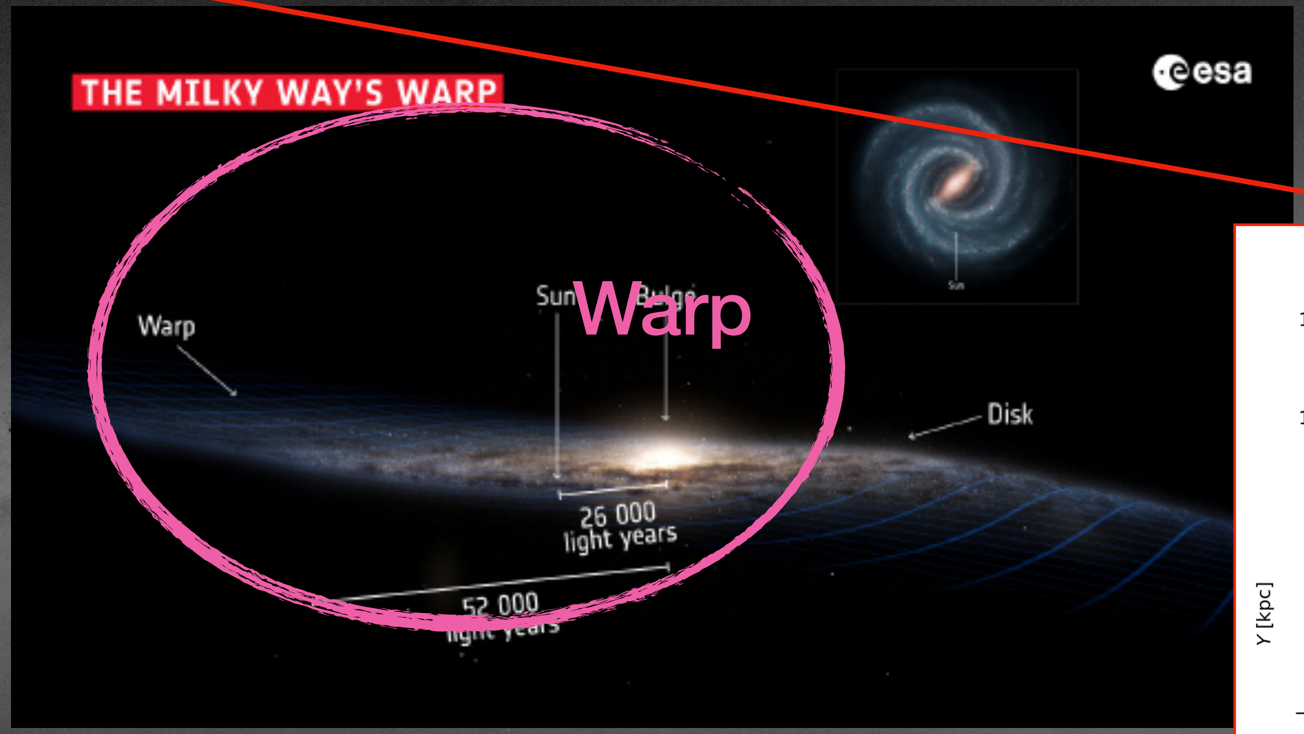

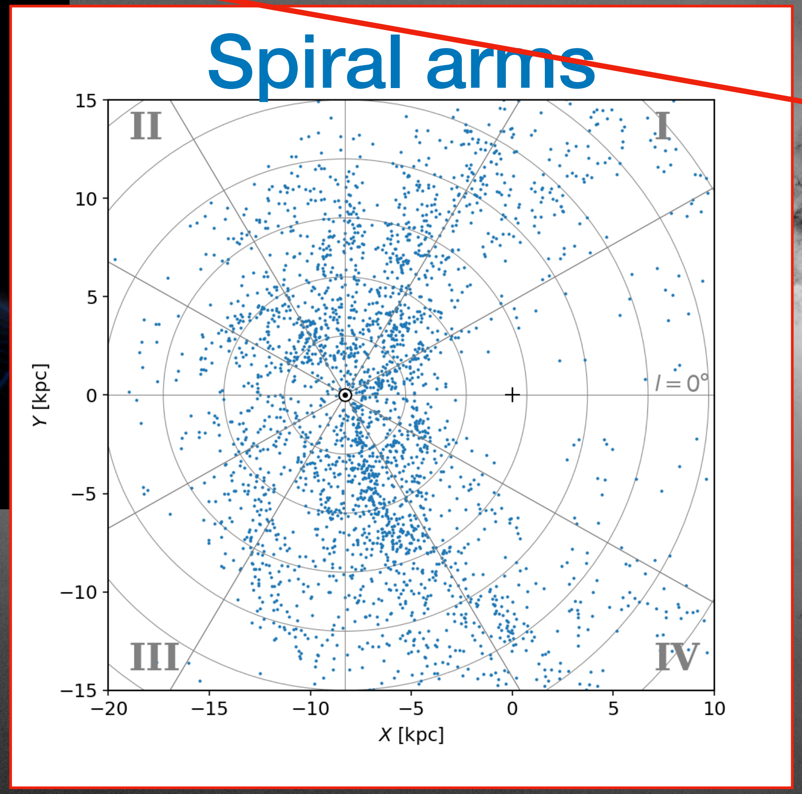

MW core Relativistic hydrodynamics for the bulge/bar?

Disc

Flaring?

Streams?

The Galaxy is a multistructured object, global solutions are unrealistic

Peering into hidden parts is utmost fundamental to establish boundary matching conditions between internal/external Einstein's solutions

Stationarity and axisymmetry spacetime may include Kerr solution for the bulge as well as different disc solutions

Regions around the bulge and the bar need relativistic hydrodynamics, where equilibrium conditions are not possible

$k^\alpha = \partial_t, m^\alpha = \partial_\phi$ $\quad u^\alpha = \Gamma\left(k^\alpha + \beta m^\alpha\right)$ **or** $u^\alpha = \gamma\left(e^\alpha_{\hat{0}} + \zeta^{\hat{\phi}} e^\alpha_{\hat{\phi}}\right)$

Relativistic kinematics, valid regardless the geometry

spatial velocity w.r.t the local non-rotating observer

$$\zeta^{\hat{\phi}} = \frac{\sqrt{g_{\phi\phi}}}{M}(\beta + M^\phi)$$

β coordinate angular velocity

$M = r/\sqrt{(r^2 - N^2)}, \quad M^\phi = N/(r^2 - N^2)$

On testing CDM and geometry-driven Milky Way rotation curve models with *Gaia* DR2- Crosta M., Giammaria M., Lattanzi M. G., Poggio E.,MNRAS, Volume 496, Issue 2, August 2020, Pages 2107–2122

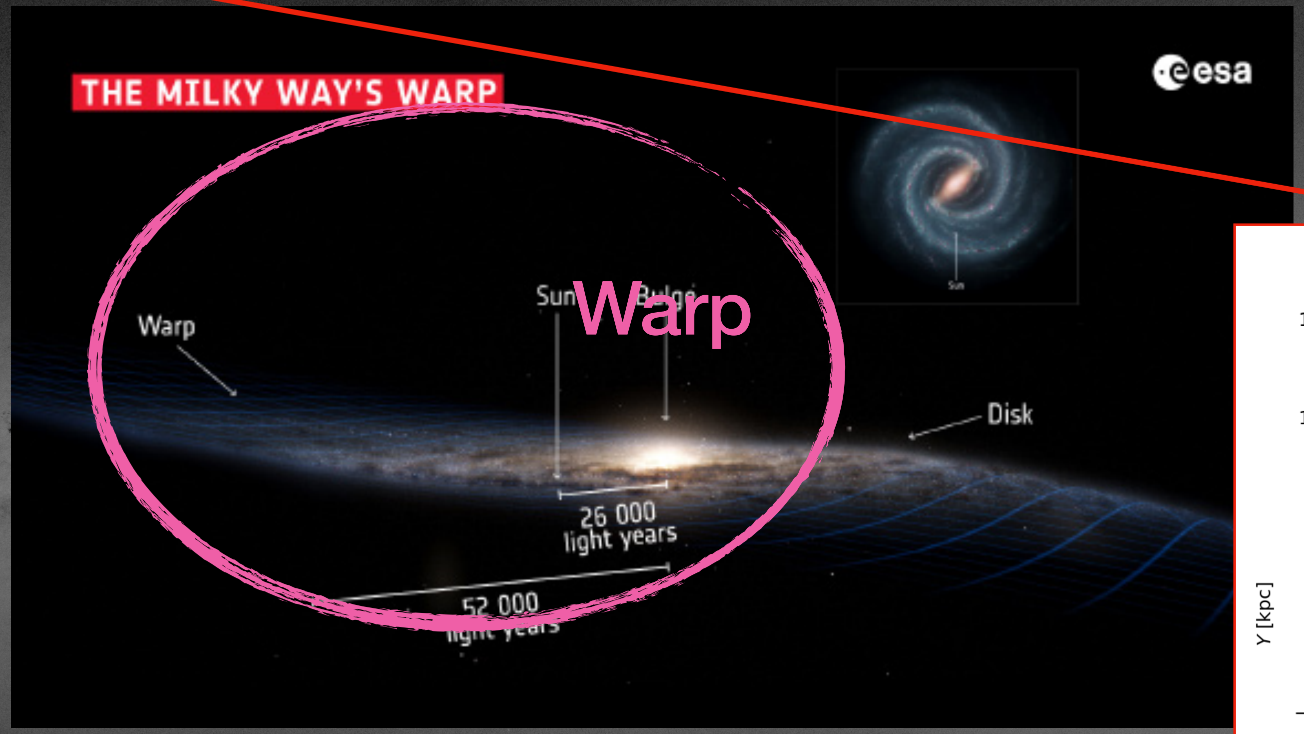

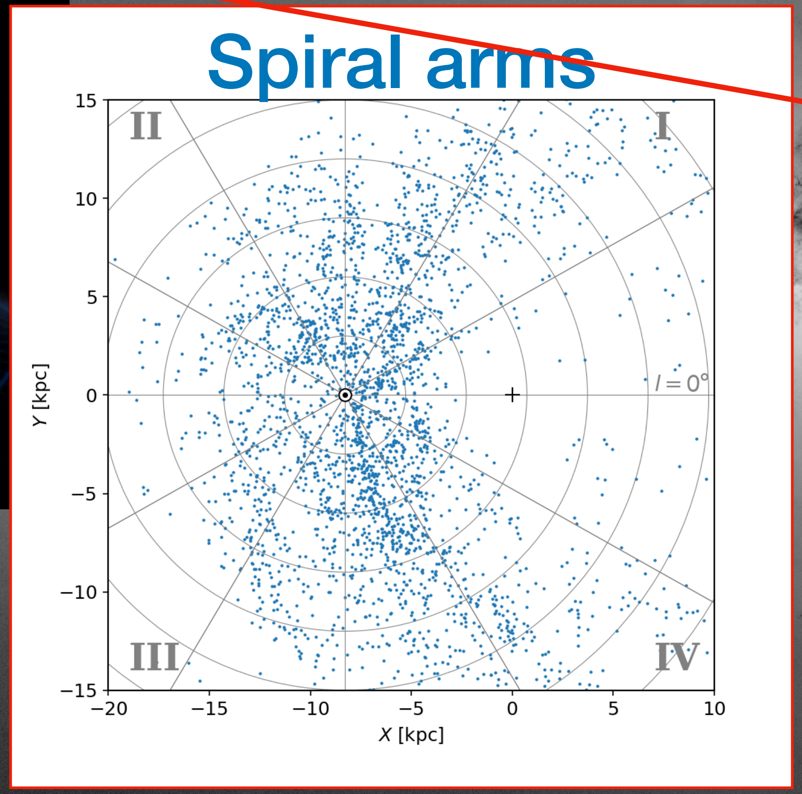

MW core Relativistic hydrodynamics for the bulge/bar?

Gravitational dragging working at disc scale?

$$\zeta^{\hat{\phi}}(r,z) = N(r,z)/r \propto g_{0\phi}$$

Flaring?

Disc

Streams?

Different from the IAU metric!

The Galaxy is a multistructured object, global solutions are unrealistic

Peering into hidden parts is utmost fundamental to establish boundary matching conditions between internal/external Einstein's solutions

Stationarity and axisymmetry spacetime may include Kerr solution for the bulge as well as different disc solutions

Regions around the bulge and the bar need relativistic hydrodynamics, where equilibrium conditions are not possible

$k^\alpha = \partial_t, m^\alpha = \partial_\phi$ $\quad u^\alpha = \Gamma\left(k^\alpha + \beta m^\alpha\right)$ **or** $u^\alpha = \gamma\left(e^\alpha_{\hat{0}} + \zeta^{\hat{\phi}} e^\alpha_{\hat{\phi}}\right)$

Relativistic kinematics, valid regardless the geometry

spatial velocity w.r.t the local non-rotating observer

$$\zeta^{\hat{\phi}} = \frac{\sqrt{g_{\phi\phi}}}{M}(\beta + M^\phi)$$

β coordinate angular velocity

$$M = r/\sqrt{(r^2 - N^2)}, \quad M^\phi = N/(r^2 - N^2)$$

On testing CDM and geometry-driven Milky Way rotation curve models with *Gaia* DR2- Crosta M., Giammaria M., Lattanzi M. G., Poggio E.,MNRAS, Volume 496, Issue 2, August 2020, Pages 2107–2122

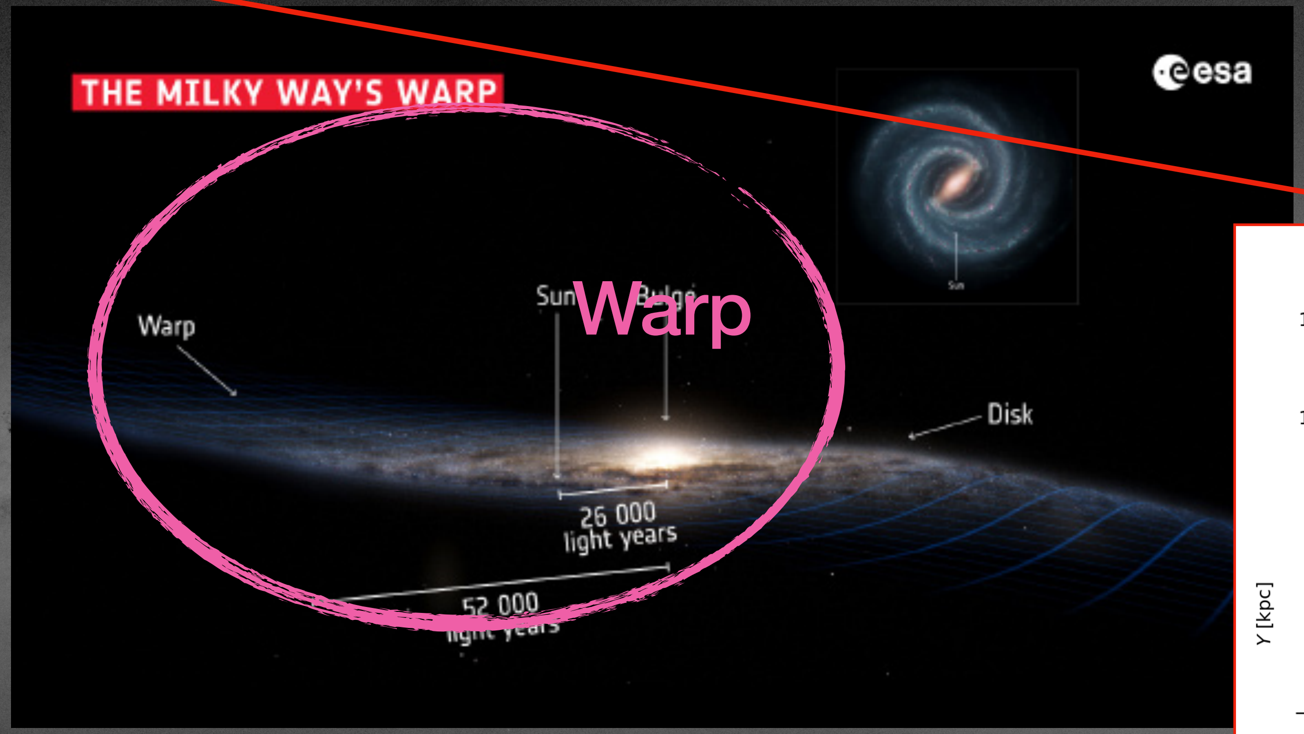

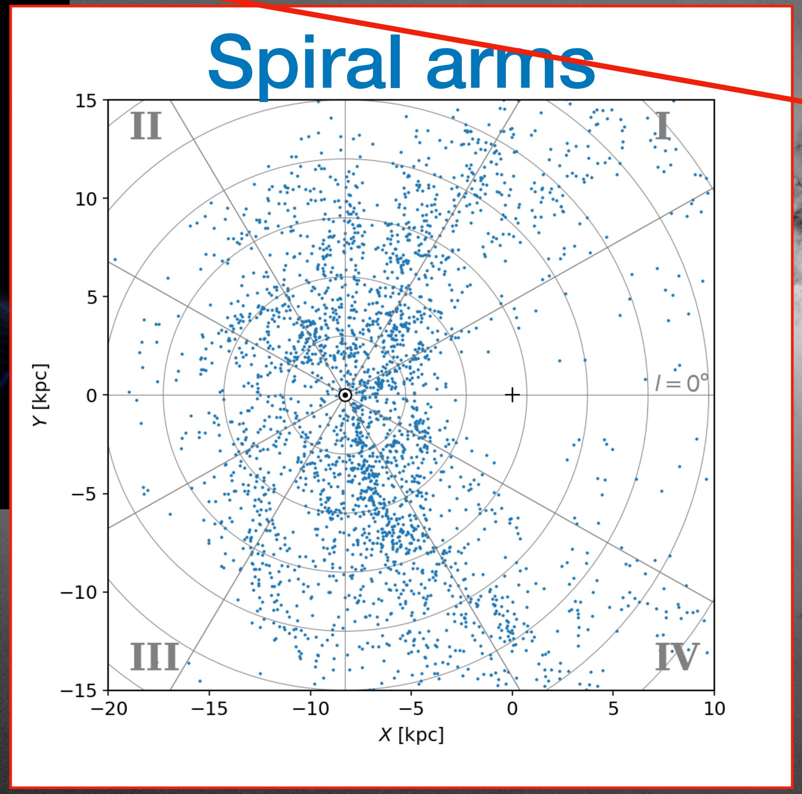

MW core Relativistic hydrodynamics for the bulge/bar?

Gravitational dragging working at disc scale?

$$\zeta^{\hat{\phi}}(r,z) = N(r,z)/r \propto g_{0\phi}$$

Flaring?

Disc

Streams?

Different from the IAU metric!

The Galaxy is a multistructured object, global solutions are unrealistic

Peering into hidden parts is utmost fundamental to establish boundary matching conditions between internal/external Einstein's solutions

Our ansatz: the MW rotation curve is geometry driven?

Data sample: full reconstruction of disc kinematics based on Gaia data only

i. **Complete Gaia astrometric dataset** and corresponding covariance matrix

ii. **Three Gaia photometric bands (G, BP, RP)** all available and RUWE < 1.4 [to discard sources with problematic astrometric solutions, astrometric binaries, and other anomalous cases]

iii. **Parallaxes good to 20%** (i.e. parallax_over_error ≥ 5) [parallaxes to better than 20% allow to deal with similar (quasi–gaussian) statistics when transforming to distances]

iv. **Gaia-measured velocity along the line of sight,** i.e. **radial velocity, with better than 20% uncertainties**

i.+ii.+iii.+iv —> proper 6D reconstruction of the phase-space location occupied by each individual star as derived by the same observer

1. Full transformation (including complete error propagation) from the ICRS equatorial to heliocentric galactic coordinates
2. translation to the galactic center

-> *independency from the local standard of rest.*

angular-momentum sustained stellar population of the Milky Way that better traces its observed RC

DR2: ***very homogenous sample of 5277 early type stars and 325 classical type I Cepheids.***

https://www.cosmos.esa.int/web/gaia/iow_20200716)

v. *Cross-matched entry in the 2MASS catalogue for the actual characterization of the sample in case of DR2 and EDR3*

Ref: On testing CDM and geometry-driven Milky Way rotation curve models with *Gaia* DR2- Crosta M., Giammaria M., Lattanzi M. G., Poggio E.,MNRAS, Volume 496, Issue 2, August 2020, Pages 2107–2122

DR3: ***a much larger sample of high-quality astrometric and spectro-photometric data of unprecedented homogeneity of***

719143 young disc stars within |z| < 1 kpc and up to R = 19 kpc

241'918 OBA stars, 475'520 RGB giants, and 1'705 Cepheides

radial cut at 4.5 kpc to avoid the bar influence

MCMC fit to the Gaia DR3 data - Classical (MWC), MOND, EINASTO ,GR
I.Results: azimuthal velocity profile of the MW

The red, blue, green, and yellow curves show the best-fitting to the BG, MWC, MOND, and ΛCDM models, respectively

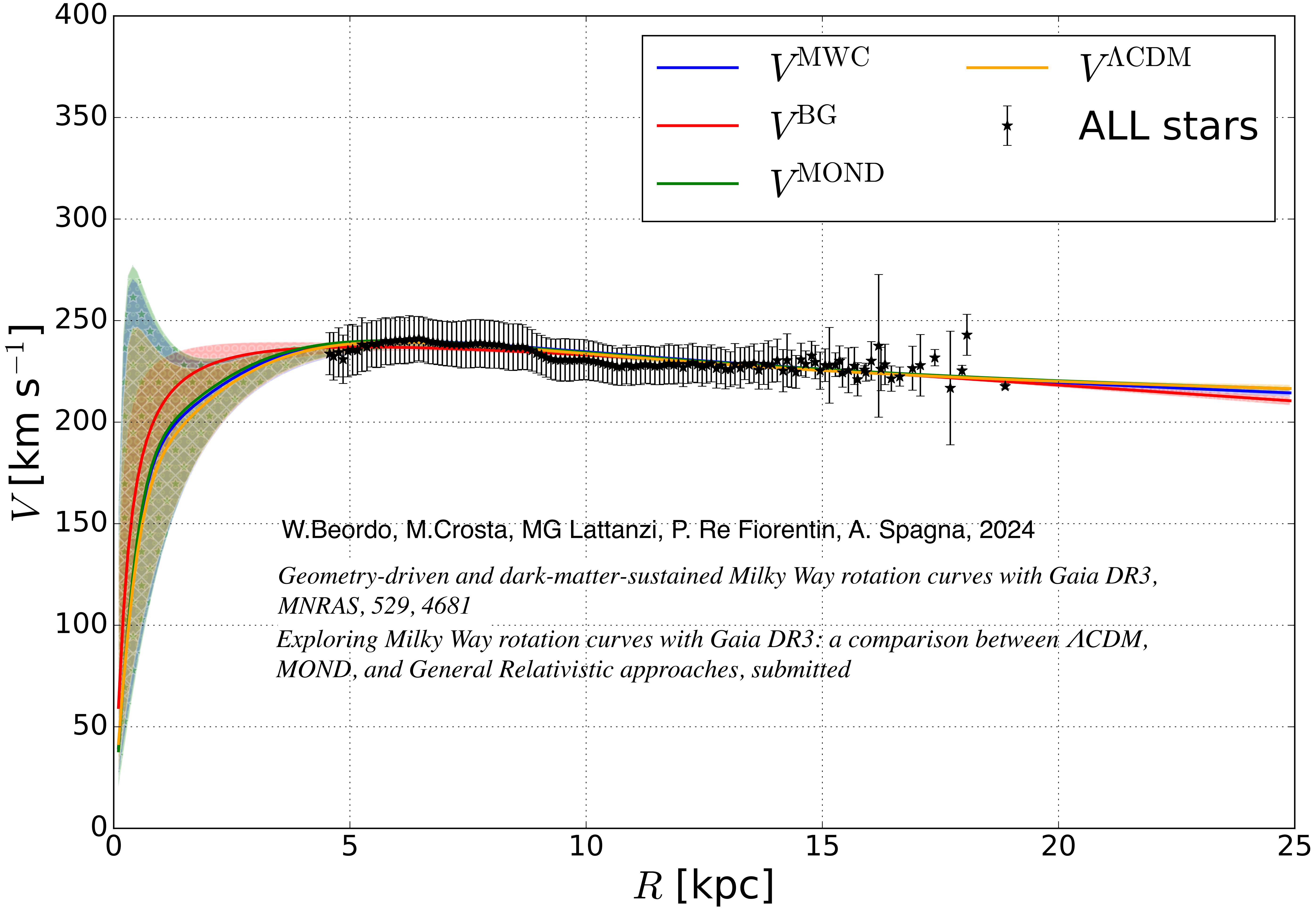

The four velocity profiles are all good representations of the observed (binned) data. **The four models are found to be statistically equivalent**

comparisons with the WAIC and LOO tests show almost identical values

-

- Black starred symbols represent the median azimutal velocity at the median distance from the galactic centre of the stellar population within each of the radial bins
- Robust Scatter Estimate (RSE) adopted as a robust measure of the azimutal velocity dispersion of the population in each radial bin
- The filled areas represent the 68 per cent reliability intervals of each rotation curve
- For R ≲ 4.5 kpc both the classical and the relativistic curves are very uncertain because of the lack of data in that region

MCMC fit to the Gaia DR3 data - Classical (MWC) and GR (BG) RC- velocity profile for each sample

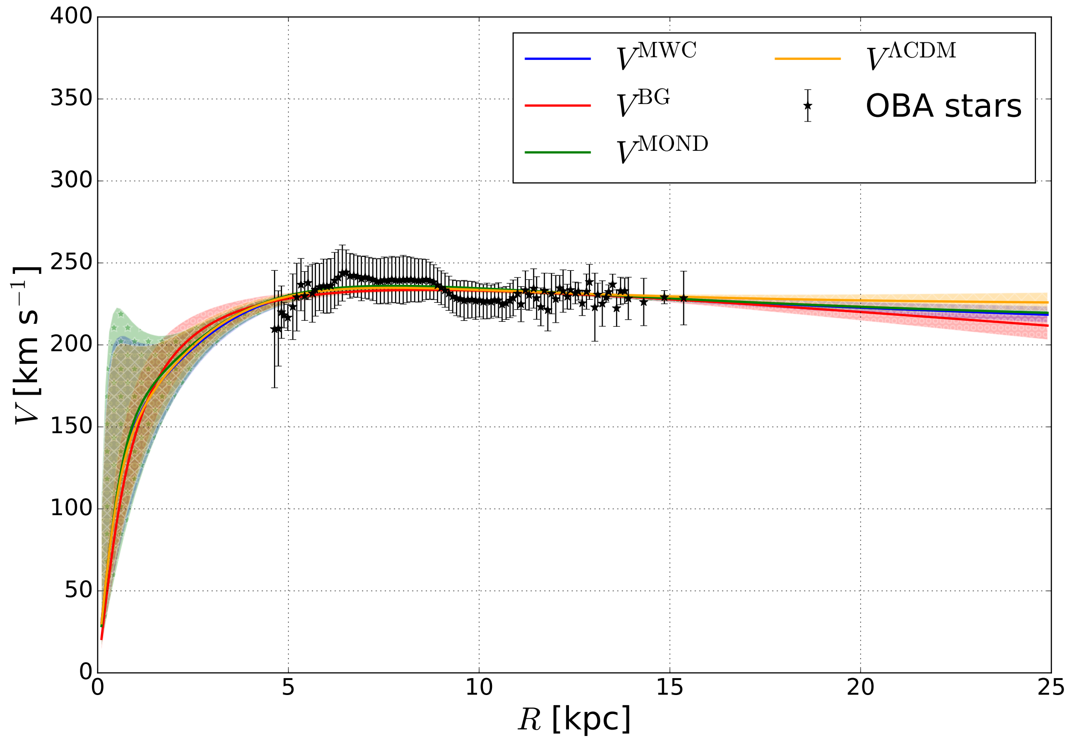

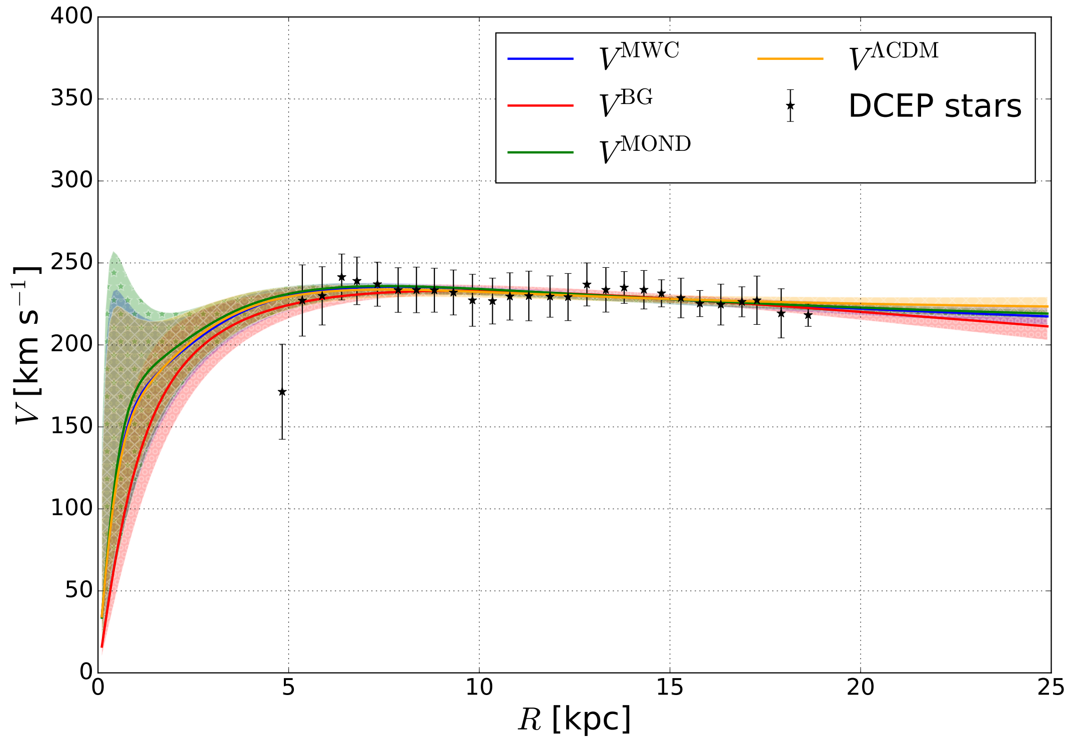

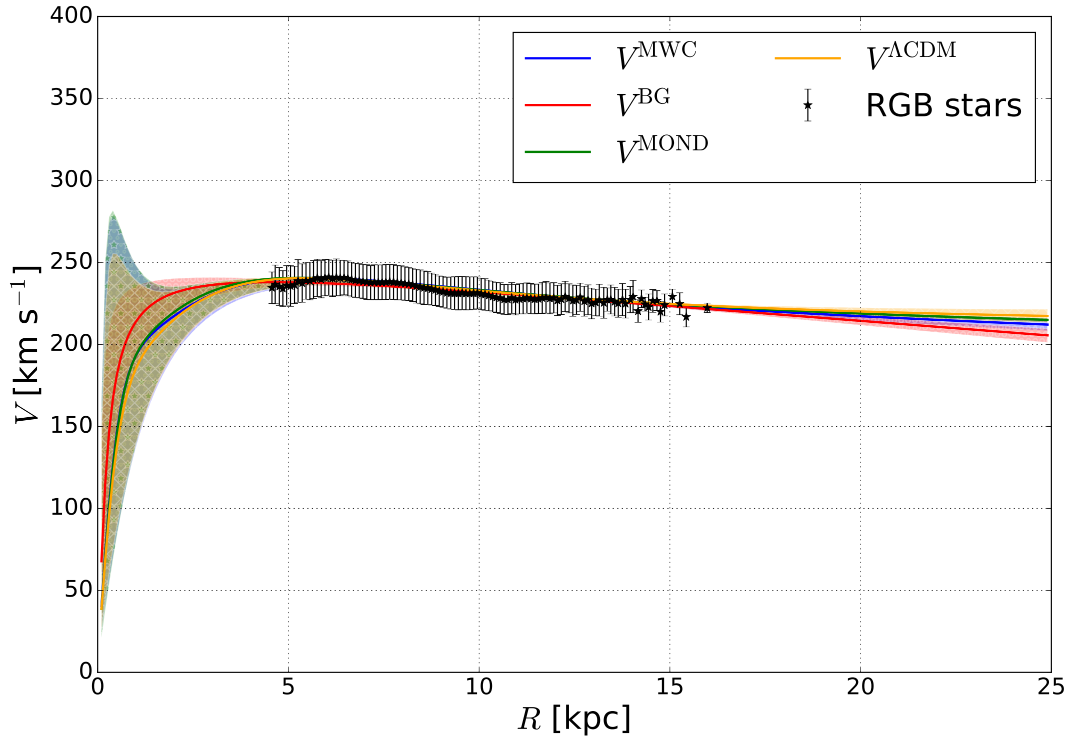

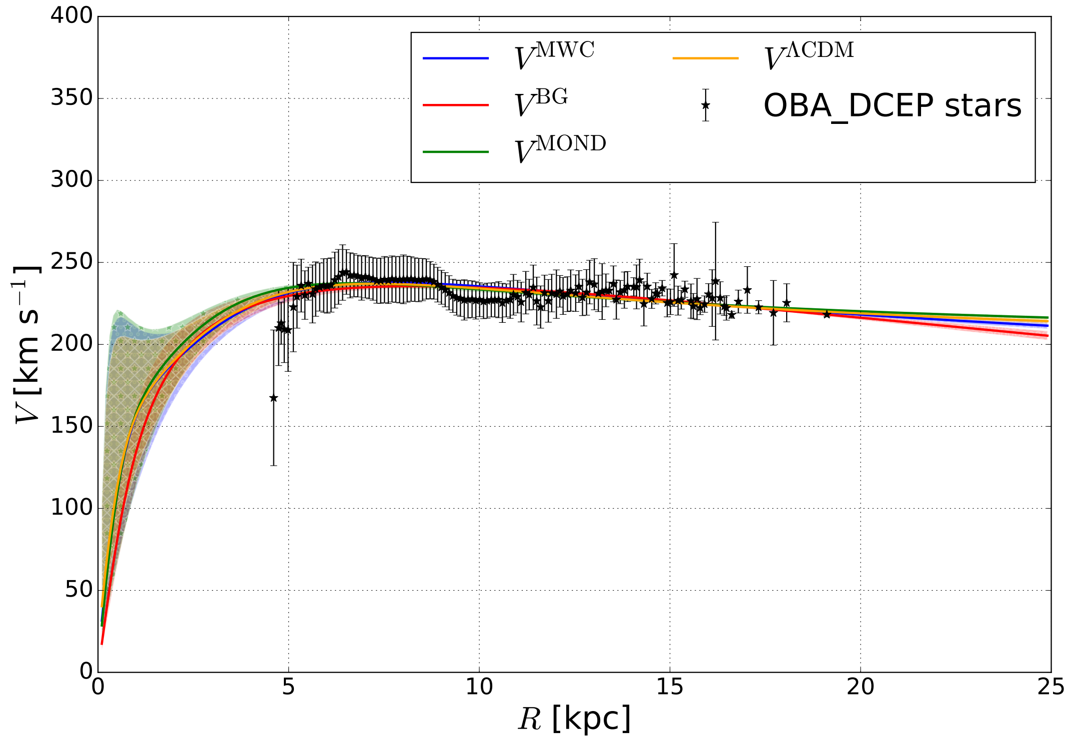

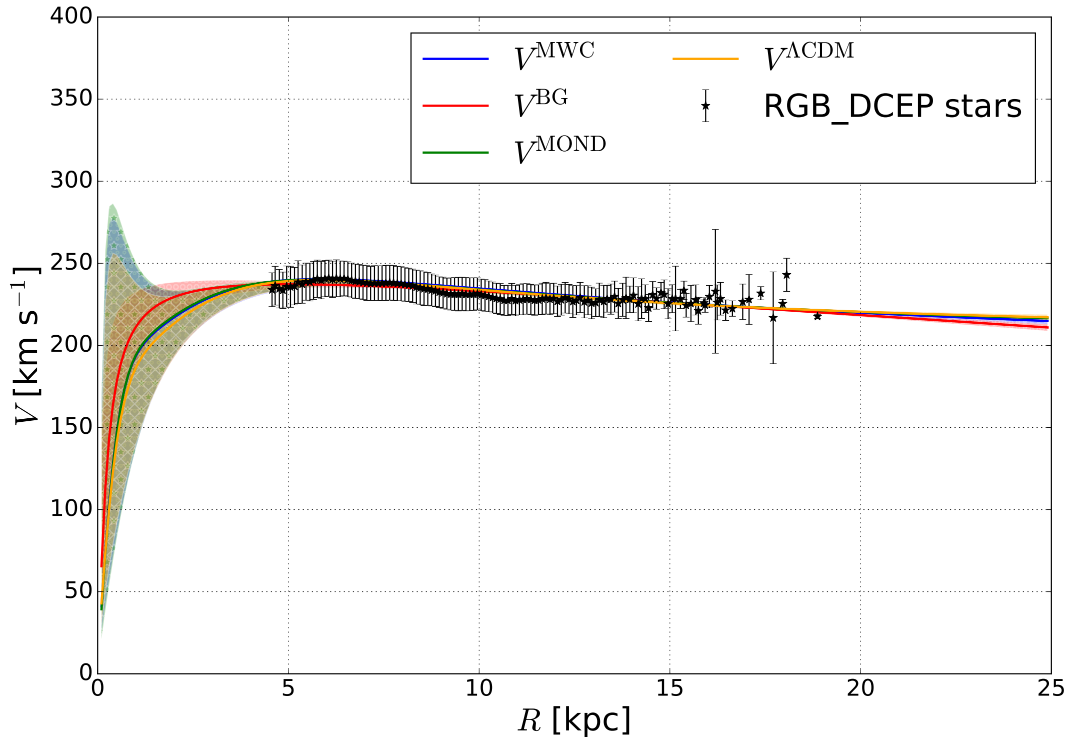

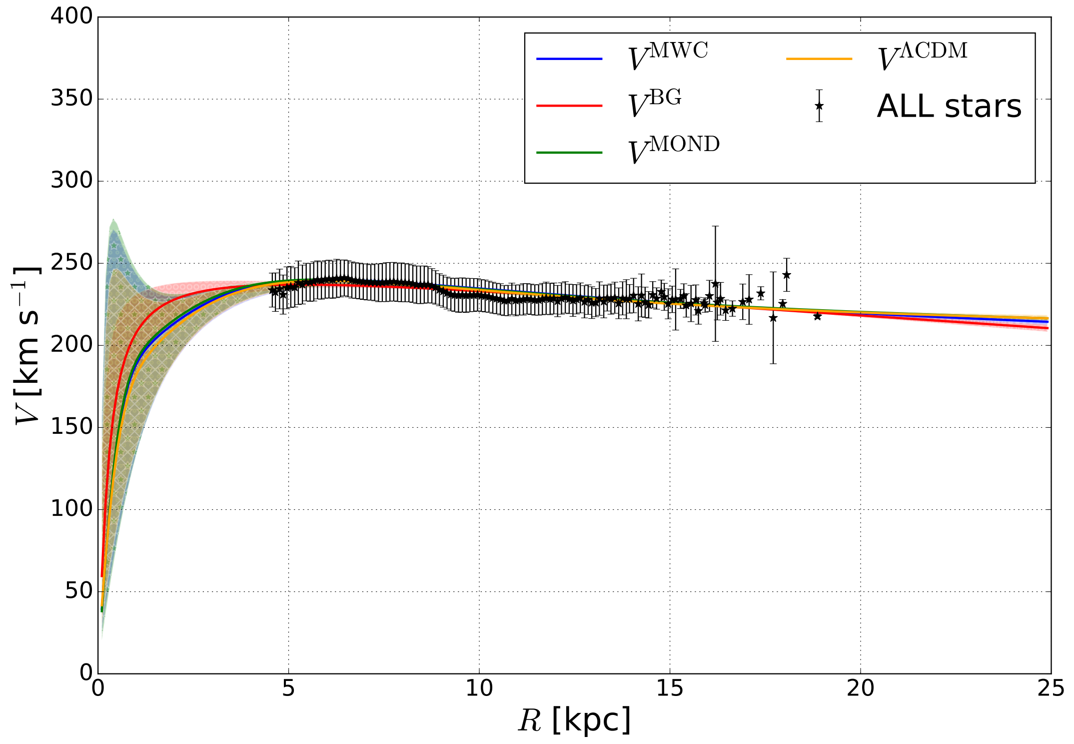

MWC model	OBA	DCEP	RGB	OBA + DCEP	RGB + DCEP	ALL
M_b [10^{10} M$_\odot$]	$0.9^{+0.6}_{-0.5}$	$1.0^{+0.6}_{-0.6}$	$1.3^{+0.6}_{-0.6}$	$1.0^{+0.6}_{-0.6}$	$1.3^{+0.6}_{-0.6}$	$1.2^{+0.6}_{-0.6}$
b_b [kpc]	$0.9^{+0.9}_{-0.6}$	$0.9^{+0.8}_{-0.6}$	$0.8^{+0.8}_{-0.5}$	$1.0^{+0.9}_{-0.6}$	$0.8^{+0.7}_{-0.5}$	$0.8^{+0.8}_{-0.5}$
M_{td} [10^{10} M$_\odot$]	$4.1^{+0.7}_{-0.8}$	$4.1^{+0.8}_{-0.8}$	$3.9^{+0.7}_{-0.7}$	$4.4^{+0.7}_{-0.7}$	$3.9^{+0.7}_{-0.7}$	$4.0^{+0.7}_{-0.7}$
a_{td} [kpc]	$5.0^{+0.9}_{-0.8}$	$5.3^{+0.9}_{-0.9}$	$5.0^{+1.0}_{-0.9}$	$5.2^{+0.8}_{-0.8}$	$5.2^{+1.0}_{-1.0}$	$5.2^{+1.0}_{-1.0}$
b_{td} [kpc]	$0.3^{+0.4}_{-0.1}$	$0.3^{+0.5}_{-0.1}$	$0.4^{+0.6}_{-0.1}$	$0.3^{+0.4}_{-0.1}$	$0.4^{+0.7}_{-0.1}$	$0.4^{+0.6}_{-0.1}$
M_{Td} [10^{10} M$_\odot$]	$4.2^{+0.9}_{-0.9}$	$4.2^{+0.9}_{-0.9}$	$4.1^{+0.8}_{-0.8}$	$4.7^{+0.9}_{-0.8}$	$4.0^{+0.8}_{-0.8}$	$4.1^{+0.8}_{-0.8}$
a_{Td} [kpc]	$3.0^{+0.6}_{-0.7}$	$3.0^{+0.7}_{-0.7}$	$2.6^{+0.6}_{-0.6}$	$3.2^{+0.6}_{-0.7}$	$2.6^{+0.6}_{-0.6}$	$2.7^{+0.6}_{-0.6}$
b_{Td} [kpc]	$0.9^{+0.9}_{-0.5}$	$0.8^{+1.0}_{-0.6}$	$0.5^{+0.8}_{-0.3}$	$1.0^{+0.9}_{-0.7}$	$0.5^{+0.8}_{-0.3}$	$0.5^{+0.8}_{-0.3}$
ρ_0^h [M$_\odot$ pc^{-3}]	$0.010^{+0.005}_{-0.003}$	$0.010^{+0.005}_{-0.004}$	$0.009^{+0.005}_{-0.003}$	$0.013^{+0.005}_{-0.004}$	$0.010^{+0.005}_{-0.003}$	$0.010^{+0.005}_{-0.003}$
A_h [kpc]	$17.2^{+4.9}_{-3.5}$	$16.4^{+4.7}_{-3.2}$	$17.2^{+5.0}_{-3.7}$	$13.6^{+3.1}_{-2.1}$	$16.5^{+4.1}_{-2.9}$	$16.3^{+4.0}_{-2.9}$
WAIC	−341 ± 3	−103 ± 3	−346 ± 2	−448 ± 5	−424 ± 5	−426 ± 5
LOO	−341 ± 3	−103 ± 3	−346 ± 2	−448 ± 5	−424 ± 6	−427 ± 5

BG model	OBA	DCEP	RGB	OBA + DCEP	RGB + DCEP	ALL
r_{in} [kpc]	$0.65^{+0.35}_{-0.27}$	$0.86^{+0.63}_{-0.49}$	$0.18^{+0.20}_{-0.12}$	$0.81^{+0.29}_{-0.28}$	$0.18^{+0.17}_{-0.12}$	$0.20^{+0.18}_{-0.13}$
R_{out} [kpc]	$60.61^{+32.83}_{-19.17}$	$55.21^{+32.68}_{-18.93}$	$61.85^{+14.42}_{-12.37}$	$45.52^{+9.38}_{-6.71}$	$73.14^{+12.53}_{-11.31}$	$71.12^{+12.97}_{-11.31}$
V_0 [km s^{-1}]	$272.58^{+24.94}_{-16.70}$	$281.40^{+40.77}_{-24.20}$	$257.16^{+12.17}_{-7.48}$	$288.23^{+17.33}_{-15.68}$	$255.01^{+8.72}_{-6.25}$	$256.17^{+9.52}_{-6.79}$
e^{ν_0}	$0.094^{+0.017}_{-0.013}$	$0.096^{+0.019}_{-0.014}$	$0.085^{+0.015}_{-0.011}$	$0.094^{+0.017}_{-0.013}$	$0.087^{+0.016}_{-0.011}$	$0.087^{+0.017}_{-0.012}$
WAIC	−343 ± 4	−103 ± 3	−346 ± 2	−448 ± 6	−422 ± 4	−425 ± 4
LOO	−343 ± 4	−103 ± 3	−346 ± 2	−448 ± 5	−423 ± 5	−426 ± 5

MOND model	OBA	DCEP	RGB	OBA + DCEP	RGB + DCEP	ALL
M_b [10^{10} M$_\odot$]	$1.1^{+0.6}_{-0.6}$	$1.2^{+0.6}_{-0.6}$	$1.3^{+0.6}_{-0.6}$	$1.1^{+0.6}_{-0.6}$	$1.4^{+0.6}_{-0.6}$	$1.3^{+0.6}_{-0.6}$
b_b [kpc]	$1.0^{+0.9}_{-0.6}$	$0.8^{+0.8}_{-0.6}$	$0.8^{+0.8}_{-0.5}$	$0.9^{+0.9}_{-0.6}$	$0.8^{+0.7}_{-0.5}$	$0.8^{+0.8}_{-0.5}$
M_{td} [10^{10} M$_\odot$]	$4.3^{+0.6}_{-0.7}$	$4.3^{+0.7}_{-0.7}$	$3.8^{+0.6}_{-0.6}$	$4.1^{+0.7}_{-0.7}$	$4.0^{+0.6}_{-0.6}$	$4.0^{+0.6}_{-0.6}$
a_{td} [kpc]	$5.0^{+0.9}_{-0.8}$	$5.2^{+0.9}_{-0.8}$	$4.7^{+0.9}_{-0.9}$	$4.4^{+0.7}_{-0.6}$	$4.9^{+0.9}_{-0.8}$	$4.8^{+0.8}_{-0.8}$
b_{td} [kpc]	$0.3^{+0.4}_{-0.1}$	$0.4^{+0.5}_{-0.1}$	$0.4^{+0.5}_{-0.1}$	$0.3^{+0.3}_{-0.1}$	$0.4^{+0.5}_{-0.1}$	$0.3^{+0.5}_{-0.1}$
M_{Td} [10^{10} M$_\odot$]	$4.7^{+0.7}_{-0.7}$	$4.5^{+0.7}_{-0.8}$	$4.2^{+0.7}_{-0.8}$	$4.4^{+0.7}_{-0.7}$	$4.2^{+0.7}_{-0.7}$	$4.3^{+0.7}_{-0.8}$
a_{Td} [kpc]	$3.0^{+0.6}_{-0.6}$	$2.9^{+0.7}_{-0.7}$	$2.4^{+0.6}_{-0.6}$	$2.8^{+0.6}_{-0.6}$	$2.5^{+0.6}_{-0.6}$	$2.5^{+0.6}_{-0.6}$
b_{Td} [kpc]	$0.9^{+0.8}_{-0.5}$	$0.8^{+0.9}_{-0.5}$	$0.4^{+0.7}_{-0.2}$	$0.7^{+0.7}_{-0.4}$	$0.5^{+0.7}_{-0.3}$	$0.5^{+0.7}_{-0.3}$
g_0 [10^{-10} m s^{-2}]	$1.20^{+0.02}_{-0.02}$	$1.20^{+0.02}_{-0.02}$	$1.20^{+0.02}_{-0.02}$	$1.20^{+0.02}_{-0.02}$	$1.20^{+0.02}_{-0.02}$	$1.20^{+0.02}_{-0.02}$
WAIC	−341 ± 3	−103 ± 3	−345 ± 2	−452 ± 5	−423 ± 5	−426 ± 5
LOO	−341 ± 3	−103 ± 3	−345 ± 2	−452 ± 5	−423 ± 5	−426 ± 5

ΛCDM model						
M_b [10^{10} M$_\odot$]	$0.8^{+0.6}_{-0.5}$	$0.9^{+0.6}_{-0.5}$	$1.1^{+0.6}_{-0.6}$	$0.8^{+0.6}_{-0.5}$	$1.1^{+0.6}_{-0.6}$	$1.0^{+0.6}_{-0.6}$
b_b [kpc]	$0.9^{+0.8}_{-0.6}$	$0.8^{+0.8}_{-0.6}$	$0.8^{+0.8}_{-0.5}$	$0.9^{+0.9}_{-0.6}$	$0.8^{+0.8}_{-0.5}$	$0.8^{+0.8}_{-0.5}$
M_{td} [10^{10} M$_\odot$]	$3.8^{+0.7}_{-0.7}$	$3.7^{+0.8}_{-0.8}$	$3.6^{+0.7}_{-0.7}$	$4.1^{+0.7}_{-0.7}$	$3.7^{+0.7}_{-0.7}$	$3.7^{+0.7}_{-0.7}$
a_{td} [kpc]	$4.8^{+0.9}_{-0.8}$	$5.1^{+0.9}_{-0.9}$	$4.7^{+1.0}_{-0.9}$	$5.0^{+0.8}_{-0.7}$	$5.0^{+1.0}_{-0.9}$	$4.9^{+0.9}_{-0.9}$
b_{td} [kpc]	$0.3^{+0.4}_{-0.1}$	$0.3^{+0.5}_{-0.1}$	$0.3^{+0.5}_{-0.1}$	$0.3^{+0.3}_{-0.1}$	$0.3^{+0.6}_{-0.1}$	$0.3^{+0.5}_{-0.1}$
M_{Td} [10^{10} M$_\odot$]	$3.9^{+0.9}_{-0.9}$	$3.7^{+0.9}_{-0.9}$	$3.8^{+0.9}_{-0.9}$	$4.2^{+0.8}_{-0.8}$	$3.7^{+0.8}_{-0.8}$	$3.8^{+0.8}_{-0.8}$
a_{Td} [kpc]	$2.9^{+0.6}_{-0.7}$	$2.8^{+0.7}_{-0.7}$	$2.5^{+0.6}_{-0.6}$	$3.1^{+0.6}_{-0.7}$	$2.6^{+0.6}_{-0.6}$	$2.7^{+0.6}_{-0.6}$
b_{Td} [kpc]	$0.8^{+0.8}_{-0.5}$	$0.7^{+0.9}_{-0.5}$	$0.5^{+0.7}_{-0.3}$	$1.0^{+0.9}_{-0.6}$	$0.5^{+0.8}_{-0.3}$	$0.6^{+0.8}_{-0.3}$
$\log(\rho_s/[M_\odot\ kpc^{-3}])$	$5.8^{+0.3}_{-0.3}$	$5.9^{+0.3}_{-0.3}$	$5.8^{+0.3}_{-0.3}$	$6.0^{+0.3}_{-0.3}$	$5.9^{+0.3}_{-0.3}$	$5.9^{+0.3}_{-0.3}$
r_s [kpc]	38^{+20}_{-12}	35^{+16}_{-10}	35^{+17}_{-11}	25^{+10}_{-7}	29^{+11}_{-8}	29^{+11}_{-8}
α	$0.15^{+0.06}_{-0.04}$	$0.14^{+0.05}_{-0.04}$	$0.14^{+0.05}_{-0.04}$	$0.11^{+0.04}_{-0.03}$	$0.12^{+0.04}_{-0.03}$	$0.12^{+0.04}_{-0.03}$
V_{200} [km s$^-1$]	192^{+27}_{-20}	186^{+22}_{-18}	179^{+20}_{-16}	164^{+12}_{-13}	174^{+13}_{-14}	173^{+13}_{-14}
C_{200}	$7.5^{+2.4}_{-1.9}$	$8.0^{+2.5}_{-2.0}$	$7.7^{+2.5}_{-1.9}$	$9.8^{+3.0}_{-2.3}$	$8.8^{+2.5}_{-2.0}$	$8.8^{+2.6}_{-2.0}$
$\log(M_{200}/[M_\odot])$	$12.39^{+0.17}_{-0.14}$	$12.35^{+0.15}_{-0.13}$	$12.30^{+0.14}_{-0.12}$	$12.19^{+0.09}_{-0.10}$	$12.26^{+0.10}_{-0.11}$	$12.26^{+0.09}_{-0.11}$
r_{200} [kpc]	286^{+40}_{-30}	278^{+33}_{-27}	267^{+30}_{-24}	245^{+17}_{-19}	259^{+20}_{-21}	258^{+19}_{-20}
WAIC	−341 ± 4	−103 ± 3	−345 ± 2	−450 ± 5	−425 ± 6	−427 ± 6
LOO	−341 ± 4	−103 ± 3	−345 ± 2	−450 ± 5	−425 ± 7	−428 ± 7

best-fit estimates, the medians of the posteriors and their 1σ credible intervals

→ Widely Applicable Information Criterion (WAIC)

→ Leave-one-out cross-validation (LOO-CV)

- BG: larger value of R_{out} due to wider radial coverage of DR3 over DR2

- The values of Mb , Mtd , MTd are slightly smaller in the ΛCDM paradigm compared to those estimated with the MOND and MWC models

prior distributions from N-body simulations within the ΛCDM cosmology

A new kinematic model of the Galaxy: analysis of the stellar velocity field from Gaia D3,
Akhmetov et al. 2024, MNRAS, 530,1

evidence of warps and non-axisymmetric bar features of the Galaxy

Distribution of 18 million high luminosity stars (i.e., young OB, giants and subgiants) from Gaia DR3

radial gradient of the Galactic: **dynamical perturbations generated by the substructures as Galactic bar, spiral arms and warp** -> within **10 km/ s kpc!**

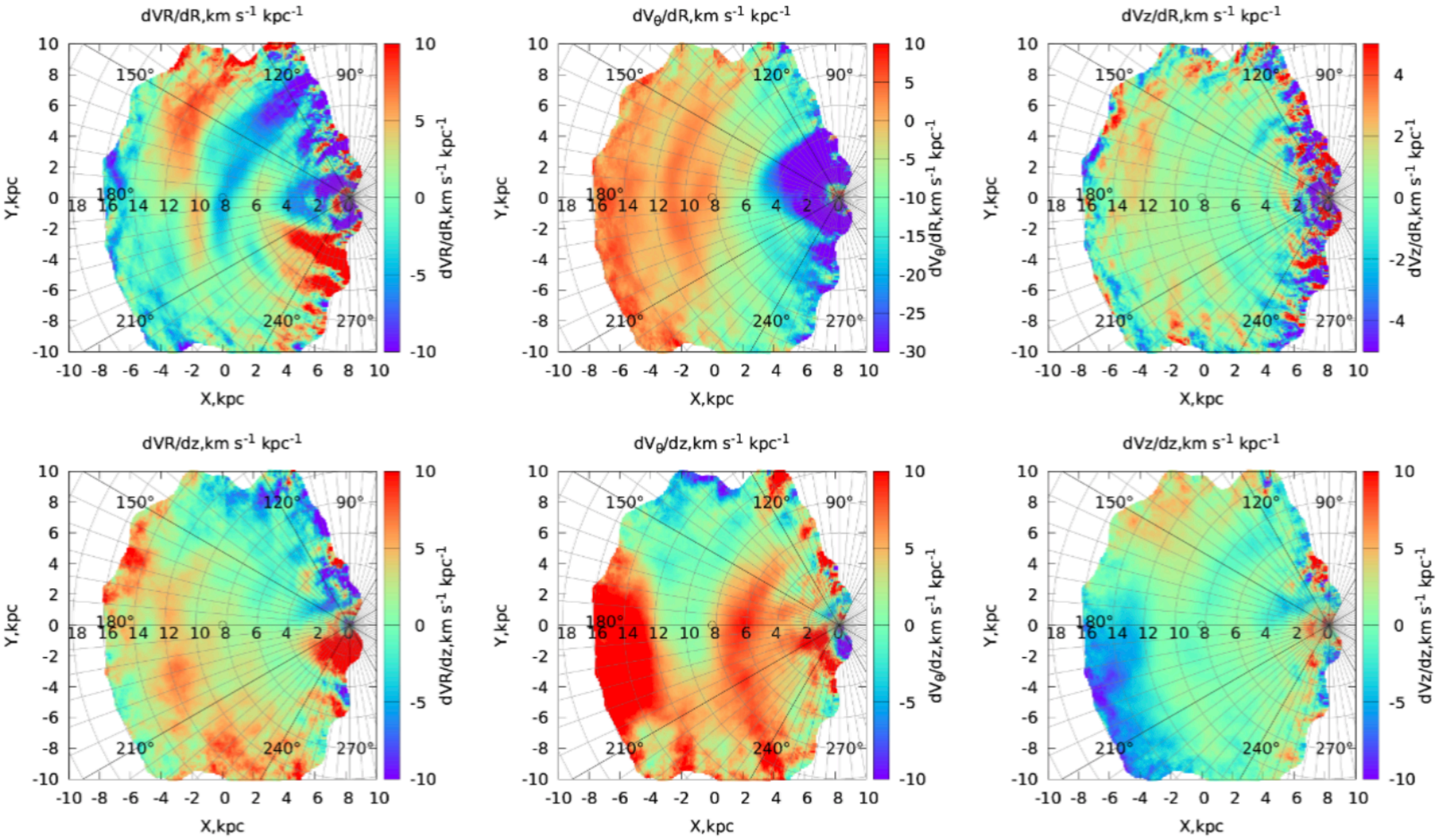

A new kinematic model of the Galaxy: analysis of the stellar velocity field from Gaia D3,
Akhmetov et al. 2024, MNRAS, 530,1

evidence of warps and non-axisymmetric bar features of the Galaxy

Distribution of 18 million high luminosity stars (i.e., young OB, giants and subgiants) from Gaia DR3

A new kinematic model of the Galaxy: analysis of the stellar velocity field from Gaia D3,
Akhmetov et al. 2024, MNRAS, 530,1

evidence of warps and non-axisymmetric bar features of the Galaxy

Distribution of 18 million high luminosity stars (i.e., young OB, giants and subgiants) from Gaia DR3

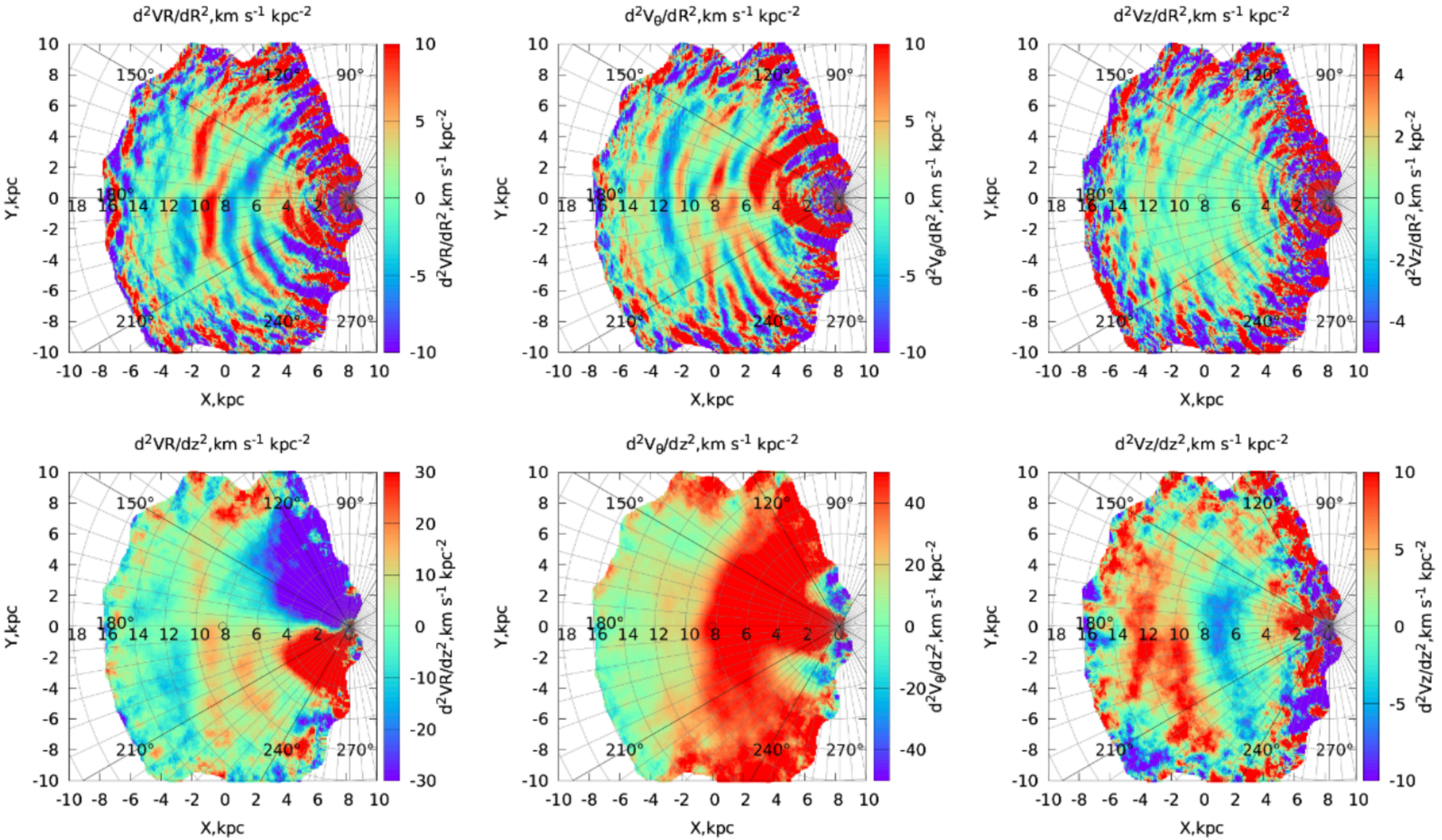

second order derivatives of the stellar velocity field in the radial direction: **wave-like dependence and ring-like signatures** on Galactic distance R **related to kinematic substructures** (spiral arms and bulge, and/or by the propagation of density, bending and breathing waves)

MCMC fit to the Gaia DR3 data - II. Results: radial density profile of the MW at z=0

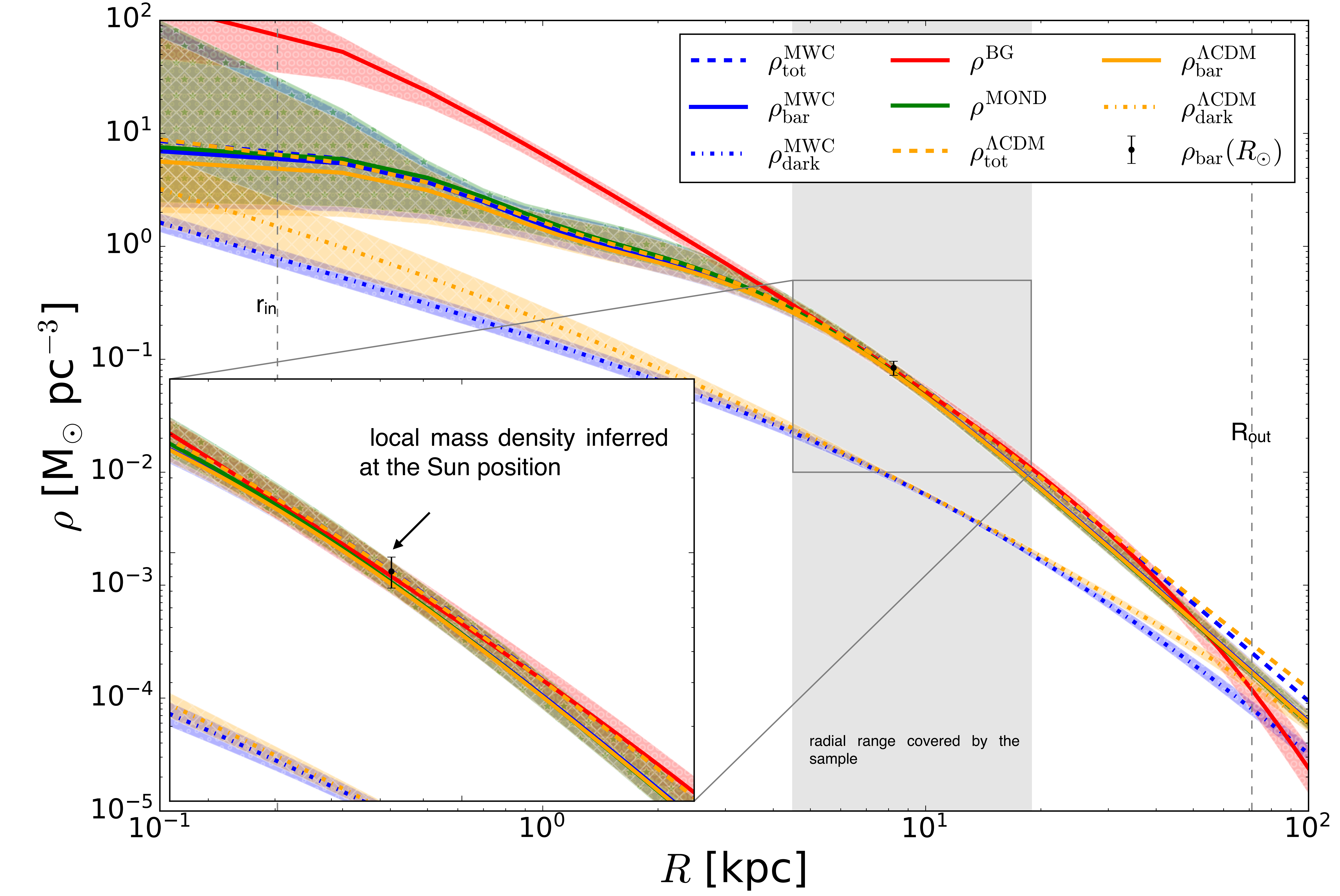

solid lines baryonic matter contributions

- MWC and ΛCDM total matter density profiles (dashed lines) are almost coincident while departing from each other only at very large radii
- Einasto profile of the ΛCDM model results larger than the NFW one both in the inner and outer parts of the Galaxy (dash-dotted lines)- > **more dark matter in the ΛCDM scenario compared to the case of an NFW halo** without cosmological constraints
- **BG and MOND** density profiles are **consistent with** both the baryonic and total density profiles of **MWC**

$$\rho(R,z) = e^{-\nu(R,z)}\frac{1}{8\pi R^2}\left[\left(\partial_R N(R,z)\right)^2 + \left(\partial_z N(R,z)\right)^2\right]$$

baryonic matter density observed at the Sun

$\varrho_{bar}(R_\odot) = 0.084 \pm 0.012\ M_\odot pc^{-3}$

estimates of the local baryonic density $\varrho^{\Lambda CDM}$ and ϱ^{MOND} around $0.080 M_\odot pc$

Crosta et. al, 2020, Beordo et al. 2024, Garbari et al. 2012; Bienaymé et al. 2014; McKee et al. 2015

MCMC fit to the Gaia DR3 data - III. Results: Total mass estimates

Density profile in agreement between all four models within the region of validity of BG

$$M = -2\int (T^0_0 - \frac{1}{2}T)\sqrt{-g}\ d^3x,$$

Komar mass for the GR model

Quantity	OBA	DCEP	RGB	OBA + DCEP	RGB + DCEP	ALL
$\rho^{MWC}_{bar,\odot}$ [$M_\odot$ pc^{-3}]	$0.080^{+0.012}_{-0.012}$	$0.080^{+0.012}_{-0.012}$	$0.080^{+0.012}_{-0.012}$	$0.080^{+0.012}_{-0.012}$	$0.080^{+0.012}_{-0.012}$	$0.080^{+0.012}_{-0.012}$
$\rho^{MWC}_{h,\odot}$ [$M_\odot$ pc^{-3}]	$0.0092^{+0.0009}_{-0.0009}$	$0.0092^{+0.0009}_{-0.0009}$	$0.0084^{+0.0007}_{-0.0007}$	$0.0083^{+0.0007}_{-0.0007}$	$0.0088^{+0.0006}_{-0.0007}$	$0.0088^{+0.0006}_{-0.0007}$
$\rho^{BG}_{\odot}$ [$M_\odot$ pc^{-3}]	$0.080^{+0.012}_{-0.012}$	$0.080^{+0.013}_{-0.012}$	$0.080^{+0.013}_{-0.012}$	$0.081^{+0.012}_{-0.012}$	$0.080^{+0.012}_{-0.012}$	$0.080^{+0.012}_{-0.012}$
M^{MWC}_{bar} [10^{10} $M_\odot$]	~1.62	~1.83	~1.25	~1.96	~1.36	~1.48
M^{BG} [10^{10} $M_\odot$]	~1.81	~2.39	~1.11	~2.37	~1.39	~1.54
$M^{MWC}_{\star}$ [10^{10} $M_\odot$]	$9.24^{+1.07}_{-1.01}$	$9.30^{+1.12}_{-1.10}$	$9.35^{+0.95}_{-0.93}$	$10.15^{+0.99}_{-0.95}$	$9.22^{+0.94}_{-0.91}$	$9.27^{+0.90}_{-0.95}$
M^{MWC}_{vir} [10^{10} $M_\odot$]	~114	~109	~103	~85	~105	~103
R^{MWC}_{vir} [kpc]	~222	~218	~214	~201	~216	~215

The **total baryonic mass** predicted by the ΛCDM scenario is around 8 × 10¹⁰ M⊙, smaller than the values of 9.2–10.2 × 10¹⁰ M⊙ expected for the MWC and MOND models

ΛCDM paradigm tends to assign less mass to the baryonic component and up to a factor of 2 more dark matter compared to the MWC model

The **virial mass** in the ΛCDM framework ranges from 1.5–2.5 × 10¹² M⊙

Quantity	OBA	DCEP	RGB	OBA + DCEP	RGB + DCEP	ALL
$\rho^{\Lambda CDM}_{bar,\odot}$ [$M_\odot$pc^{-3}]	$0.080^{+0.012}_{-0.012}$	$0.080^{+0.012}_{-0.012}$	$0.080^{+0.012}_{-0.012}$	$0.080^{+0.012}_{-0.012}$	$0.080^{+0.012}_{-0.012}$	$0.080^{+0.012}_{-0.012}$
$\rho^{\Lambda CDM}_{h,\odot}$ [$M_\odot$pc^{-3}]	$0.0099^{+0.0008}_{-0.0008}$	$0.0098^{+0.0008}_{-0.0008}$	$0.0088^{+0.0078}_{-0.0007}$	$0.0085^{+0.0006}_{-0.0006}$	$0.0091^{+0.0006}_{-0.0006}$	$0.0090^{+0.0006}_{-0.0006}$
$\rho^{MOND}_{\odot}$ [$M_\odot$pc^{-3}]	$0.080^{+0.012}_{-0.012}$	$0.080^{+0.012}_{-0.012}$	$0.081^{+0.012}_{-0.012}$	$0.081^{+0.012}_{-0.012}$	$0.081^{+0.012}_{-0.012}$	$0.081^{+0.012}_{-0.012}$
$M^{\Lambda CDM}_{bar}$ [10^{10} $M_\odot$]	$8.49^{+1.10}_{-1.03}$	$8.31^{+1.11}_{-1.04}$	$8.51^{+1.06}_{-0.95}$	$9.23^{+0.95}_{-0.93}$	$8.43^{+0.96}_{-0.91}$	$8.49^{+0.96}_{-0.89}$
M^{MOND} [10^{10} $M_\odot$]	$10.12^{+0.33}_{-0.30}$	$10.05^{+0.48}_{-0.45}$	$9.32^{+0.27}_{-0.24}$	$9.59^{+0.19}_{-0.18}$	$9.59^{+0.21}_{-0.19}$	$9.56^{+0.21}_{-0.19}$
$M^{\Lambda CDM}_{200}$ [10^{12} $M_\odot$]	$2.45^{+1.16}_{-0.68}$	$2.24^{+0.88}_{-0.59}$	$1.99^{+0.74}_{-0.49}$	$1.53^{+0.35}_{-0.33}$	$1.82^{+0.44}_{-0.40}$	$1.80^{+0.43}_{-0.39}$

MCMC fit to the Gaia DR3 data - IV.Results: Non-Newtonian contributions vs dark matter halo

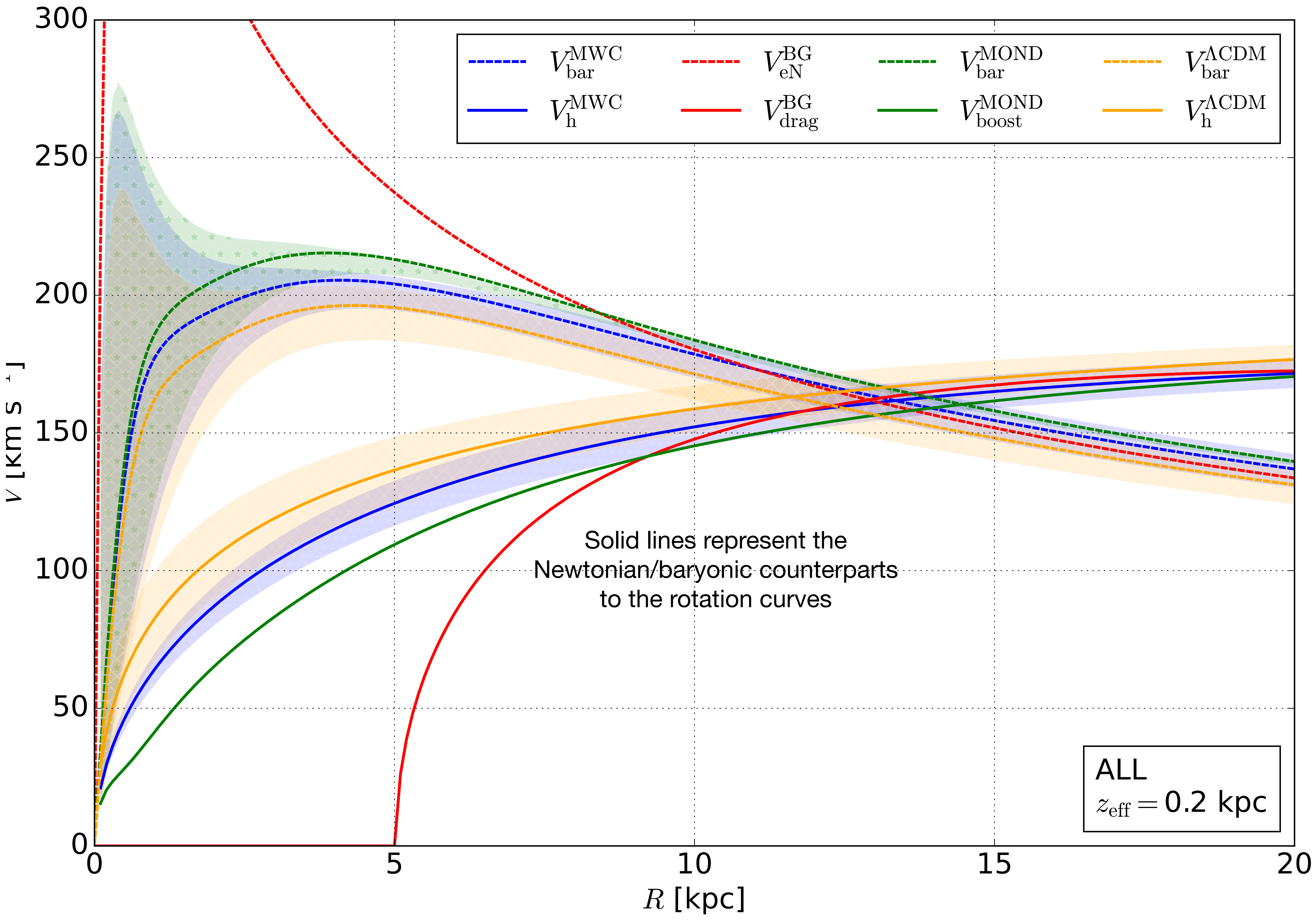

Non-Newtonian contributions to the rotation curve are consistent with that of the dark matter halo: they become predominant over the classical baryonic counterpart from 10-15 kpc outwards and, at the Sun distance, they are responsible for the 30-37% of the velocity profile.

Dragging effect vs. halo effect

The relativistic dragging effect has no newtonian counterpart, thus we compared:

(i) the MWC baryonic-only contribution with the effective Newtonian profile (Binney & Tremaine 1988) calculated by using the BG density:

(ii) the MWC dark matter-only contribution (halo) with the "dragging curve" traced by subtracting *effective Newtonian profile* to V_{BG} .

$$(V^{BG}_{drag}(R_i; |z|_{eff}|) = \sqrt{(V^{BG}(R))^2 - (V^{BG}_{eN}(R; |z|_{eff}))^2}$$

$$V_{\rm drag}^{\rm BG} = \sqrt{V_{\rm BG}^2 - V_{\rm eN}^2}$$

amount of rotational velocity across the MW plane <u>due to gravitational dragging</u>

$$V_{\rm boost}^{\rm MOND} = \sqrt{V_{\rm MOND}^2 - V_{\rm bar}^2} = V_{\rm bar}\sqrt{\eta(R, V_{\rm bar}) - 1}$$

pure Mondian boost

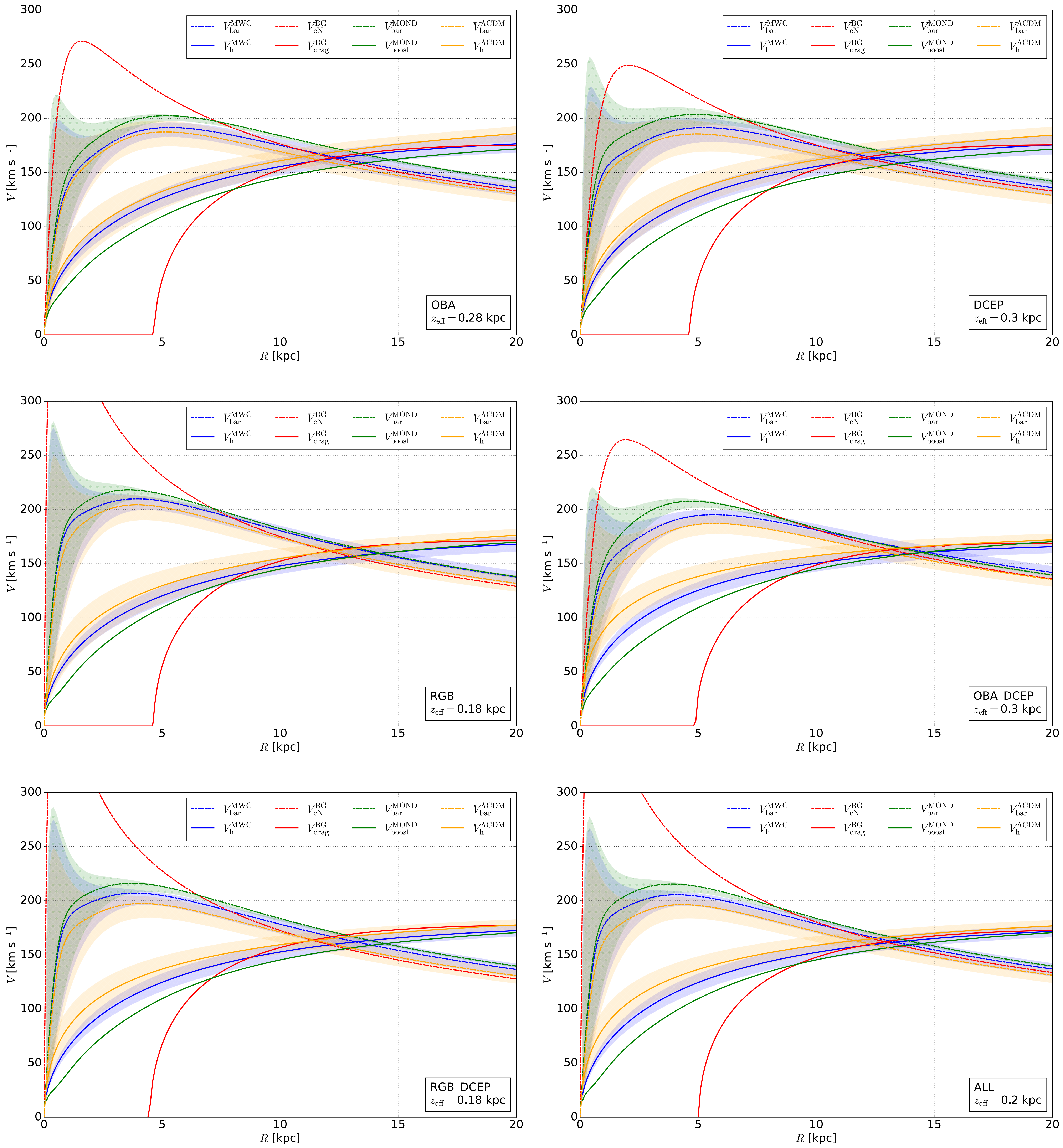

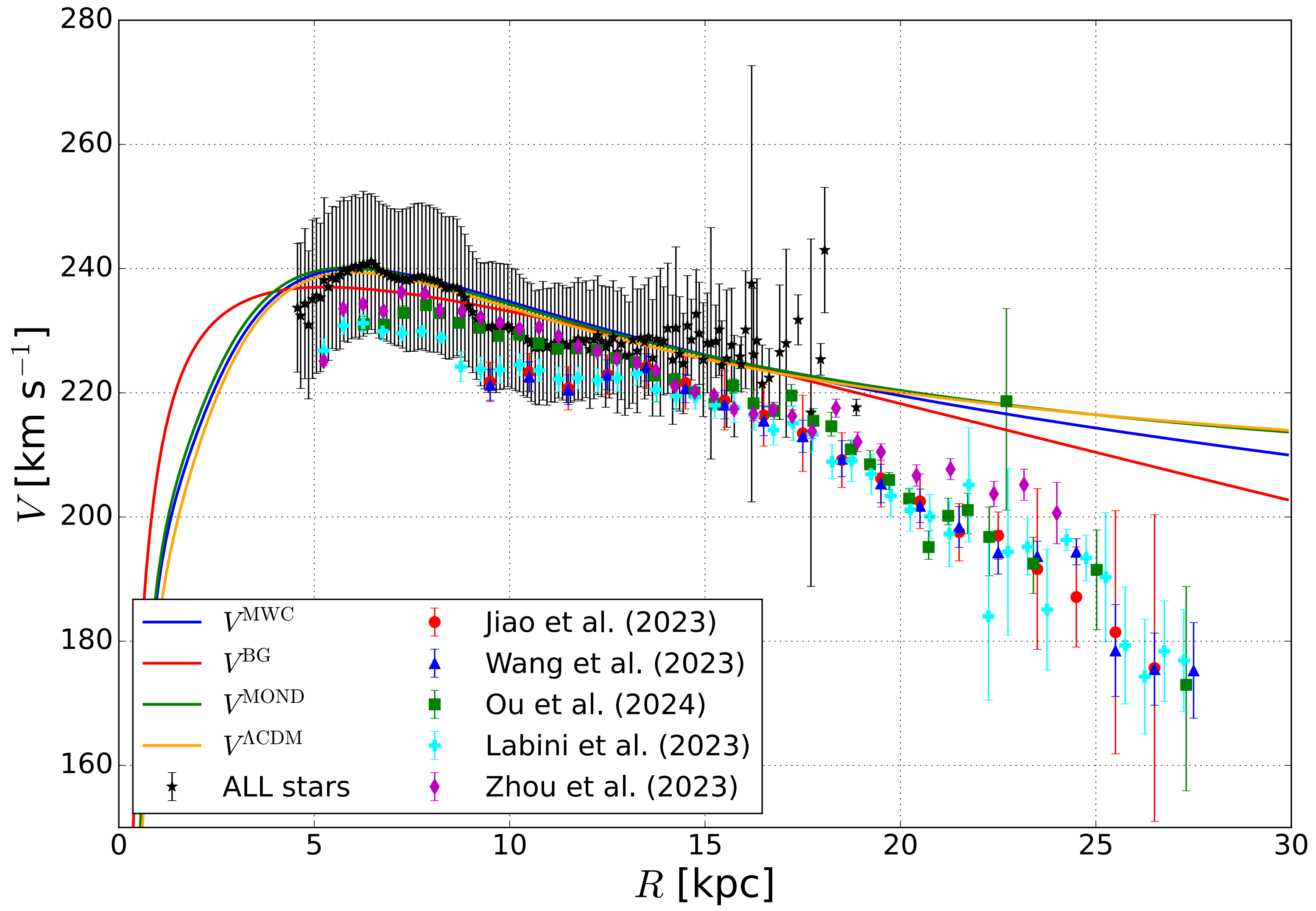

our rotation curves exhibit slightly declining profiles, aligning with recent findings that indicate a pronounced decline only beyond 18–19 kpc

we imposed a stringent requirement of errors on parallaxes smaller than 20%

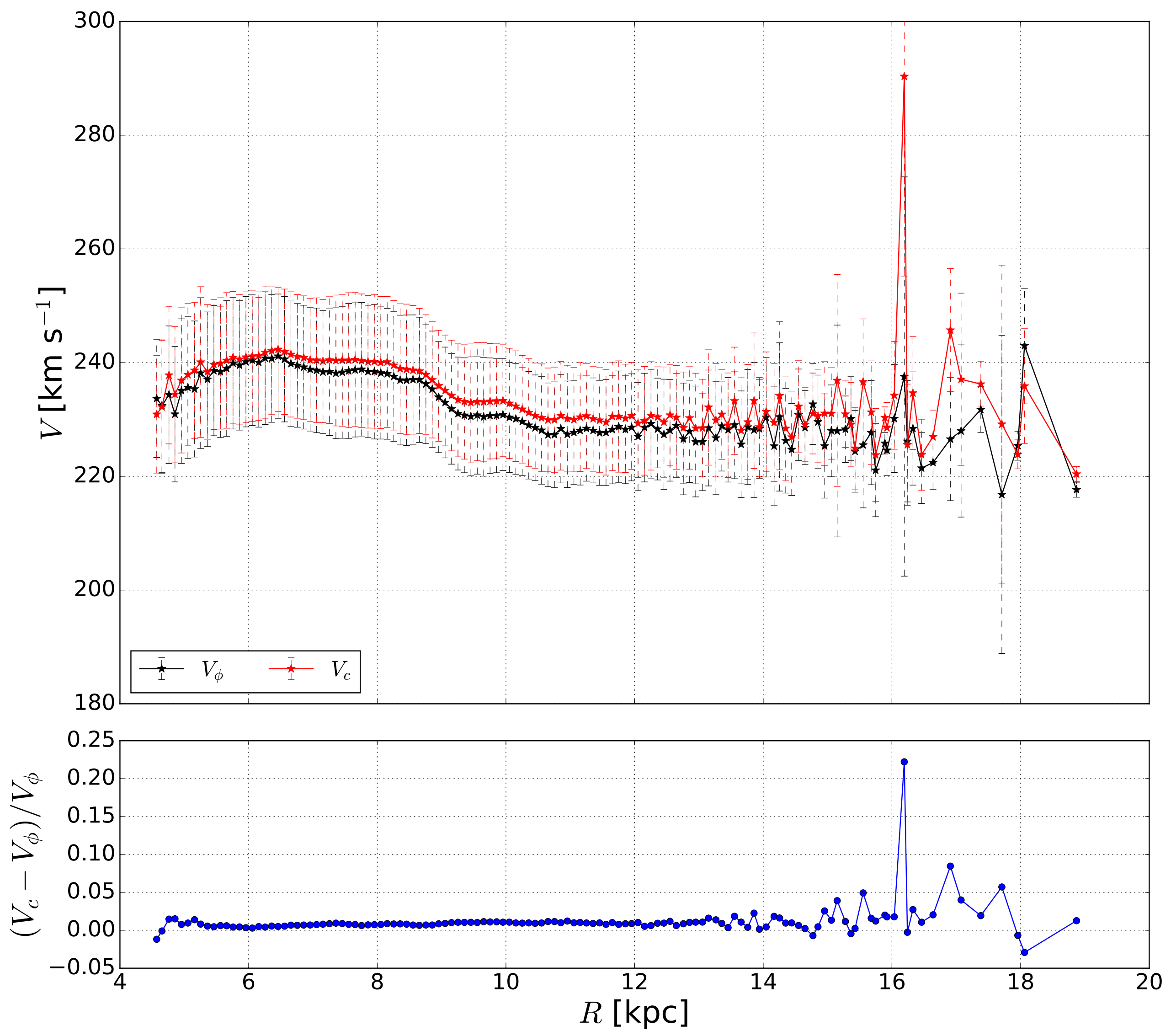

Wrap-up

Data are independent from the theoretical models that we use for the predictions

For our likelihood analysis the three models appear almost identically consistent with the data

- GR model has only 4 parameters, the classical model needs at least 10 parameters +1 for MOND , +3 for Lambda CDM

DM: does not absorb or emit light but it exerts and responds only to the gravity force; it enters the calculation as extra mass (halo) required to justify the flat galactic rotational curves.

MOND requires an adjustment ad hoc in the low acceleration regime

Einasto ΛCDM model results larger than the NFW one, dynamical mass supplied by more dark matter in the ΛCDM scenario compared to the case of an NFW halo without cosmological constraints

GR could imply a gravitational dragging "DM-like" effect driving the Galaxy velocity rotation curve, i.e. the geometry - unseen but perceived as manifestation of gravity according to Einstein’s equation - is responsible of the flatness at large Galactic radii.

Our interpretation with Gaia DR2/DR3 **depends only on the background geometry**

“space tells mass how to move”

GR is the standard theory of gravity over 60 order of magnitudes

Hypotehsis non fingo&occam's razor

By setting a coherent GR framework, we are pursuing to:

✓ Treat separately velocities and density with Einstein's equations [contrary to what is done in classical models]

✓ Establish to what extent the MW structure is dictated by the standard theory of gravity [avoiding replica of the common assumption that invalidate GR, i.e the GR effects are small in the linear approximation, and the star velocity as source of gravitomagnetism]

✓ Use **new mathematical solutions** & **new observables** [i.e. metric solutions to describe the structure and evolution of a multistructured Galaxy]

- At Galactic scale MW dynamics can be dominated, e.g., by Weyl, Lewis-Papapetrou spacetimes, whereas the Newtonian approximation is valid locally (e.g in the Solar System, binaries, …)
- Fix boundary matching conditions between internal/external Einstein's solutions
- Set comparisons at the scale of the Milky Way disc with the Lambda-CDM model predictions
- Explore more "geometrical" effects
- …….

✓ Extend the MW "geometries" to other galaxies:, the "geometries" of the Galaxy can play a reference role for other galaxies, just like the Sun for stellar models

MCMC fit to external Galaxies

Velocity profiles (SPARC data)

Classical (MWC)   GR (BG)

Best fit estimates as the median of the posteriors and their 1σ level credible interval

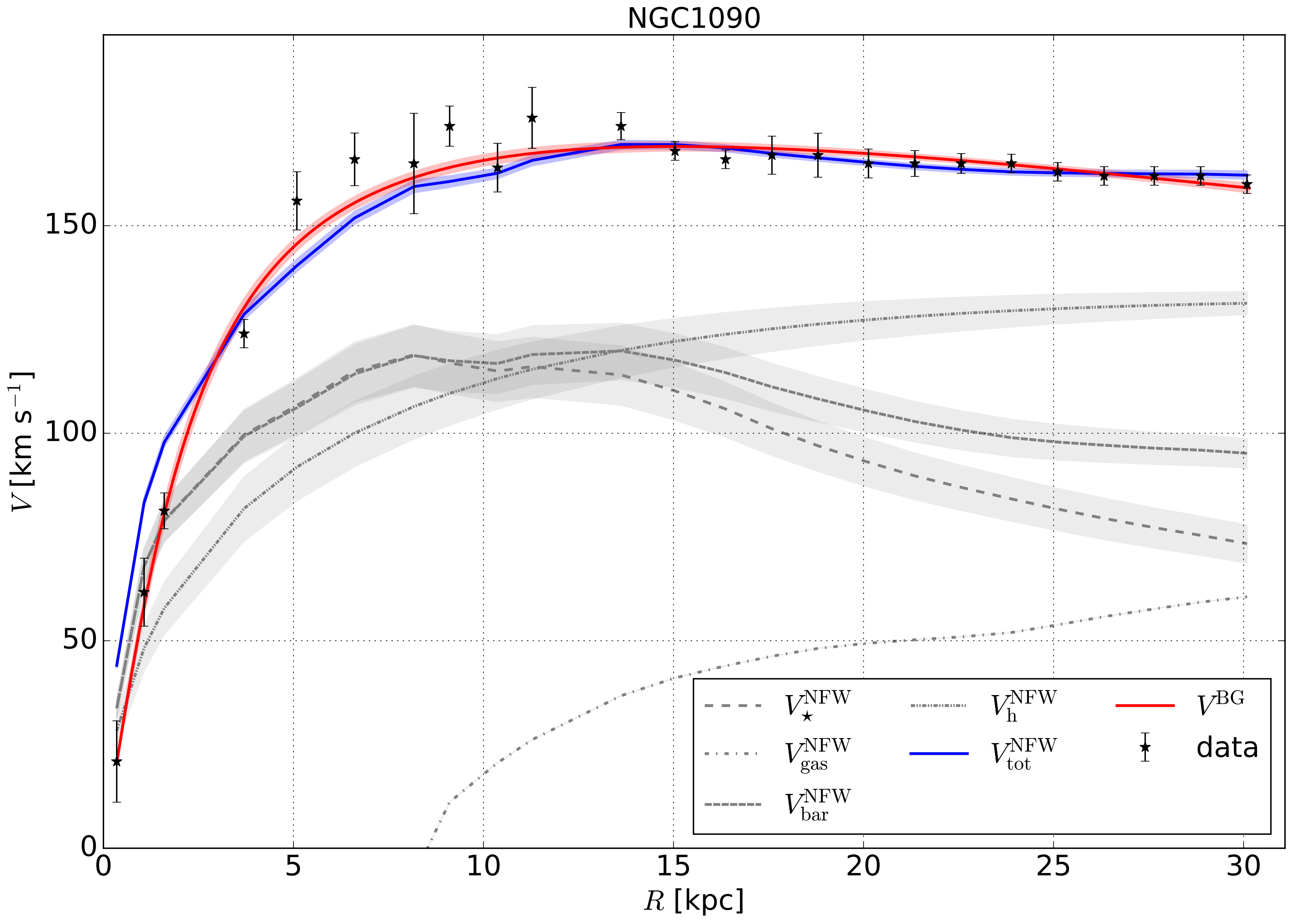

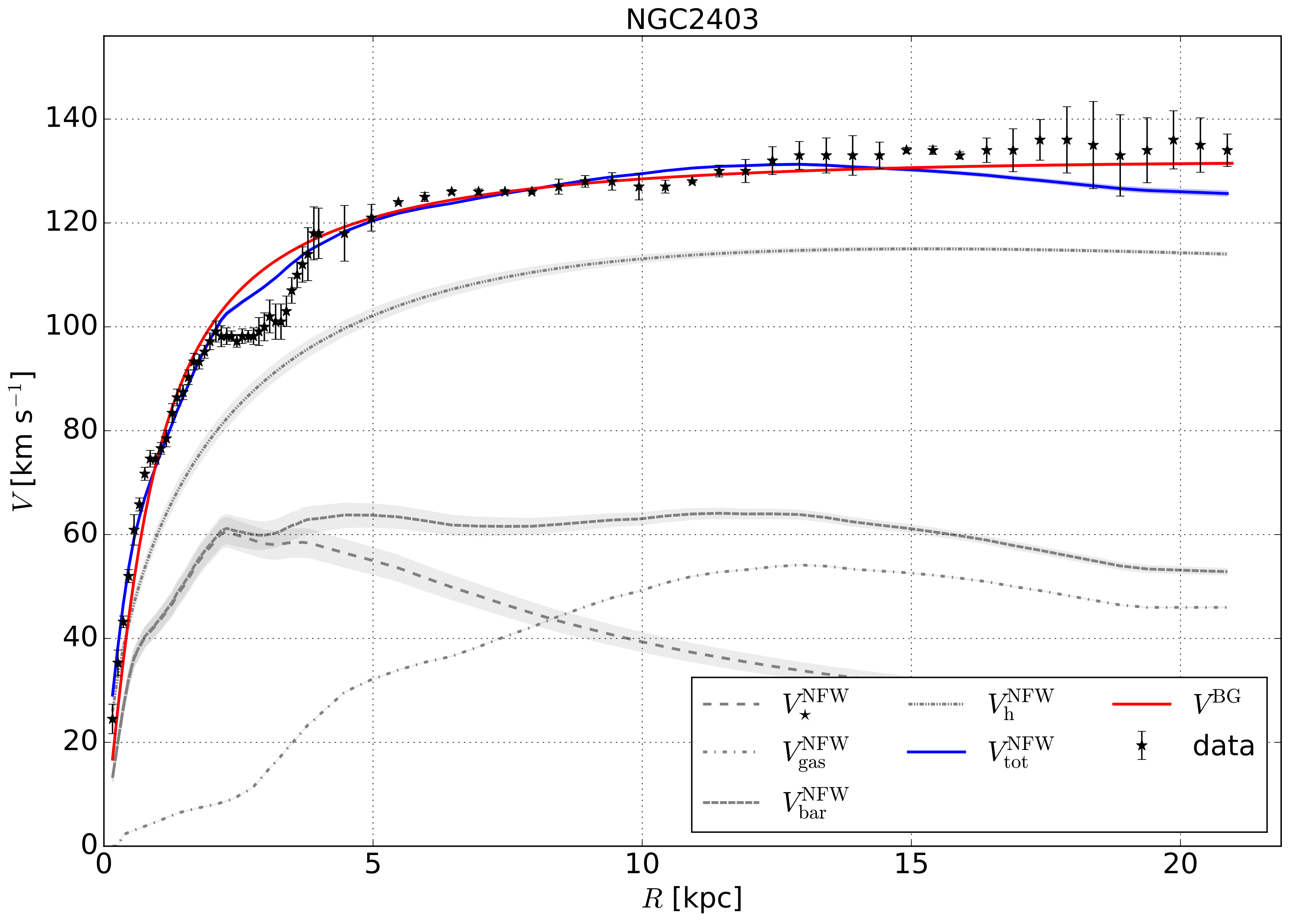

Conclusions

- The mandatory use of GR for astrometry in space has opened new possibilities and strategies to apply Einstein's Theory in classical astronomy domain, providing new coherent methods and "laboratories" to exploit at best the standard theory of gravity and the LDCM scnario

- Any GR tests performed by using Gaia @SS or @MW scale can play a reference role for other tests, much like the Sun for the stars, our Galaxy for other galaxies and so on..

- For the first time, there was quantitative evidence of the differences between the Newtonian and GR approaches to MW dynamics pushing towards more mathematical solutions of Einstein's equations, i.e. any modification of GR is done with GR as background theory

Conclusions

- The mandatory use of GR for astrometry in space has opened new possibilities and strategies to apply Einstein's Theory in classical astronomy domain, providing new coherent methods and "laboratories" to exploit at best the standard theory of gravity and the LDCM scnario

- Any GR tests performed by using Gaia @SS or @MW scale can play a reference role for other tests, much like the Sun for the stars, our Galaxy for other galaxies and so on..

- For the first time, there was quantitative evidence of the differences between the Newtonian and GR approaches to MW dynamics pushing towards more mathematical solutions of Einstein's equations, i.e. any modification of GR is done with GR as background theory

the "ether" was cured by a new kinematics (i.e. special relativity) instead of "new" dynamic as inspired by the FitzGerald-Lorentz contraction phenomena ("extra molecular force")

"*We know that electric forces are affected by the motion of the electrified bodies relative to the ether and it seems a not improbable supposition that the molecular forces are affected by the motion and that the size of the body alters consequently.*" FitzGerald, Science, 1889

Conclusions

- The mandatory use of GR for astrometry in space has opened new possibilities and strategies to apply Einstein's Theory in classical astronomy domain, providing new coherent methods and "laboratories" to exploit at best the standard theory of gravity and the LDCM scnario

- Any GR tests performed by using Gaia @SS or @MW scale can play a reference role for other tests, much like the Sun for the stars, our Galaxy for other galaxies and so on..

- For the first time, there was quantitative evidence of the differences between the Newtonian and GR approaches to MW dynamics pushing towards more mathematical solutions of Einstein's equations, i.e. any modification of GR is done with GR as background theory

> the "ether" was cured by a new kinematics (i.e. special relativity) instead of "new" dynamic as inspired by the FitzGerald-Lorentz contraction phenomena ("extra molecular force")
>
> "*We know that electric forces are affected by the motion of the electrified bodies relative to the ether and it seems a not improbable supposition that the molecular forces are affected by the motion and that the size of the body alters consequently.*" FitzGerald, Science, 1889

- [x] **What do we really know about the dark matter in the Universe?**
- [x] **How can we indirectly infer its existence and its nature from cosmology and astrophysics?**

- [ ] How can we directly detect its presence in experimental apparatus on Earth?
- [ ] What is the status of indirect dark matter experiments and searches at accelerators?
- [ ] Is it possible to build a consistent and comprehensive theoretical framework for the dark matter, as emerging from physics beyond the Standard Model?

- [x] **How can we advance further with theory, phenomenology, and experiments from the current standpoint?**

Conclusions

- The mandatory use of GR for astrometry in space has opened new possibilities and strategies to apply Einstein's Theory in classical astronomy domain, providing new coherent methods and "laboratories" to exploit at best the standard theory of gravity and the LDCM scnario

- Any GR tests performed by using Gaia @SS or @MW scale can play a reference role for other tests, much like the Sun for the stars, our Galaxy for other galaxies and so on..

- For the first time, there was quantitative evidence of the differences between the Newtonian and GR approaches to MW dynamics pushing towards more mathematical solutions of Einstein's equations, i.e. any modification of GR is done with GR as background theory

> the "ether" was cured by a new kinematics (i.e. special relativity) instead of "new" dynamic as inspired by the FitzGerald-Lorentz contraction phenomena ("extra molecular force")
>
> *"We know that electric forces are affected by the motion of the electrified bodies relative to the ether and it seems a not improbable supposition that the molecular forces are affected by the motion and that the size of the body alters consequently."* FitzGerald, Science, 1889

☑ **What do we really know about the dark matter in the Universe?**
☑ **How can we indirectly infer its existence and its nature from cosmology and astrophysics?**

☐ How can we directly detect its presence in experimental apparatus on Earth?
☐ What is the status of indirect dark matter experiments and searches at accelerators?
☐ Is it possible to build a consistent and comprehensive theoretical framework for the dark matter, as emerging from physics beyond the Standard Model?

☑ **How can we advance further with theory, phenomenology, and experiments from the current standpoint?**

Many thanks for your attention!